# Vicarious calibration of the HYDROPT algorithm with support of fixed monitoring stations in the Dutch coastal zone

S.W.M. Peters, H.J. van der Woerd, M.A. Eleveld

Report number R-08/12

2008

This report was commissioned by: Adviesdienst Geo-Informatie en ICT van Rijkswaterstaat, Delft.

It was internally reviewed by: Dr. M. Blaas, Delft Hydraulics

IVM

Institute for Environmental Studies
Vrije Universiteit
De Boelelaan 1087
1081 HV Amsterdam
The Netherlands

T +31-20-598 9555
F +31-20-598 9553
E info@ivm.vu.nl

# Contents

# Abstract

Over the last years the HYDROPT algorithm has been developed and perfected for operational processing of ocean colour images. The algorithm converts sea spectral reflectance to concentrations of the three optically active components in coastal waters, Chlorophyll-a, Total Suspended Matter and Coloured Dissolved Organic Matter. The standard calibration is based on Specific Inherent Optical Properties (absorption and scattering properties) that have been derived from an extensive set of measurements for the North Sea, collected in the EC FP5 project REVAMP.

In this report the HYDROPT calibration is investigated by comparing a four year dataset of in-situ Chlorophyll-a (Chl-a) and Total Suspended Matter (TSM) observations from Rijkswaterstaat with MERIS (ESA) and MODIS AQUA (NASA) ocean colour observations. The main conclusion is that the HYDROPT calibration can be improved for the Dutch coastal zone by so-called "vicarious calibration". In vicarious calibration, measurements (in this case MWTL measurements), independent of those that were used for the primary calibration, are used to correct for incomplete characterisation of the optical system (sensor calibration, atmospheric correction, air-water interface and errors in SIOP measurements).

It was found, using the highest quality data screening, that the SIOP set that was derived for 2006 performed best for all years, as can be seen in the figure below. At each point the 4 year geometric mean is calculated of MERIS and MWTL observations. The Chl-a regression line is almost perfectly on the 1:1 line; the TSM regression line has a very small deviation. RMS error values are extremely low.

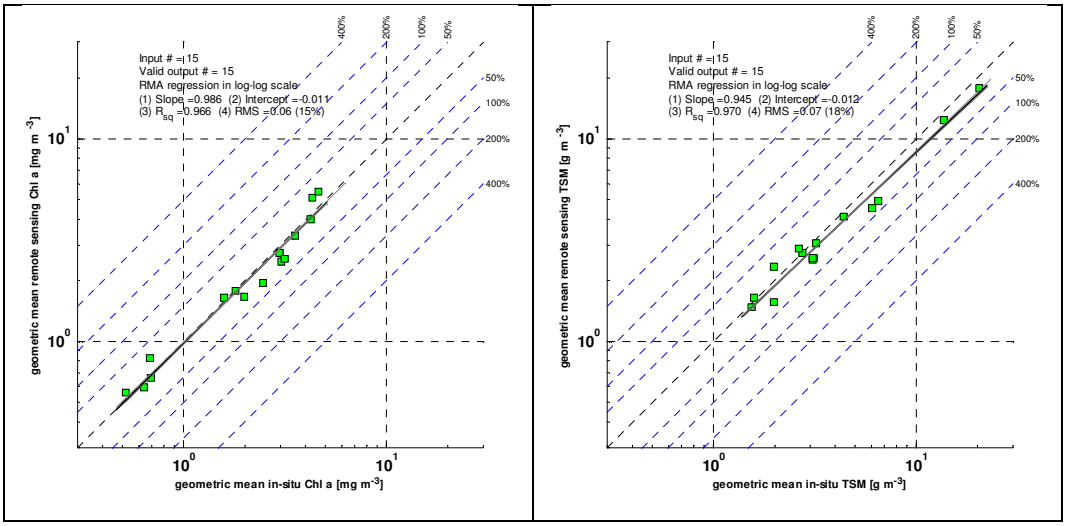


In this study also a data screening method was developed to provide the highest number of observations of good quality. As a results the HYDROPT MERIS optimized algorithm provides for each station about 80 MERIS observations per year that are well tied in to the MWTL monitoring results.

# Samenvatting

Gedurende de laatste jaren is het HYDROPT algoritme verder ontwikkeld en verbeterd ten behoeve van de operationele verwerking van satellietbeelden. Het algoritme berekent uit de gemeten reflectie van het zeeoppervlak de concentratie van de drie optisch actieve componenten in kustwateren, te weten chlorofyl a, zwevende stof en de gekleurde fractie van opgelost organisch materiaal. De standaard ijking van dit algoritme is gebaseerd op de specifiek inherent optische eigenschappen (absorptie en verstrooiing eigenschappen) van deze componenten, afgeleid van een grote database van metingen op de Noordzee, verzameld binnen het EC FP5 project REVAMP.

In dit rapport wordt de ijking van het HYDROPT algoritme onderzocht door een vergelijk te maken van een 4-jarige reeks van *in-situ* metingen van chlorofyl a (Chl-a) en zwevende stof (TSM) met een reeks satelliet waarnemingen door MERIS (ESA) en MODIS AQUA (NASA). De belangrijkste conclusie is dat de ijking van HYDROPT voor de Nederlandse kustzone verbeterd kan worden door middel van “vervangende ijking”. Bij vervangende ijking worden extra metingen gebruikt (in dit geval de MWTL metingen van Rijkswaterstaat die onafhankelijk zijn van de oorspronkelijke ijk metingen) om onvolkomenheden te corrigeren in de kennis van het hele optische systeem (ijking van de sensor in de ruimte, atmosferische correctie, verstrooiing aan lucht-water overgang en fouten in de metingen van de specifiek inherent optische eigenschappen (SIOP)).

Uit deze studie blijkt dat, met de hoogste kwaliteitscontrole, de SIOP gegevens die zijn afgeleid voor het jaar 2006 het beste presteert voor alle jaren (2003-2006), zoals blijkt uit de onderstaande figuur. Elk punt geeft voor één van de MWTL stations op de Noordzee het geometrisch gemiddelde van vier jaar metingen door middel van in-situ analyse en vier jaar MERIS waarnemingen. De regressielijn voor Chl-a ligt vrijwel perfect op de 1:1 lijn en de TSM regressielijn heeft slechts een kleine afwijking. De gemiddelde fout is bijzonder laag.

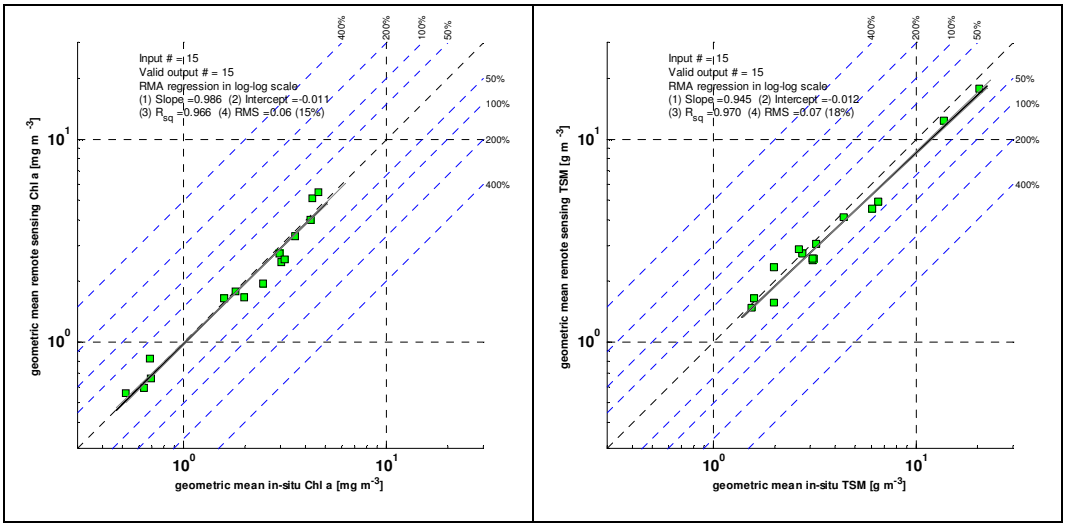

Binnen deze studie is ook een methode ontwikkeld om de satelliet gegevens te selecteren op goede kwaliteit, waarbij zoveel mogelijk metingen behouden blijven. Hierdoor levert HYDROPT algoritme voor elk station op de Noordzee gemiddeld 80 MERIS waarnemingen per jaar die door de herijking zeer sterk zijn gekoppeld aan de MWTL waarneem resultaten.

# 1. Description of the HYDROPT algorithm

## 1.1 Short history

The HYDROPT algorithm was developed during the REVAMP and AAN projects by R. Pasterkamp. The results of the algorithm as applied to MERIS images of 2003 and some validation results were published in Peters et al. (2005). The algorithm itself was described by Pasterkamp (2004, manuscript submitted to Applied Optics) and published by Van der Woerd & Pasterkamp (2005 and 2008). In a conference proceeding, Pasterkamp et al. (2005) outline a modification/extension of the algorithm for the purpose of calibrating the algorithm. This vicarious calibration uses long term datasets of in-situ Chlorophyll-a (Chl-a) and Total Suspended Matter (TSM) observations from Rijkswaterstaat instead of measured inherent optical properties. This extension was further developed and validated during this project. The results are presented in this report. In this section a description of the HYDROPT algorithm is given using excerpts from the papers by Pasterkamp et al. (2005) and Peters et al. (2005) and Van der Woerd & Pasterkamp (2008). Some of the text and findings of these papers overlap with reports from the AAN project (Van der Woerd & Pasterkamp, 2005).

## 1.2 Background of the HYDROPT algorithm

The sea spectral reflectance measured by satellites ("ocean colour") is linked to the optical properties of the sea, i.e. absorption and scattering. These optical properties, in turn, are determined by the constituents in the water. The basic challenge of each remote sensing algorithm is to calculate the concentrations of these optically active constituents from the measured sea spectral reflectance. The approach of the algorithm HYDROPT is to iteratively adjust the concentrations by minimizing the difference between a measured reflectance spectrum and the reflectance spectrum generated by a "forward" radiation transfer model. A detailed description of the underlying method is published in Van der Woerd & Pasterkamp (2008). Here we will restrict ourselves to a short explanation that is divided in two parts: 1) the description of the forward model and 2) the description of the inverse method.

## 1.3 Forward model

The forward model is the core of the HYDROPT algorithm. It calculates the sea spectral reflectance (Rrs) at optical wavelengths ($\lambda$) given a set of concentrations (see Figure 1.1). The forward model underlying HYDROPT is the HydroLight radiation transfer code (see http://www.sequoiasci.com/p-roducts/HydroLight.aspx). HydroLight is a well documented (Mobley, 1994) numerical solution of the radiation transfer equation, and is known for its accuracy (Mobley et al., 1993) and flexibility. For practical reasons some assumption were made, which are listed in Table 1.1. An advantage of the HydroLight code is that all angular dependency (solar and viewing angles) is fully resolved. A drawback is that the model takes too much computational time to make it suitable for real-time satellite processing (this is a general drawback of numerical models as compared to analytical approximations such as the equations proposed by Gordon (1988).

*Table 1.1 Main HydroLight Model Assumptions.*

| Main assumptions | Critical | Remarks |
|---|---|---|
| Vertically homogeneous water column | Moderate | North Sea can be thermally stratified in summer (Otto et al., 1990). |
| No bottom influence / infinitely deep water | Low | Violation in clear, shallow area's (e.g. Dogger Bank in Summer), but the effect is low. |
| Single scattering phase function | Moderate | Effect on retrieved TSM concentration mainly by backscatter to scatter ratio (Mobley et al., 2002). |
| Simple sky model | Low | model is appropriate for sunny conditions |
| No inelastic scattering (fluorescence, Raman) | Low | Main influence is to be expected in the chlorophyll-a fluorescence band (~ 680nm), but this band was omitted from inversion as a precaution. |

To facilitate fast computation, Pasterkamp designed an interface to HydroLight which consists of a tabulation of the output in a Look Up Table (LUT) and a polynomial equation that approximates the LUT (see Figure 1.1 and subsequent paragraphs).

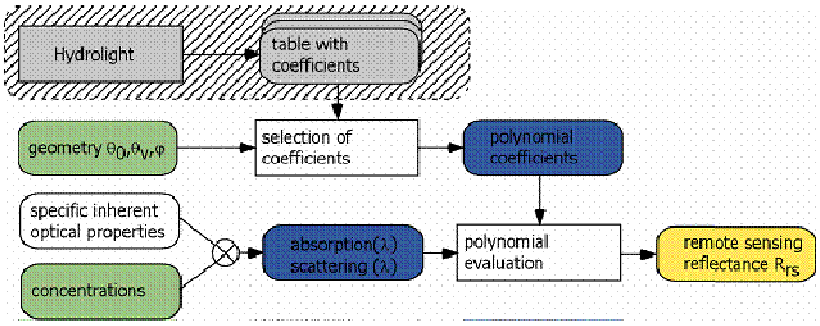


*Figure 1.1 Illustration of the forward model (from Pasterkamp et al., 2005).*

## 1.4 Approximating the forward model with look-up tables and polynomial functions

### 1.4.1 Design and content of the HydroLight LUT

To bypass the problem of computational time limitations, the output of the forward model is approximated first by a look-up table (LUT).

The LUT tabulates the relationship between remote sensing reflectance and a range of inherent optical properties, as calculated by HydroLight. The range over which the LUT is calculated is determined by estimating the minimum and maximum absorption (a $m^{-1}$) or scattering values (b $m^{-1}$) that might occur in the area of interest. Also the scattering over absorption ratio $\omega$=b/a is limited to the range 0.01 to 47. The optical properties are assumed to be invariant with depth and influence of bottom reflectance was neglected. The air water interface properties are fixed for a wind speed of 5 m $s^{-1}$, because the transfer properties of the air–water surface for that wind speed, based on Cox–Munk capillary wave slope statistics are already included in the HydroLight model.

In order to keep the conversion of concentrations to optical properties outside the model, LUT and polynomial approximation, the total absorption and scattering are used as independent variables instead of their specific subparts. As a result, this conversion can be defined on a regional or even pixel-by-pixel basis without the need to run HydroLight or recalculate the polynomial coefficients. To retain the angular dependence of the remote sensing reflectance, and to include the pure water volume scattering function for each wavelength, the polynomial coefficients are computed and stored for each combination of MERIS-wavelength, solar zenith angle ($\theta_0$), viewing zenith angle ($\theta_v$) and differential azimuth angle ($\Phi$). The standard HydroLight quad layout is used, with a nominal angular resolution of $\Delta\theta = 10°$ and $\Delta\Phi = 15°$, resulting in 10 viewing nadir angles and 24 azimuth angles.

The LUT is filled by evaluating first the minimum and maximum absorption and scattering values that can be encountered in the Dutch coastal zone. In this report this evaluation is based on the specific inherent optical properties that have been measured in the REVAMP project (Peters et al., 2005) for all permutations of the concentrations of Chl-a (0.01–150 mg $m^{-3}$), TSM (0.1–200 g $m^{-3}$) and Gelvin (CDOM 0–2 $m^{-1}$), for each wavelength of interest. The 20 discrete absorption and scattering values for which the LUT is generated are logarithmically spaced between the minimum and maximum for each wavelength, and a selection of absorption and scattering combinations is based on the minimum and maximum $\omega$.

Remote sensing reflectance is an apparent optical property and, although it is normalized to down-welling irradiance, shows a weak but significant variation with the illumination (sky radiance distribution) and observation angle (Mobley, 1994). Several models exist for the sky radiance distribution in clear sky conditions. In this study a hypothetical sky model is used, where the sun is shining in a uniform background sky. The relative contribution of the direct solar irradiance is controlled by the fraction diffuse irradiance, Fdiff. The sky radiance distributions in the LUT are limited to solar zenith angle ($\theta_0$) of 0–80° with the two options Fdiff=0 or 1. The remote sensing reflectance for any Fdiff can be found by using Equation 5 from Van der Woerd & Pasterkamp (2008).

In the end a 5-dimensional LUT is constructed, containing the remote sensing reflectance as a function of (i) solar zenith angle (including an entry with totally diffuse skylight), (ii) viewing nadir angle, (iii) azimuth angle, (iv) absorption and (v) scattering, adding up to 10×10×24×20×20=960,000 entries per wavelength. This grid sufficiently covers the solution space to allow interpolation with adequate accuracy.

For the purpose of the OVATIE-2 project this LUT was constructed based on the spectral properties of MERIS and a separate LUT based on the spectral characteristics of the MODIS sensor.

### 1.4.2 Polynomial approximations of the LUT

In order to be able to find the corresponding remote sensing reflectance with any absorption, scattering, and angular configuration the LUT was approximated by a polynomial expression containing all parameters of relevance. This allows fast interpolation in the LUT during the inversion procedure.

Because Rrs varies slowly with illumination and observation geometry, it is sufficient to use nearest neighbour interpolation for $\theta_0$, $\theta_v$ and $\Phi$. On a logarithmic scale, Rrs can well be well approximated by a polynomial function of the natural logarithm of total absorption (a) and scattering (b). A polynomial function of degree (n=m=4) has been fitted to the LUT values. After the fitting, a table was constructed that contained the 15 coefficients for each combination of $\theta_0$, $\theta_v$ and $\Phi$. Now, for a given a, b, Fdiff and geometry, Rrs can be calculated by first selecting the appropriate coefficients belonging to $\theta_0$, $\theta_v$, and $\Phi$ and than evaluating Eqs. (5) and (6) in Van der Woerd & Pasterkamp (2008).

A major advantage is that the polynomial can be differentiated analytically to yield ($\partial$Rrs/$\partial$a) and ($\partial$Rrs/$\partial$b), and partially differentiated to ($\partial$Rrs/$\partial$Chl-a), ($\partial$Rrs/$\partial$TSM) and ($\partial$Rrs/$\partial$CDOM). This enables the construction of the Jacobian matrix that is necessary for the Levenberg–Marquardt least-squares fitting (optimization) and the calculation of the standard errors. The polynomial equation is defined by equation 6 in Van der Woerd & Pasterkamp (2008).

The Levenberg-Marquardt routines, the calculation of the error products from the partial derivates and the software to determine the table of polynomial coefficients were elegantly programmed into a fast JAVA routine by R. Pasterkamp. This routine is controlled from MATLAB. In principle all settings (polynomial coefficients) and SIOP values are passed to the JAVA routine, including a measured Rrs spectrum and the observation geometry. The routine subsequently returns a fitted Rrs spectrum, the concentrations of Chl-a, TSM and CDOM and their associated standard errors. How this exactly is achieved is described in the next section.

It is important to realize that the LUT and the polynomial coefficients are completely defined by the spectral band widths of the sensor under consideration. In the course of the OVATIE-2 project LUT and the polynomial coefficients were recalculated for the MODIS sensor whose band settings are quite different from MERIS. Since HydroLight is computationally intensive, the calculation of the LUT takes several days to complete, but needs to be done only once for each sensor configuration. A special software interface controlling HydroLight from MATLAB was developed by Pasterkamp and developed further by Eleveld and Van der Woerd during this project.

## 1.5 Inverse modelling and concentration determination

The principle of the algorithm (in inverse mode) is to minimize (optimize) the difference between the observed reflectance spectrum and the HydroLight calculated reflectance spectrum for any number of spectral bands of the specific sensor, by varying the absorption and scattering properties. The ‘best-fit’ concentrations belonging to the minimum difference are then assumed to be the most likely concentrations corresponding to the measured spectrum. The ‘difference’ between the observation and the model is defined by the chi-square merit function. To be less vulnerable for bias errors introduced by

inaccurate atmospheric correction, the $\chi 2$ merit function is not based on the squared differences in the remote sensing reflectance for each band, but is based on the squared difference in the consecutive bands.

In the JAVA routine by R. Pasterkamp the simulated (consecutive differences) spectrum is constructed using the polynomial equation together with formulations for the derivation of the concentrations using the total absorption and scattering for all bands and user-given functions for the Specific Inherent Optical Properties (SIOP). Since the system of equations is non-linear, Levenberg- Marquardt optimization is used to find the simulated reflectance spectrum with the highest similarity to the measured reflectance spectrum. The process is illustrated by Figure 1.2.

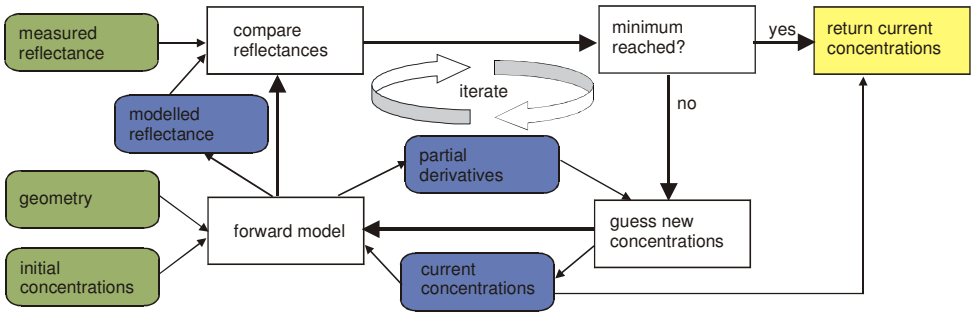


*Figure 1.2 Process of fitting a measured reflectance spectrum with HydroLight output, using the table of polynomial coefficients (from Pasterkamp et al., 2005).*

## 1.6 Performance of the HYDROPT algorithm

Van der Woerd & Pasterkamp (2008) tested the performance of the algorithm by first simulating a number of spectra with HydroLight (based on known distributions of concentrations of Chl-a, TSM and CDOM in the Dutch part of the North Sea). These spectra were subsequently simulated by HYDROPT to obtain (via inverse modelling) the concentrations back.

The RMS errors for Chl-a, TSMs and CDOM were 20%, 3% and 9% respectively (See Figure 1.3). For chlorophyll-a the error increases for decreasing concentrations, related to the fact that the chlorophyll-a absorption signature becomes less pronounced in spectra that are dominated by sediment backscatter and high CDOM absorption at the blue bands. Since these spectra are simulated and undisturbed (no measurement errors), this is the ideal situation. Determining the concentrations from satellite observed spectra containing a number of various potential spectral and bias errors will lead to larger uncertainties.

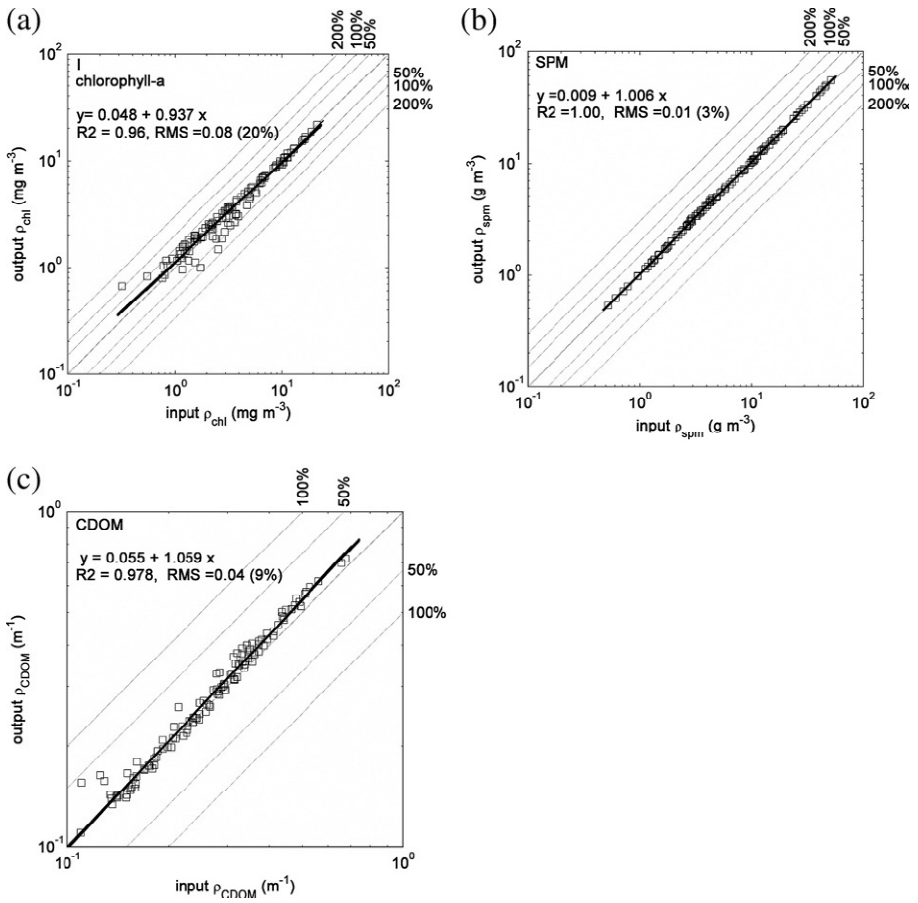


*Figure 1.3 Results of the inverse modelling test for concentrations of (a) chlorophyll-a, (b) suspended particulate matter and (c) the absorption of coloured dissolved organic matter. Diagonal dotted lines indicate 50, 100 and 200% error bounds. The thick line follows from log–log linear regression. (From Van der Woerd & Pasterkamp, 2008)*

## 1.7 Additional error products

Besides the standard errors in the concentrations, HYDROPT provides the $\chi 2$ value, which is a measure for the likelihood that the difference between the measured and simulated spectrum is accidental. Van der Woerd & Pasterkamp (2008, based on discussions in Pasterkamp, 1999) argue that, in order to avoid inconsistencies in the interpretation of $\chi 2$ it is probably better to use the cumulative $\chi 2$ distribution probability values (Pchi2).

During this study we found that it is convenient to take the –log10(Pchi2) as an indicator of inversion success. This parameter is called P in the output of HYDROPT. P is on a scale from 0 to 10+; large values for P indicate inaccurate fits because of low quality input data (bad spectra) or completely unsuitable input data (usually thin clouds and intertidal areas).

# 2. Application of HYDROPT to spectra

## 2.1 Comparison by match-up data

One way to evaluate the skill of the REVAMP-HYDROPT algorithm was to apply it to spectra observed in-situ with ship-borne or hand-held spectrometers. By calculating Chl-a from these spectra with HYDROPT an assessment could be made of the performance of the algorithm on real spectra. By comparing the Chl-a results to simultaneously observed traditional (HPLC or photometric) Chl-a measurements from samples one can get a good idea of the performance of the algorithm for various water types and conditions.

Based on the REVAMP SIOP observations a calibration dataset was calculated for the HYDROPT algorithm (Table 2.1). To this moment this calibration set of SIOPs is the best possible set of measurements for the North Sea using data not only from REVAMP but also from COLORS and COASTLOOC projects (Tilstone et al., 2008).

*Table 2.1 Coefficients of the optical model for the North Sea used for match-up comparison. The absorption and scattering of pure water, and the absorption and scattering per unit concentration of chlorophyll-a, suspended particular matter and coloured dissolved organic matter are presented for wavelengths corresponding to the MERIS bands. (Van der Woerd & Pasterkamp, 2008). These are REVAMP median values as described in Tilstone et al., 2008*

| **Wavelength (nm)** | **Absorption (m−1)** | | | | **Scattering (m−1)** | | |
|---|---|---|---|---|---|---|---|
| | Pure water | CHL (1/mg m−3) | SPM (1/g m−3) | CDOM(m−1) at 440 nm | Pure water | CHL (1/mg m−3) | SPM (1/g m−3) |
| 413 | 0.01 | 0.023 | 0.035 | 1.28 | 0.007 | 0.005 | 0.43 |
| 442 | 0.01 | 0.025 | 0.026 | 0.98 | 0.005 | 0.005 | 0.41 |
| 490 | 0.02 | 0.015 | 0.017 | 0.64 | 0.003 | 0.018 | 0.38 |
| 510 | 0.03 | 0.012 | 0.014 | 0.54 | 0.003 | 0.019 | 0.37 |
| 560 | 0.07 | 0.006 | 0.011 | 0.34 | 0.002 | 0.024 | 0.35 |
| 619 | 0.28 | 0.006 | 0.008 | 0.20 | 0.001 | 0.018 | 0.32 |
| 665 | 0.40 | 0.011 | 0.006 | 0.13 | 0.001 | 0.008 | 0.31 |
| 681 | 0.43 | 0.009 | 0.007 | 0.12 | 0.001 | 0.013 | 0.30 |
| 708 | 0.71 | 0.002 | 0.005 | 0.09 | 0.001 | 0.033 | 0.29 |

The results of the comparison are illustrated in Figure 2.1 (Peters et al., 2005). It was found that inversion of 85 observed spectra from the REVAMP dataset (Tilstone et al., 2008 in prep) lead to acceptable correlations for Chl-a in complex case-2 waters but to weak correlations in case-1 waters (Figure 2.1), which was explained by Van der Woerd & Pasterkamp (2008) by the fact that for all waters one single set of specific optical properties was used, which was more representative for case-2 waters than for case-1 waters.

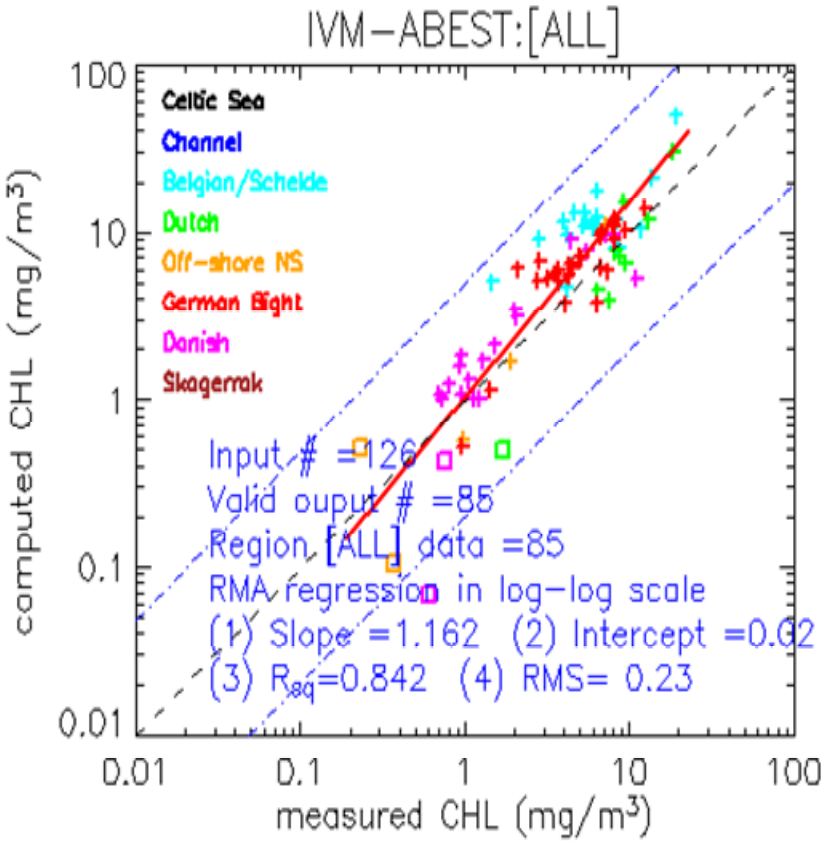


*Figure 2.1 Outcome of the chlorophyll retrieval by the HYDROPT algorithm on a set of 85 reflectance spectra collected in the REVAMP project. Note that the chlorophyll concentration covers almost two orders of magnitude and seven different water masses with variations in IOP and concentrations in the optical properties of SPM and CDOM. The log–log linear fit is described by $y=0.022+1.16x$, $R^2=0.84$, RMS error is 0.23(from Peters et al., 2005).*

## 2.2 Comparison by match-up data and time series

Remote sensing observations can provide a synoptic overview of the Chl-a concentrations in the North Sea, on a day-to-day basis and can be used to investigate the seasonal and spatial variations at high resolution, which can teach us more about the underlying processes that drive the 'North Sea' system (see e.g. Eleveld et al., 2008).

However, to be useful for long-term trend detection, we need to establish the relationship between actual and historical in-situ data (measured routinely by national monitoring agencies) to verify whether remote sensing and in-situ measurements of Chl-a and TSM give consistent measurements. There are a number of points that need to be considered when comparing in situ and remotely sensed Chl-a and TSM data.

- First of all, the measurement scales are of different orders of magnitude; while in-situ measurements typically sample about 1 to 2 litres of water, a remote sensing measurement covers tens of hectares, averaged over a specific surface layer.

- Second, in-situ measurements typically extract the algal pigments from the cell, whereas remote sensing 'sees' intact algal cells with an array of pigments as they interact with the underwater light field.
- Third, because of the rapidly changing conditions on the North Sea, remote sensing and in-situ measurements are only directly comparable when sampled within a small time window (~1 hour). It is often very difficult to fulfil this criterion.
- Finally, the measurement protocols that are used by national monitoring agencies can differ from agency to agency and from those used by other research laboratories (Sørensen et al., 2007).

The advantage of remote sensing is that it could provide a uniform measurement method for the whole North Sea. Validation of the results is however required to study the effect of above mentioned errors on the retrieval results. There have been a small number of relevant validation studies, each with their own scope and approach. For example, independent validation for research purposes was conducted during the REVAMP project mainly on matchup point samples (REVAMP atlas: Peters et al. 2005, Figure 2.1) where it was proven that the "REVAMP algorithm" (=HYDROPT) outperformed the standard MERIS Neural Network algorithm.

But, in order to evaluate the performance of the algorithm in reproducing in-situ observed Chl-a and SPM data at Dutch monitoring stations, other approaches were chosen. These are inspired by the fact that there is a relatively large volume of in-situ data collected by RWS: the Dutch monitoring network (MWTL) collects in-situ samples regularly with a frequency between 3 $yr^{-1}$ to 18 $yr^{-1}$.

A method of comparison was devised, inspired by the work of Dury et al. (2004), whereby time series of in situ Chlorophyll-a measurements for one year (initially 2003) are used for a number of fixed monitoring stations on the Dutch (Rijkswaterstaat). During REVAMP this method was tested and also used for other locations such as the Southern UK (PML) coast station L4 (16 data points in total).

Based on these time series one can either compare the yearly average mean value per station from satellite and in-situ samples, or one can plot the time series together on the same time axis to study similarities/discrepancies in time (see e.g. Eleveld for SPM time series of SPM). By using yearly mean values based on time series, random differences introduced by scale dissimilarity and a-synchronous sampling are averaged out to a certain extent and the systematic offsets can then be investigated.

## 2.3 The Dutch monitoring station network

In-situ samples are taken for measurement of (amongst others) SPM and chlorophyll-a along a set of transects, at several distances off the coast, on either a two week (summer) or monthly schedule (see Figure 2.2). The monitoring stations are listed in Table 2.2. Thus Walcheren 2 is the location 2 km offshore along the Walcheren transect.

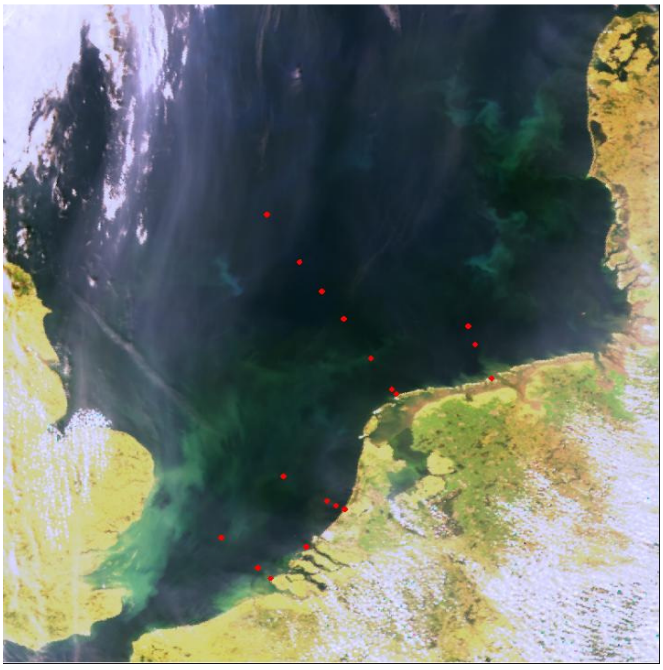

*Figure 2.2 Data is collected at the locations shown, along several transects, through the ship-based MWTL programme. From south to north, the transects are called: Walcheren, Goeree (single point), Noordwijk, Terschelling, and Rottumerplaat (from Dury et al., 2004).*

*Table 2.2 Location codes of 17 MWTL stations included in this study*

| Location code | Location description |
|---|---|
| WALCRN2 | Walcheren, 2 km from the coastline |
| WALCRN20 | Walcheren, 20 km from the coastline |
| GOERE6 | Goeree 6, 6 km from the coastline |
| NOORDWK2 | Noordwijk 2, 2 km from the coastline |
| NOORDWK10 | Noordwijk 10, 10 km from the coastline |
| NOORDWK20 | Noordwijk 20, 20 km from the coastline |
| NOORDWK70 | Noordwijk 70, 70 km from the coastline |
| TERSLG4 | Terschelling 4, 4 km from the coastline |
| TERSLG10 | Terschelling 10, 10 km from the coastline |
| TERSLG50 | Terschelling 50, 50 km from the coastline |
| TERSLG100 | Terschelling 100, 100 km from the coastline |
| TERSLG135 | Terschelling 135, 135 km from the coastline |
| TERSLG175 | Terschelling 175, 175 km from the coastline |
| TERSLG235 | Terschelling 235, 235 km from the coastline |
| ROTTMPT3 | Rottumerplaat 3, 3 km from the coastline |
| ROTTMPT50 | Rottumerplaat 50, 50 km from the coastline |
| ROTTMPT70 | Rottumerplaat 70, 70 km from the coastline |

## 2.4 Review of HYDROPT application to MERIS spectra at MWTL locations

### 2.4.1 REVAMP results

The first comparison of annual mean values from MERIS and MWTL (plus one UK station L4) was published in Peters et al. (2005). It was shown that an acceptable correlation exists between annual median Chl-a at MWTL stations from samples and from MERIS (Figure 2.3).

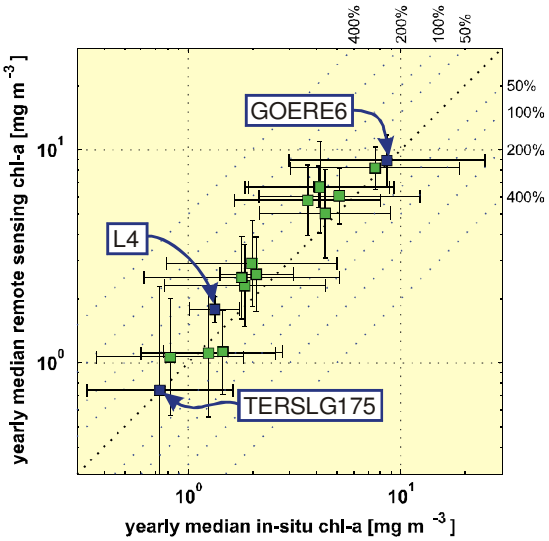


*Figure 2.3 yearly geometric median Chlorophyll-a per station (in-situ vs MERIS results)(from the REVAMP atlas Peters et al., 2005).*

In Figure 2.1 the green squares represent the yearly mean chlorophyll-a for each measurement station. The horizontal and vertical error bars represent the standard deviation over all measurements at each station, for in-situ and remote sensing measurements, respectively. The relative root-mean square difference between remote sensing and in-situ is 33%, the correlation coefficient equals 0.93. Part of this difference can be attributed to the statistical uncertainty in the median value (calculated as the geometric mean). This exercise demonstrates a lack of systematic offset between both datasets.

In the calculation of the MERIS Chl-a values the following properties / criteria / flags were applied:

| | |
|---|---|
| MERIS processing version | MEGS 7.0 |
| PCD-1-13 flag applied | YES |
| High glint flag applied | YES |
| Negative values screening | NO |
| Maximum values screening | NO |
| Spectral bands allowed | B1-7 + B9 |
| -log(P) screening | NO |

## 2.5 AAN results

In a later stage, after the REVAMP project the HYDROPT algorithm was improved further during the AAN project (Van der Woerd & Pasterkamp, 2005) to reduce the influence of high TSM on Chl-a retrievals from MERIS. The adjustment mainly involved increasing the order of the polynomial fitting equation (Pasterkamp, private communication), with the following results

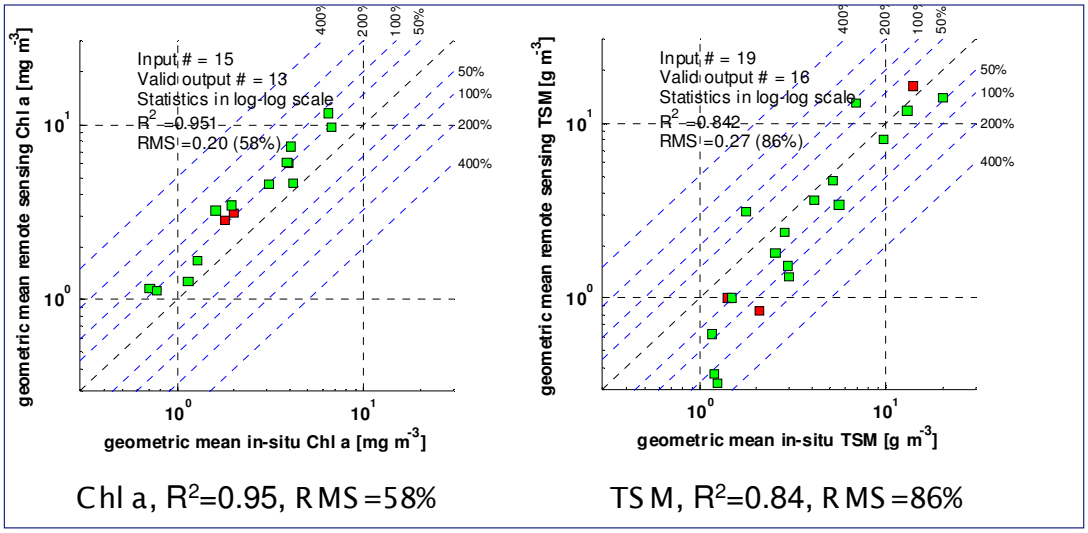


*Figure 2.4 Adjusted REVAMP algorithm calibrated with in-situ observed SIOP values.*

As a consequence of the adaptation, the algorithm now produces a higher correlation coefficient for Chl-a but it is introducing also a bias which increases the RMS error. In this case also the results for TSM are given, showing a somewhat lower $R^2$ and a relatively large RMS mainly due to relatively large errors at stations with relative low SPM concentrations. As we will show in the next sections, the interpretation of these graphs is hampered by the fact that not all MWTL stations are sampled with the same frequency. In the calculation of the MERIS Chl-a values calculation the following properties / criteria / flags were applied:

| | |
|---|---|
| MERIS processing version | MEGS 7.0 |
| PCD-1-13 flag applied | YES |
| High glint flag applied | YES |
| Negative values screening | NO |
| Maximum values screening | NO |
| Spectral bands allowed | B1-7 + B9 |
| -log(P) screening | No |

These results have inspired Pasterkamp and his co-workers to look for alternative methods for further improvement of the remote sensing results. They had arrived at a point where the underlying optical model and the transfer of the reflectance-concentrations relationships via Look-up-tables and polynomial approximations can hardly be improved, unless HydroLight itself would be improved significantly, which would be out of scope.

From REVAMP and predecessors (COLOURS and COASTLOOK) an inherent variability of measured SIOPs was shown which suggested that additional measurements would not directly contribute to a more accurate determination of North Sea model calibration parameters. One alternative would be to improve the model calibration by allowing regional/temporal subsets of SIOPs leading to a fine-tuning of the algorithm for local situations (endeavoured by Tilstone et al., 2008, in prep). Another alternative would be to use the relatively high density of MWTL observations of Chl-a and TSM to perform a vicarious calibration of HYDROPT on these observations with the SIOPs as free parameters. If possible, such a calibration would by definition automatically deliver the best possible fit between MWTL data and MERIS results for the area under consideration.

## 2.6 Results for MEGS 7.4 for the years 2003, 2004, 2005 and 2006

In 2005 the MERIS atmospheric and products processors from the European Space Agency (ESA) were upgraded from version MEGS7.0 to MEGS7.4. Although it was announced that this would be a major update, the reported differences were not altogether evident or positive (Peters, 2006). During the Ovatie-2 project an evaluation was made of the performance of HYDROPT algorithm calibrated with the REVAMP SIOP data for these new MEGS7.4 observations. The results are shown in Figure 2.5. A detailed explanation of the screening and flag setting is provided in chapter 6.

| | |
|---|---|
| MERIS processing version | MEGS 7.4 |
| PCD-1-13 flag applied | NO |
| High glint flag applied | NO |
| Negative values screening | YES |
| Maximum values screening | YES |
| Spectral bands allowed | B1-7 + B9 |
| -log(P) screening | YES 2=LQ 3=BI |

For 2003 the results can be compared to earlier validation efforts reported above, albeit that in this case the data screening was less strict. Allowing more data in the comparison by making the data screening less strict results in slightly lower correlation coefficients for Chl-a and a higher correlation coefficient for TSM for 2003 data. The same is true for the RMS which is larger for Chl-a as compared to earlier results and smaller for TSM.

But the same general conclusions can be drawn from this comparison for the years 2003-2006 as for the year 2003 alone: If we take the latest MERIS processing (MEG 7.4) and apply the REVAMP Median2 SIOP set (Table 2.1) we find that Chl-a is significantly and systematically overestimated for all 4 years and TSM is significantly and systematically underestimated by HYDROPT. One may further conclude from these comparisons that the deviations between in-situ data and remote sensing results are not likely to be caused by data screening but are determined mostly by the choice of SIOPs. This option is the focus of this study and is described in the subsequent chapters. Improvements in the correlation coefficient of TSM are probably due to the upgrade from MEGS 7.0 to MEGS 7.4. One might conjecture that this upgrade mainly has influenced the bias in the reflectance spectra.

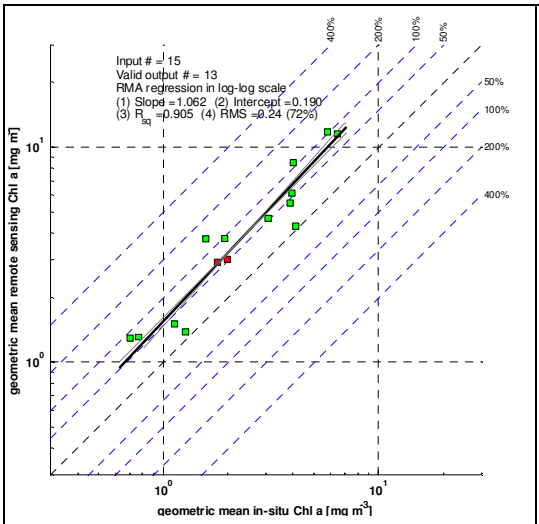


SIOP: Revampmedian2

Parameter: CHL

Year: 2003 flag settings: 1001

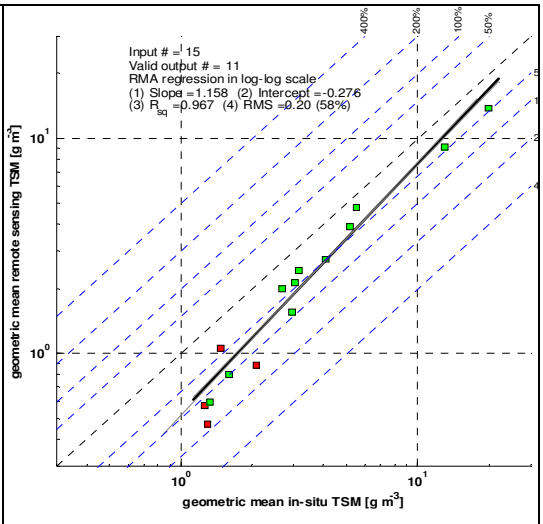


SIOP: Revampmedian2

Parameter: TSM

Year: 2003 flag settings: 1001

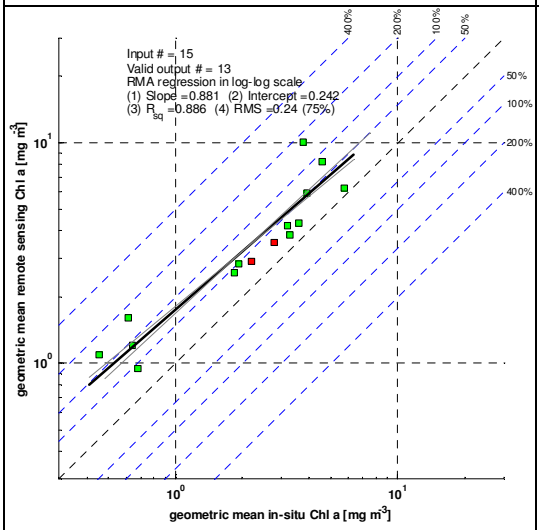


SIOP: Revampmedian2

Parameter: CHL

Year: 2004 flag settings: 1001

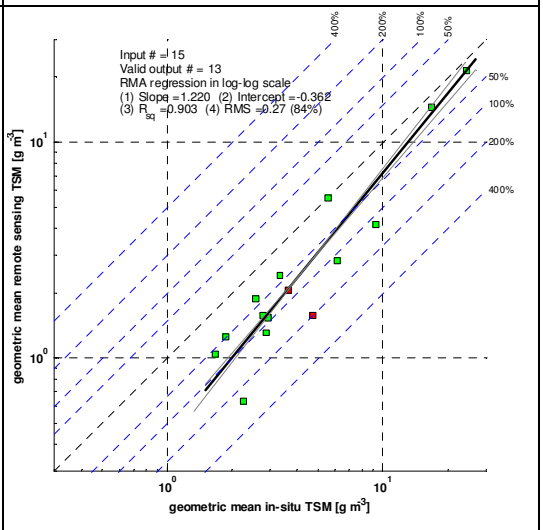


SIOP: Revampmedian2

Parameter: TSM

Year: 2004 flag settings: 1001

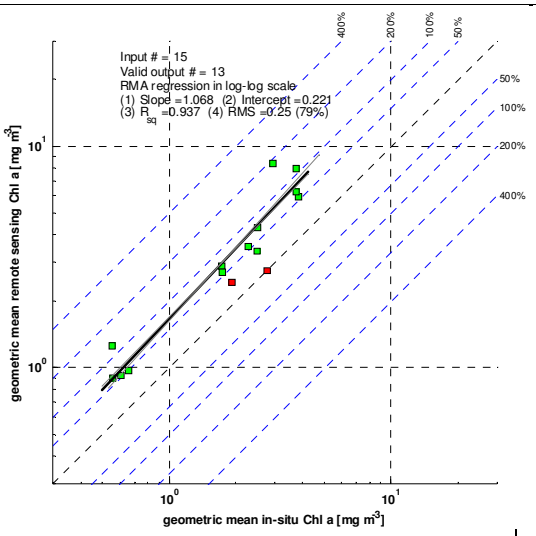


SIOP: Revampmedian2

Parameter: CHL

Year: 2005 flag settings: 1001

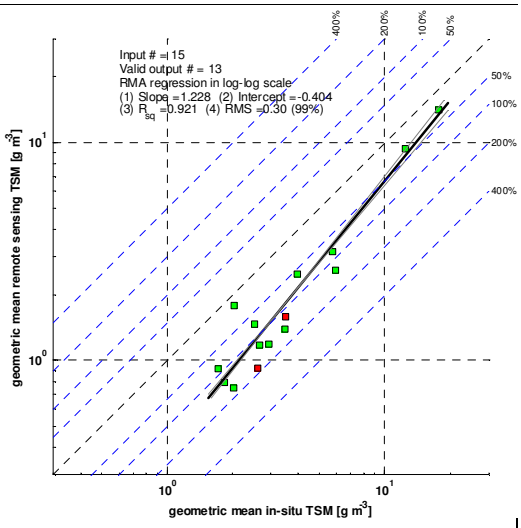


SIOP: Revampmedian2

Parameter: TSM

Year: 2005 flag settings: 1001

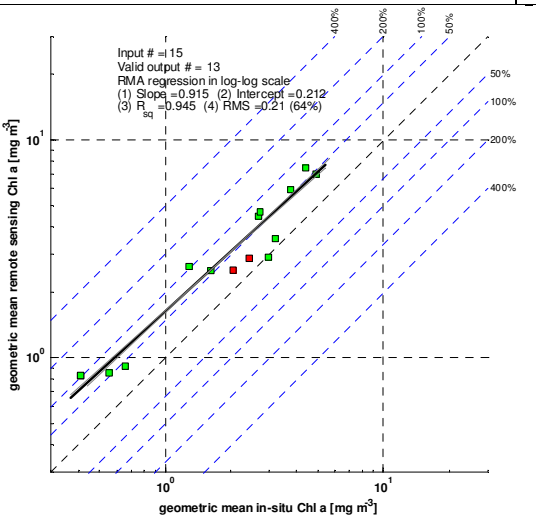


SIOP: Revampmedian2

Parameter: CHL

Year: 2006 flag settings: 1001

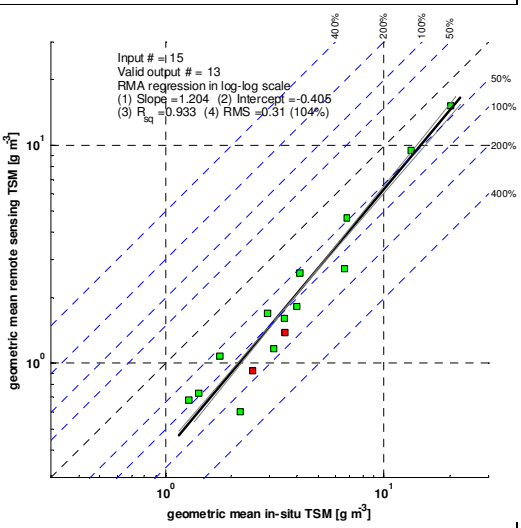


SIOP: Revampmedian2

Parameter: TSM

Year: 2006 flag settings: 1001

*Figure 2.5 Validation results for Chl-a and TSM. The yearly averaged median in-situ values at MWTL stations are compared to the median HYDROPT retrieved concentrations for each year. Processing included the REVAMP-median2 SIOP set, MEGS7.4 MERIS data and specific data screening, summarized in the flag setting.*

# 3. Further calibration of the HYDROPT algorithm: using in-situ observed data of TSM and Chl-a to optimize regional specific inherent optical properties

## 3.1 Rationale for further calibration

Evaluation of HYDROPT results (based on calibration with REVAMP SIOPs) of Chl-a and TSM by Pasterkamp et al. (2005) and Van der Woerd & Pasterkamp (2008) led to the conclusion that there are a number of errors that may influence the accuracy of the derived concentrations:

1. SIOPs vary in space and in time: It is not easy to collect a large enough dataset to cover all these variations for the North Sea.
2. The measurements of SIOPs are quite difficult and prone to errors.
3. There may be systematic and random errors in the satellite observations, mainly due to inaccurate atmospheric correction; leading to bias errors and spectral errors if wrong aerosol types were used. Bias errors can also be introduced if the atmospheric correction procedure assumes zero absorption by the water surface at the red/Nir wavelengths.
4. There may also be errors in the in-situ data used for validation of the satellite results leading to an erroneous estimate of the actual accuracy.
5. There may be errors introduced by the inaccuracies in the HydroLight code itself, the definition of SIOPs, or from the assumptions made in building the LUT from HydroLight simulations.

The fact that it seems difficult to obtain a true representative estimate of the synoptic long-term true SIOPs by field measurements, leads to the conclusion that alternative ways to obtain such representative estimate should be looked for. Since there is ample evidence of systematic errors in the atmospheric correction of MERIS and MODIS observations of case-2 waters it makes sense to design a procedure that calculates optimized (synthetic) SIOPs from these observations to compensate for these errors to some extent.

Early attempts to estimate the SIOPs from observed spectra and observed concentrations are described in the work of Hoogenboom et al. (1998) and Pasterkamp (1999). In the OPMOD study (Pasterkamp, 1999) it was concluded that retrieval of all SIOPs simultaneously from single sets of observations of reflectance and concentrations requires very accurate spectra, otherwise the shape of the retrieved SIOPs becomes unrealistic, due to the fact that multiple solutions may be possible. Therefore any a priori knowledge about the shape of the SIOP functions should be superimposed in these calculations. In the OPMOD study linearized versions of the Gordon model were used to obtain estimates for SIOPs from reflectance and concentrations measurements. To solve the system of equations, relative simple matrix inversion techniques were used.

### 3.2 Method of optimizing HYDROPT for MWTL data

Pasterkamp et al. (2005) describe a new procedure of SIOP retrieval based on the HYDROPT non-linear algorithm. The aim of this approach is to make the forward model of HYDROPT perform optimally for MERIS observations of the Dutch coastal waters. They propose to calculate SIOPs from in situ-observed water quality parameters CHL and TSM as observed on the Dutch monitoring network (MWTL). This procedure uses an optimisation approach whereby in a number of steps the difference between yearly averaged in-situ CHL and TSM concentrations on MWTL stations and yearly averaged (yearly geometric mean) remote sensing CHL and TSM on MWTL stations is minimised. During the process of fitting remote sensing estimates to in-situ estimates the calibration dataset (SIOPs) is varied until the best similarity in CHL and TSM is achieved (See Figure 3.1).

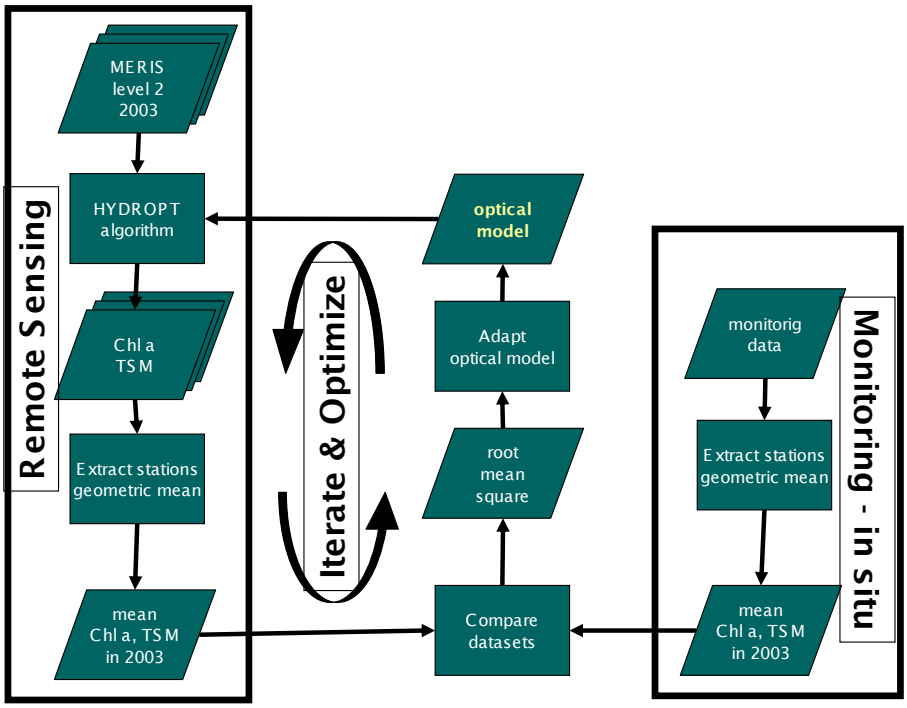


*Figure 3.1 Procedure to derive synthetic SIOPs from mapping remote sensing results on in-situ observations (Van der Woerd and Pasterkamp, 2005).*

A three component model (Chl-a, TSM and coloured dissolved organic matter (CDOM)) was thought to be sufficient to explain the optical domain of the North Sea without creating overlapping SIOP ('overtraining'). The solution space was further limited by fixing the absorption of bleached particulate matter and the absorption of dissolved matter to an exponential function (with varying slope) of wavelength ($\lambda$), and setting the scattering of CDOM and Chl-a to zero.

This procedure leads to synthetic SIOPS that may be quite different from in-situ observed values, partly because the optimisation procedure also compensates for (systematic) errors in the remote sensing observations (e.g. due to errors in the atmospheric correction). This procedure was shown to give good results for the year 2003 (Pasterkamp et al., 2005) but its results could only be checked using the same in-situ data that

was used for the optimisation. The results of the analysis of yearly geometric means for Dutch monitoring stations are shown in Figure 3.2. The green squares represent the yearly geometric mean (labelled 'median', because the geometric mean is an estimator for median when the underlying distribution is log-normal) for the Chl-a and TSM for each measurement station.

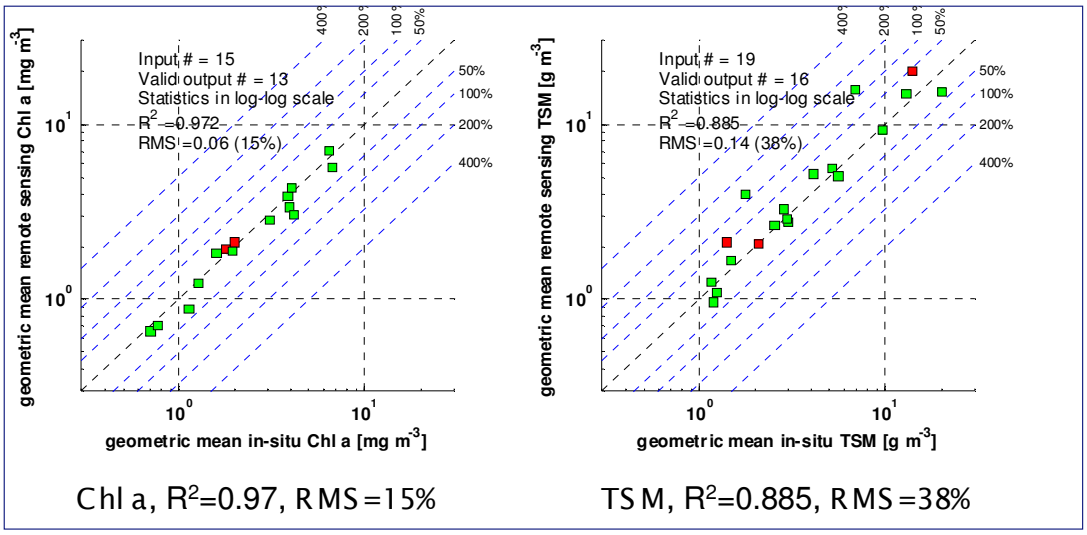


*Figure 3.2 From Pasterkamp et al., (2005). Evaluation of the optimised results using synthetic SIOPs derived from 2003 data*

In the calculation of the MERIS concentration values the following properties / criteria / flags were applied:

| | |
|---|---|
| MERIS processing version | MEGS 7.0 |
| PCD-1-13 flag applied | YES |
| High glint flag applied | YES |
| Negative values screening | NO |
| Maximum values screening | NO |
| Spectral bands allowed | B1-7 + B9 |
| -log(P) screening | No |

Compared to the results for measured SIOPs (Figure 2.) there is a significant improvement in the bias of Chl-a and TSM results. The relative root-mean square difference (RMS) between remote sensing and in-situ decreases to 15% and 38%, and the correlation coefficient increases to 0.97 and 0.87 for Chl-a and TSM, respectively. Part of the residual errors can be attributed to the statistical uncertainty in the geometric mean, possibly caused by in-situ data under-sampling and temporal heterogeneity in the remote sensing results.

This exercise shows well the removal of systematic offsets between both datasets, as the algorithm now performs well for low and high ranges of chlorophyll-a. Considering the fact the RMS includes the effect of atmospheric correction errors, scale differences and temporal differences (i.e. the temporal distribution of measurement over the year for in situ and remote sensing can be slightly different), the effective RMS error of 15% is probably the best that can be achieved under these circumstances.

Since independent validation of the results was not possible using only the 2003 data it was decided that in this study the validation of the stability of the procedure should be tested for subsequent years, based on the latest ESA MERIS processing (MEG 7.4).

# 4. Upgrading the optimisation results for MEGS 7.4 data: consistency checks on performance of the optimised calibration

## 4.1 Changes in the MERIS reflectance between MEGS7.0 and MEGS7.4

Between the study of Pasterkamp et al. (2005) and the OVATIE-2 project the MERIS atmospheric and products processor was upgraded from version MEGS7.0 to version MEGS7.4. The effect on observed MERIS spectra is illustrated in Figure 4.1 by a series of match-up comparison, as presented by Peters (2006):

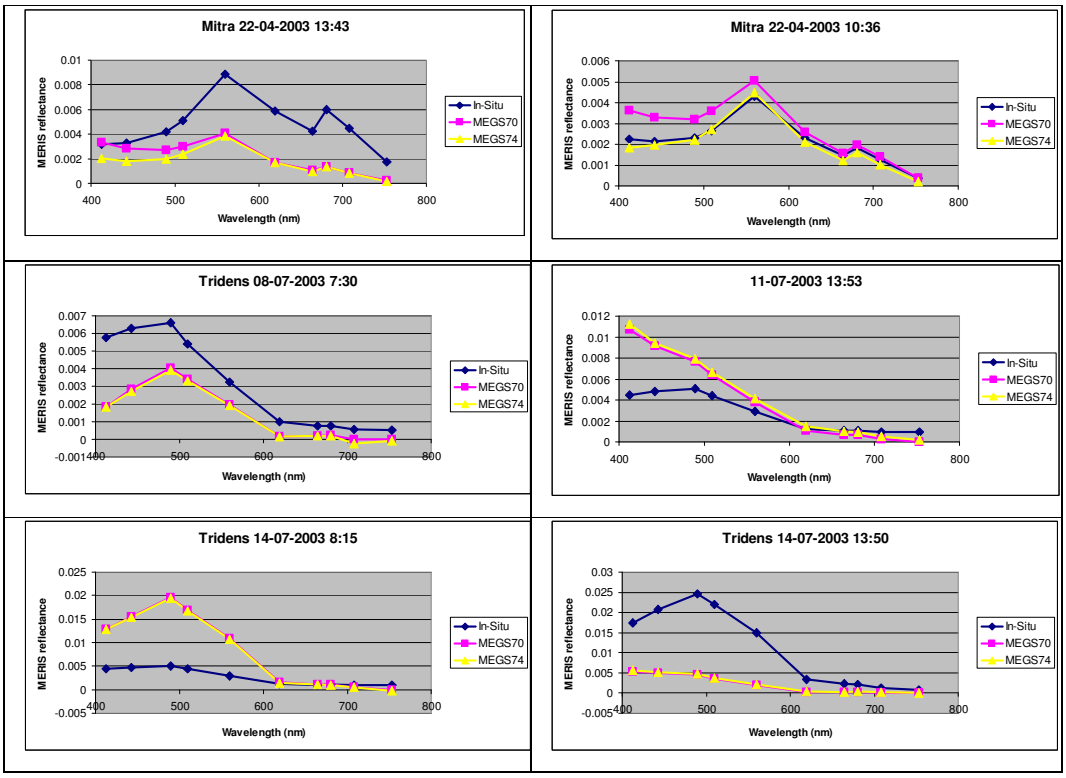


*Figure 4.1 Spectral observations from the RV Mitra and RV Tridens cruises. The Mitra cruise is relatively close to the coast; the spectrum is influenced by relatively high concentrations of TSM, CDOM and Chlorophyll-a. The matchup spectral observations on the Tridens cruise are all in open North Sea water, with relatively low concentrations of Chlorophyll-a only.*

Analyzing the near coastal water spectra of the Mitra cruise it seems that MEGS7.4 processing causes lower values in the blue-green spectral range but the number of observations is too small to draw firm conclusions. When looking at open water spectra (the Tridens series) there are few changes between MEGS7.0 and MEGS7.4. Because there is a variety of differences in again the blue-green spectral range (large over- and underestimations) between in-situ observations and the MERIS reflectance it is not clear how to

interpret the match-up results**.** **(**NB: *Matchup spectra were used only if the PCD_1_13 flag was not raised)***.**

## 4.2 Recalculation of the optimized synthetic SIOPs for MEGS7.4 for 2003

One of the objectives of this project was to recalculate the synthetic SIOPs for 2003 for MEGS7.4 version MERIS data, because of the changes in reflectance data (Level-2) delivered by ESA. Since the optimization procedure compensates for systematic errors in the MERIS reflectance, it also is sensitive to systematic changes in these reflectances. This illustrates nicely one of the strong points of the optimization approach. When MERIS processing versions change, it is always possible to accommodate the HYDROPT calibration by recalculation of the optimized SIOPs. In this way, long and consistent time series can be build, always based on state of the art atmospheric correction for the whole of the series.

Using the same procedures as Pasterkamp et al., 2005 the following results were obtained for the 2003 data (Figure 4.2). Note that some of the stations (15) have a very limited number of observations (red squares). These stations are plotted but not taken into account in the least-square fit.

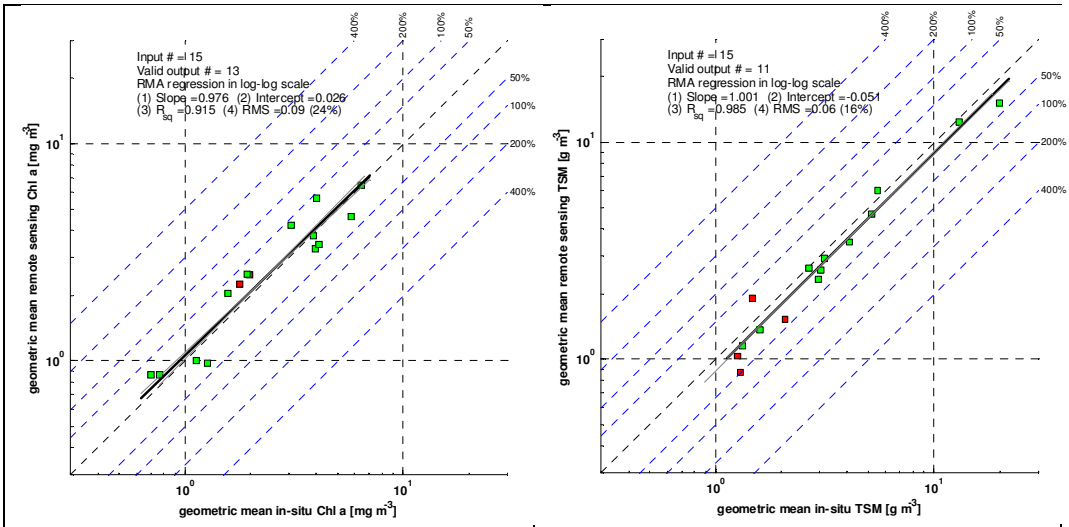


| | |
|---|---|
| SIOP: MatlaboptimisedMEGS74-2003<br>Parameter: CHL<br>Year: 2003 flag settings: 1001 | SIOP: MatlaboptimisedMEGS74-2003<br>Parameter: TSM<br>Year: 2003 flag settings: 1001 |

*Figure 4.2 Comparison of 2003 annual geometric mean values of Chl-a and TSM as observed in-situ on MWTL monitoring stations and derived from HYDROPT MERIS observations at MWTL locations. (SIOPs optimized for MEGS7.4 data)*

It is interesting to observe that the change from MEGS7.0 to MEGS7.4 improves the retrieval of TSM from the re-optimised algorithm. Since TSM and Chl-a are solved simultaneously by HYDROPT this has some consequences for the Chl-a retrieval of which the correlation coefficient has decreased a fraction compared to the MEGS7.0

result. Still the RMS values between in-situ data and satellite results are much lower as compared to the results from REVAMP calibrated HYDROPT runs.

For the calculation of the synthetic SIOPs the same strict data screening settings were applied as in Pasterkamp et al. (2005):

| | |
|---|---|
| MERIS processing version | MEGS 7.4 |
| PCD-1-13 flag applied | YES |
| High glint flag applied | YES |
| Negative values screening | NO |
| Maximum values screening | NO |
| Spectral bands allowed | B1-7 + B9 |
| -log(P) screening | No |

This MatlaboptimisedMEGS74 SIOP calibration dataset, based on the MERIS MEGS 7.4 data of 2003, was used for the operational NRT processing of 2006 and 2007 MERIS data for early warning for HABs.

Note that for the check on the performance of the calibration (Figure 4.2) more data were allowed by the data screening in order to evaluate the performance under operational conditions:

| | |
|---|---|
| MERIS processing version | MEGS 7.4 |
| PCD-1-13 flag applied | NO |
| High glint flag applied | NO |
| Negative values screening | YES |
| Maximum values screening | YES |
| Spectral bands allowed | B1-7 + B9 |
| -log(P) screening | YES |

# 5. Testing the stability of the MEGS7.4 calibration for 2004, 2005 and 2006 data

An important question of RWS to the OVATIE-2 project team was to test the stability of the MEGS7.4 2003 calibration for subsequent years. Calibration on one year of MWTL observation data might result in too specific SIOPs valid only for e.g. certain algae types only occurring in that year. Or there may be year to year variability of SIOPs caused by differences in algal species composition, silt composition etc., which might lead to unrealistic concentration retrievals. The results of the test are given in Figure 5.1, Figure 5.2 and Figure 5.3. In all cases the following data screening settings were used:

| | |
|---|---|
| MERIS processing version | MEGS 7.4 |
| PCD-1-13 flag applied | NO |
| High glint flag applied | NO |
| Negative values screening | YES |
| Maximum values screening | YES |
| Spectral bands allowed | B1-7 + B9 |
| -log(P) screening | YES |

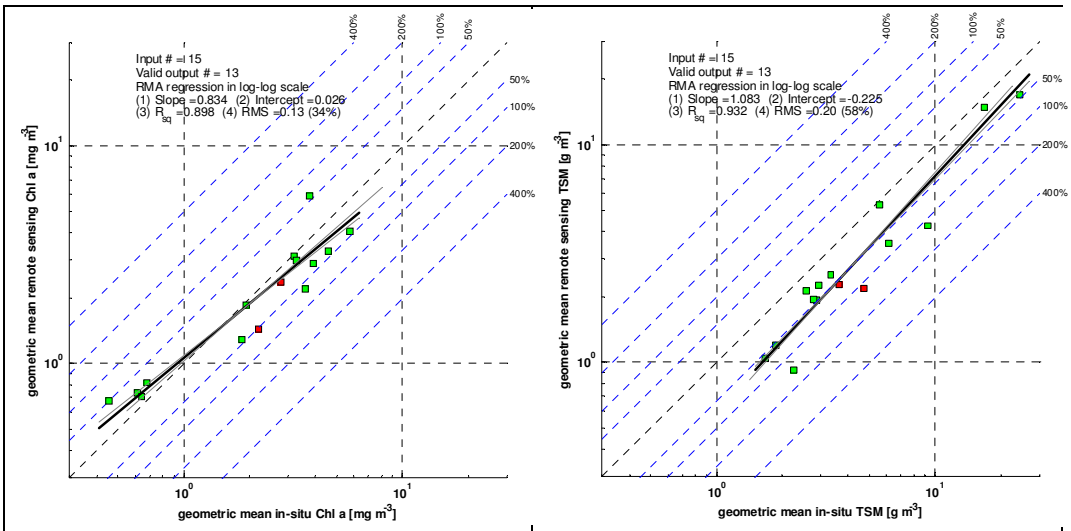


| | |
|---|---|
| SIOP: MatlaboptimisedMEGS74-2003<br>Parameter: CHL<br>Year: 2004 flag settings: 1001 | SIOP: MatlaboptimisedMEGS74-2003<br>Parameter: TSM<br>Year: 2004 flag settings: 1001 |

*Figure 5.1 Comparison of 2004 annual geometric mean values of Chl-a and TSM as observed in-situ on MWTL monitoring stations and derived from HYDROPT MERIS observations at MWTL locations. (SIOPs optimized for MEGS7.4 data)*

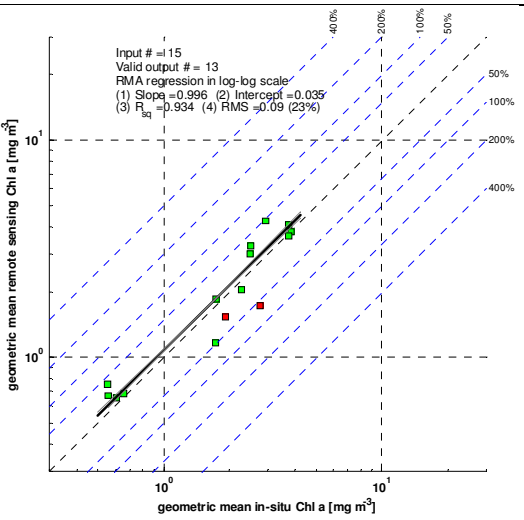


SIOP: MatlaboptimisedMEGS74-2003

Parameter: CHL

Year: 2005 flag settings: 1001

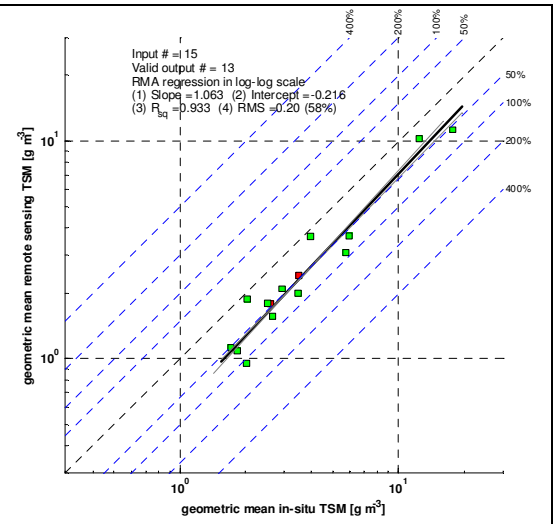


SIOP: MatlaboptimisedMEGS74-2003

Parameter: TSM

Year: 2005 flag settings: 1001

*Figure 5.2 Comparison of 2005 annual geometric mean values of Chl-a and TSM as observed in-situ on MWTL monitoring stations and derived from HYDROPT MERIS observations at MWTL locations. (SIOPs optimized for MEGS7.4 data).*

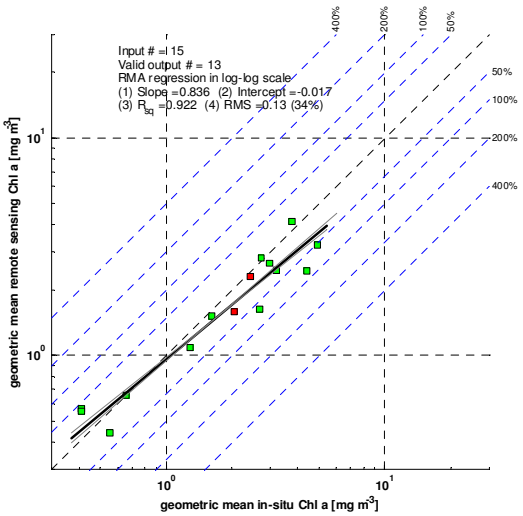


SIOP: MatlaboptimisedMEGS74-2003

Parameter: CHL

Year: 2006 flag settings: 1001

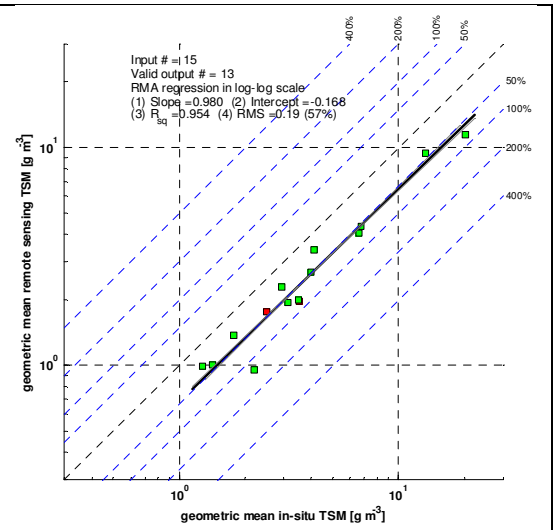


SIOP: MatlaboptimisedMEGS74-2003

Parameter: TSM

Year: 2006 flag settings: 1001

*Figure 5.3 Comparison of 2006 annual geometric mean values of Chl-a and TSM as observed in-situ on MWTL monitoring stations and derived from HYDROPT MERIS observations at MWTL locations. (SIOPs optimized for MEGS7.4 data).*

Figure 5.1 shows that in 2004 the 2003-calibrated SIOPs perform reasonable for Chl-a and somewhat worse (bias) for TSM retrievals. This is partially due to the fact that 2004 had prolonged cloudy periods during the spring bloom period (see chapter 7). Figure 5.2 shows that in 2005 the 2003-calibrated SIOPs again perform reasonable for Chl-a and somewhat worse (negative bias) for TSM retrievals. Figure 5.3 shows that in 2006 the 2003-calibrated SIOPs again perform reasonable for Chl-a and somewhat worse (negative bias) for TSM retrievals.

Overall, one may conclude from this stability test that Chl-a retrieval based on 2003 MEGS7.4 optimised SIOPs is relatively stable with a small tendency for overestimation of low values and underestimation of high values in 2004 and 2006. TSM retrieval behaves quite stable between the years 2004-2005-2006; but they all have a bias of approximately minus 0.2 in log-log space.

Despite of the calculation of the correlation in log-log space, the correlation coefficient and hence also the optimization results for Chl-a are probably still quite influenced by 2 or 3 stations that have overall very low Chl-a concentrations (open water stations). The correlation coefficient of TSM, however, is markedly influenced by 2 stations with overall high values (near coastal stations).

Based on these results it was decided to do an extensive test in which HYDROPT is calibrated subsequently on each year (2003, 2004, 2005 or 2006) and tested for stable performance in all years. In this way it is attempted to find the SIOP set that is most representative for the inter-annual variability over MWTL stations.

However, before engaging in this experiment it was considered important to study the effect of two major influences on the result of this experiment, namely:

1. Data screening methods (Chapter 6);
2. The availability of MWTL and remote sensing results (Chapter 7).

# 6. Data screening methods for pixel selection

## 6.1 Introduction: data screening for operational use

Besides obtaining high accuracy results for MERIS and MODIS, the operational embedding of the resulting CHL and TSM data in the monitoring of RWS poses some additional constraints on the tuning procedure (finding the optimal calibration SIOP set). Operational use requires well documented procedures, algorithms and calibration datasets ensuring reproducibility of the procedure. The operational processing should also contain transparent quality control mechanisms. It was voiced by RWS during this project that, for operational use, quality control mechanisms should be installed in such a way that:

- They allow a maximum yield of observations with acceptable to high quality.
- They provide ways to discard obviously erroneous results without omitting extreme but still realistic values which may represent important conditions such as sand mining activities e.g.

Quality control procedures can operate at two different levels for HYDROPT optimisation:

- They can be used to select observations that may participate in the determination of the optimal calibration.
- They can be used to select results that can be presented in the outcome maps.

In practice there can be a decoupling of data screening methods for the first step (tuning of HYDROPT) and the second step (presentation of the results). Applying very strict data screening methods in the first step could prevent "pollution" of the resulting optimal synthetic SIOPs. But, since strict data screening might lead e.g. to omission of many winter observations, it might also lead SIOPs that are less representative for the whole year.

Both data screening methods were tested, in order to investigate the consequences of both strategies. Before discussing the results of this testing, first the data screening methods are described in more detail. Data screening methods can be based on:

A priori data selection methods: "does the input make sense"?

- The inherent quality of the spectral observations;
- Additional quality indicators (data quality flags) provided by the data provider (which is ESA in the case of MERIS and NASA in the case of MODIS) are based on intermediate results in the processing from raw detector counts to water-leaving radiance products.

A posteriori data selection methods: "does the output make sense"?

- Quality indicators based on the HYDROPT processing results.

ESA and NASA have developed complicated procedures to either compensate for a number of effects on spectra, or to develop flags that indicate the inferior quality of spectra as a result of identified problems (see next paragraph). Unfortunately, the quality

screening and compensation algorithms are not identical leading to different flags for both sensors. For operational purposes this is a handicap because it is impossible to apply identical data screenings based on ESA and NASA flags. An additional problem attached to the use of standard flags (especially the ESA PCD-1-13 flag) is that they may be too strict. As a result many (sometimes to 50%) of the data are screened out while visual analysis of HYDROPT results shows that there was no obvious degradation of the spectra and the resulting concentrations.

Therefore ample attention was paid in this project to develop and test additional data screening methods based on alternative and generic a priori and a posteriori criteria.

## 6.2 A priori data screening methods based on quality of spectral observations

Atmospheric correction of spectra observed by sensors like MERIS and MODIS normally leads to water reflectance spectra of reasonable quality. There are some major disturbances that may not be treated completely by standard atmospheric correction procedures:

- Aircraft contrails and thin cirrus clouds ;
- Cloud shadows (mainly a problem at low solar angles) ;
- Wave tips (white foam);
- Floating layers of algae (seen as land vegetation).

There also some situations that sometimes are not corrected adequately:

- Waters with extremely high sediment loads may be flagged as being “land”;
- Aerosols that differ from the standard catalogue of aerosols may cause errors in the retrieved reflectance spectra.

Also of consequence, but often unmentioned: the presence of highly reflecting surfaces on ships during the taking of matchup pixels.

During the course of this OVATIE-2 study it was found that obviously erroneous results of HYDROPT can be attributed to

- Spectra with one or more negative values;
- Spectra with more than two zero values in wavelengths shorter than 750 nm;
- Spectra with one or more unrealistically high values (>0.3).

These criteria were subsequently used as data screening for all further analysis

## 6.3 Comparison of MERIS and MODIS AQUA bands and quality control flags

MERIS and MODIS-AQUA have comparable spectral band settings with some differences: the MERIS band-pass function is a block-shaped function, while the MODIS band-pass function has the shape of a normal distribution. Band widths at Full Width Half Maximum are approximately the same for most bands (see Table 6.1). Due to these

differences MERIS probably observes the Chl-a absorption maximum around 666 nm more accurately.

*Table 6.1 Comparison of MERIS and MODIS spectral band characteristics*

| AQUA band No. | Name in file | AQUA width[1] | AQUA Centre wave-length[2] | MERIS band No. | Name in file | MERIS Centre +width[3] | MERIS Detector averaged centre wave-length[4] | MERIS Detector av-eraged centre wavelength[5] |
|---|---|---|---|---|---|---|---|---|
| **8** | **412** | **405-420 (15)** | **412.5** | **1** | **412** | **412.5 (10)** | **412.3** | **412.7** |
| **9** | **443** | **438-448 (10)** | **442.2** | **2** | **442** | **442.5 (10)** | **442.3** | **442.6** |
| **10** | **488** | **483-493 (10)** | **487.4** | **3** | **490** | **490 (10)** | **489.7** | **489.9** |
| **11** | **531** | **526-536 (10)** | **530.1** | **4** | **510** | **510 (10)** | **509.6** | **509.7** |
| **12** | **551** | **546-556 (10)** | **547.2** | **5** | **560** | **560 (10)** | **559.5** | **559.8** |
| | | | | **6** | **620** | **620 (10)** | **619.4** | **619.6** |
| **13** | **667** | **662-672 (10)** | **666.0** | **7** | **665** | **665 (10)** | **664.3** | **664.6** |
| 14 | 678 | 673-683 (10) | 677.6 | 8 | 681 | 681.25 (7.5) | 680.6 | 680.9 |
| | | | | **9** | **709 *** | **708.75 (10)** | **708.1** | **708.3** |
| **15** | **748** | **743-753 (10)** | **746.8** | 10 | 754 | 753.75 (7.5) | 753.1 | |
| | | | | 11 | 760? | 760.625 (3.75) | | |
| | | | | 12 | 778? | 778.75 (15) | | |
| 16 | 869 | 863-877 (15) | 866.9 | 13 | 865 | 865 (20) | 778.15 | |
| | | | | 14 | 885 | 10 | 864.6 | |
| | | | | 15 | 900 | 10 | | |

Sources:

[1] http://modis.gsfc.nasa.gov/about/specifications.php

[2] http://oceancolor.gsfc.nasa.gov/DOCS/RSR/spectral_response_comp.html

[3] Meris Product handbook Table 1.1, http://www-loa.univ-lille1.fr/simbadA/MAVT2003_proc_val_2003.pdf

[4] http://envisat.esa.int/workshops/mavt_2003/MAVT-2003_801_MERIS-protocols_issue1.3.5.pdf

[5] HYDROPT setting (Pasterkamp et al., 2005)

[*] Variants 705-708-715

A distinctive advantage of MERIS over MODIS for case-2 water remote sensing is the presence of the 709 nm band, which is essential for high quality Chl-a mapping in CDOM and TSM rich waters (see. e.g. Gons et al., 2002).

A summary of the multiple flags that are defined by ESA (ESA, 2002) and NASA (NASA, 2007) is given in the Tables 6.2 and 6.3.

ESA guarantees good quality spectra if spectra pass the PCD-1-13 flag. This means amongst others that the spectra do not have negative values, they are not saturated and they are not affected by high glint. Especially this last criterion makes the flag often too strict. This is because the occurrence of high glint is calculated from geometry, while in reality the glint-affected area is usually much smaller. Therefore, for operational processing in Dutch waters this flag has been discarded. Another handicap in using this flag is the fact that there is no MODIS-AQUA flag of the same definition. Partly this is because MODIS is much less influenced by glint because of the tilted sensor.

*Table 6.2 MERIS Product Confidence Flags, taken from the MERIS handbook (ESA, 2002)*

| Bit num. | Symbol & Description | Type | Relevant to Surface Type | | |
|---|---|---|---|---|---|
| | | | Water | Land | Cloud |
| 23 | LAND: Land product available | class | 1 | 1 | 1 |
| 22 | CLOUD: Cloud product available | class | 1 | 1 | 1 |
| 21 | WATER: Water product available | class | 1 | 1 | 1 |
| 20 | PCD_1_13: Confidence flag for MDS 1 to 13 | confidence | 1 | 1 | 1 |
| 19 | PCD_14: Confidence flag for MDS 14 | confidence | 1 | 1 | 1 |
| 18 | PCD_15: Confidence flag for MDS 15 | confidence | 1 | 1 | 1 |
| 17 | PCD_16: Confidence flag for MDS 16 | confidence | 1 | 0 | 0 |
| 16 | PCD_17: Confidence flag for MDS 17 | confidence | 1 | 1 | 0 |
| 15 | PCD_18: Confidence flag for MDS 18 | confidence | 1 | 1 | 1 |
| 14 | PCD_19: Confidence flag for MDS 19 | confidence | 1 | 1 | 1 |
| 13 | COASTLINE: Coastline flag | science | 1 | 1 | 1 |
| 12 | COSMETIC: Cosmetic flag (from level-1b) | science | 1 | 1 | 1 |
| 11 | SUSPECT: Suspect flag (from level-1b) | science | 1 | 1 | 1 |
| 10 | ABSOA_CONT: Continental absorbing aerosol | science | 1 | 0 | 0 |
| 9 | ABSOA_DUST: Dust-like absorbing aerosol | science | 1 | 0 | 0 |
| 8 | CASE2_S: Turbid water | science | 1 | 0 | 0 |
| 7 | CASE2_ANOM: Anomalous scattering water | science | 1 | 0 | 0 |
| 6 | CASE2_Y: Yellow substance loaded water | science | 1 | 0 | 0 |
| 5 | ICE_HAZE: Ice or high aerosol load pixel | science | 1 | 0 | 0 |
| 4 | MEDIUM_GLINT: Corrected for glint | science | 1 | 0 | 0 |
| 3 | DDV: Dense dark vegetation | science | 0 | 1 | 0 |
| 2 | HIGH_GLINT: High (uncorrected) glint | science | 1 | 1 | 1 |
| 1 | P_CONFIDENCE: The two pressure estimates do not compare successfully | science | 1 | 1 | 1 |
| 0 | LOW_PRESSURE: Computed pressure lower than ECMWF one | science | 1 | 1 | 1 |

*Table 6.3 MODIS quality control flags, taken from the Ocean Level-2 Data Product document (NASA, 2007)*

| Bit Set = 1 | Condition Indicated | Algorithm Name |
|---|---|---|
| 1 | atmospheric correction failure from invalid inputs | ATMFAIL |
| 2 | land | LAND |
| 3 | missing ancillary data | BADANC |
| 4 | severe Sun glint | HIGLINT |
| 5 | total radiance above knee in any band | HILT |
| 6 | satellite zenith angle above limit | HISATZEN |
| 7 | shallow water | COASTZ |
| 8 | negative water-leaving radiance in any band | NEGLW |
| 9 | stray light contamination | STRAYLIGHT |
| 10 | clouds and/or ice | CLDICE |
| 11 | coccolithophore | COCCOLITH |
| 12 | turbid, case-2 water | TURBIDW |
| 13 | solar zenith angle above limit | HISOLZEN |
| 14 | high aerosol concentration | HITAU |
| 15 | low water-leaving radiance at 555 nm | LOWLW |
| 16 | chlorophyll not calculable | CHLFAIL |
| 17 | questionable navigation (e.g. tilt change) | NAVWARN |
| 18 | absorbing aerosol index above threshold | ABSAER |
| 19 | trichodesmium | TRICHO |
| 20 | maximum iterations of NIR algorithm | MAXAERITER |
| 21 | moderate Sun glint | MODGLINT |
| 22 | chlorophyll out of range | CHLWARN |
| 23 | epsilon out of range | ATMWARN |
| 24 | dark pixel (Lt - Lt < 0) for any band | DARKPIXEL |
| 25 | sea ice in pixel (based on climatology) | SEAICE |
| 26 | navigation failure condition indicated in nav flags | NAVFAIL |
| 27 | insufficient valid neighboring pixels for epsilon filtering | FILTER |
| 28 | sea surface temperature warning flag (MODIS only) | SSTWARN |
| 29 | sea surface temperature falure flag (MODIS only) | SSTFAIL |
| 30 - 31 | spare flags | SPARE |
| 32 | clear ocean data (no clouds, land or ice) | OCEAN |

## 6.4 A posteriori criteria based on HYDROPT output

As explained in section 1.7, HYDROPT produces the standard error per pixel per parameter (TSM, Chl-a and CDOM). HYDROPT also provides a measure of the quality of the spectral fit between the simulated and the measured spectrum of a sensor (-log(P( $\chi^2$)). The advantage of these criteria is that they can be applied to any sensor.

Experience shows that the standard errors do not provide unambiguous screening of results. This is because a large standard error in a low concentration range is more likely to point to a calculation error than a large standard error in a high concentration range. Experiments to normalise the standard error with the concentration could be performed in future to see if this can be remedied.

The (-log(P($\chi^2$)) statistic has proved to be (from visual inspection) a very good discriminator between high quality and low quality input spectra and results. Therefore this data screening criterion is used in the following analysis.

# 7. Temporal variability of the in-situ and remote sensing data

## 7.1 Availability of in-situ measurements

Based on the data delivered as product in OVATIE-2 a report was published on the validation results (Uhlig et al., 2007). In this report use the same numbering of the stations to facilitate a comparison. Uhlig et al. (2007) number the MWTL stations as follows (Table 7.1):

*Table 7.1 Station name, distance to shore [in km], abbreviation and code for 17 North Sea stations*

| Station name | Distance to shore [km] | abbreviation | Code |
|---|---|---|---|
| Goeree 6 km uit de kust | 6 | GOERE6 | 1 |
| Noordwijk 2 km uit de kust | 2 | NOORDWK2 | 2 |
| Noordwijk 10 km uit de kust | 10 | NOORDWK10 | 3 |
| Noordwijk 20 km uit de kust | 20 | NOORDWK20 | 4 |
| Noordwijk 70 km uit de kust | 70 | NOORDWK70 | 5 |
| Rottumerplaat 3 km uit de kust | 3 | ROTTMPT3 | 6 |
| Rottumerplaat 50 km uit de kust | 50 | ROTTMPT50 | 7 |
| Rottumerplaat 70 km uit de kust | 70 | ROTTMPT70 | 8 |
| Terschelling 4 km uit de kust | 4 | TERSLG4 | 9 |
| Terschelling 10 km uit de kust | 10 | TERSLG10 | 10 |
| Terschelling 100 km uit de kust | 100 | TERSLG100 | 11 |
| Terschelling 135 km uit de kust | 135 | TERSLG135 | 12 |
| Terschelling 175 km uit de kust | 175 | TERSLG175 | 13 |
| Terschelling 235 km uit de kust | 235 | TERSLG235 | 14 |
| Walcheren 2 km uit de kust | 2 | WALCRN2 | 15 |
| Walcheren 20 km uit de kust | 20 | WALCRN20 | 16 |
| Walcheren 70 km uit de kust | 70 | WALCRN70 | 17 |

Figure 7.1 and Figure 7.2 illustrate the temporal variability of the data. Figure 4.1 provides an overview for 15 years of MWTL monitoring (1992-2006). In Figure 7.2 the availability of observations for each months of the year are plotted. These figures show that the availability of Chl-a measurements is not the same at all MWTL stations. Data of locations NOORDWK20 (4), NOORDWK70 (5), ROTTMPT3 (6), ROTTMPT50 (7), ROTTMPT70 (8), WALCRN2 (15) and WALCRN20 (16) are only available for selected periods. Station 3 (NOORDWK10) has an exceptionally high data density.

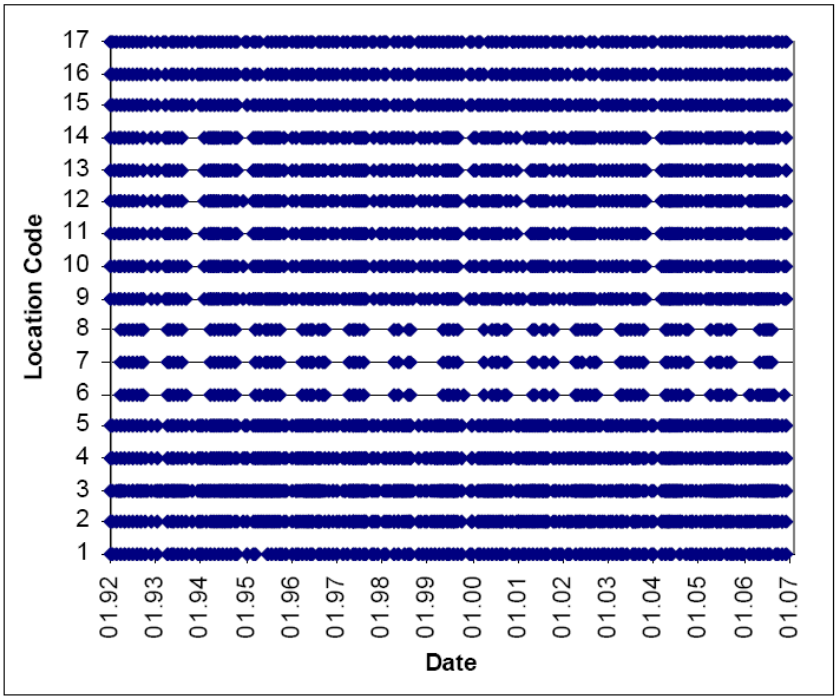


*Figure 7.1 The temporal distribution of Chl-a measurements at MWTL stations from 1992 to 200 (copied from Uhlig et al., 2007)*

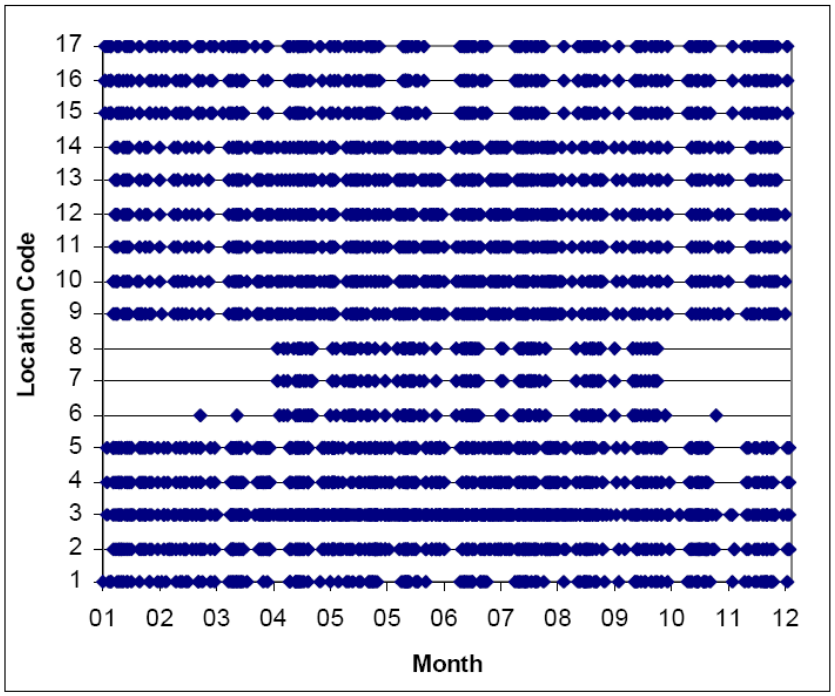


*Figure 7.2 The monthly availability of Chl-a at MWTL stations (copied from Uhlig et al., 2007)*

## 7.2 Availability of MERIS results at MWTL locations

From the MERIS results delivered as result of this OVATIE-2 project a graph was made with the number of valid observations per 4 years (2003-2006) and the arithmetic mean Chl-a and TSM concentrations over these 4 years (Figure 7.3).

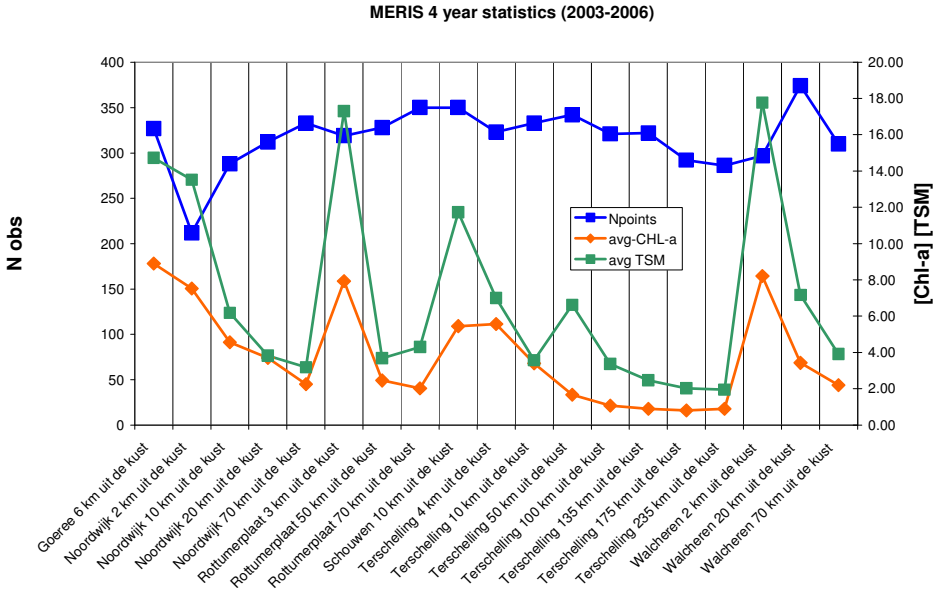


*Figure 7.3 Availability of valid MERIS observations at MWTL locations together with the 4-year mean value of observed Chl-a and TSM*

Figure 7.3 shows that the overall availability of valid MERIS observations is between 300 and 350 data points in 4 years, which are on the average about 80 data points per year, much higher in frequency than the MWTL coverage (3 – 18 times per year). The orbit of the MERIS instrument determines that the Dutch coastal zone is only visible 2 out of 3 days, which leads to 243 out of 365 days in a year. The average cloud coverage is 55% in the Netherlands. Therefore we expect that the sea surface is on average visible for 45% of 243 days = 109 days per year.

There is a distinct correlation between mean Chl-a and TSM with the distance to coast-line (see also Eleveld et al., 2008). This is illustrated in Figure 7.4, which shows that there is a nice linear correlation between log(Chl-a) and log(distance) ($R^2 = 0.91$) and a somewhat lesser but still significant linear correlation between log(TSM) and log(distance) ($R^2 = 0.78$). When looking at the residuals from the regression of Chla- and TSM as illustrated by Figure 7.5 it seems that Goeree6, Noordwijk20, Schouwen10, Ter-schelling 4, 10 and 50 deviate most from the model. Other factors than the proximity to the coast probably also determine the TSM concentration at these locations.

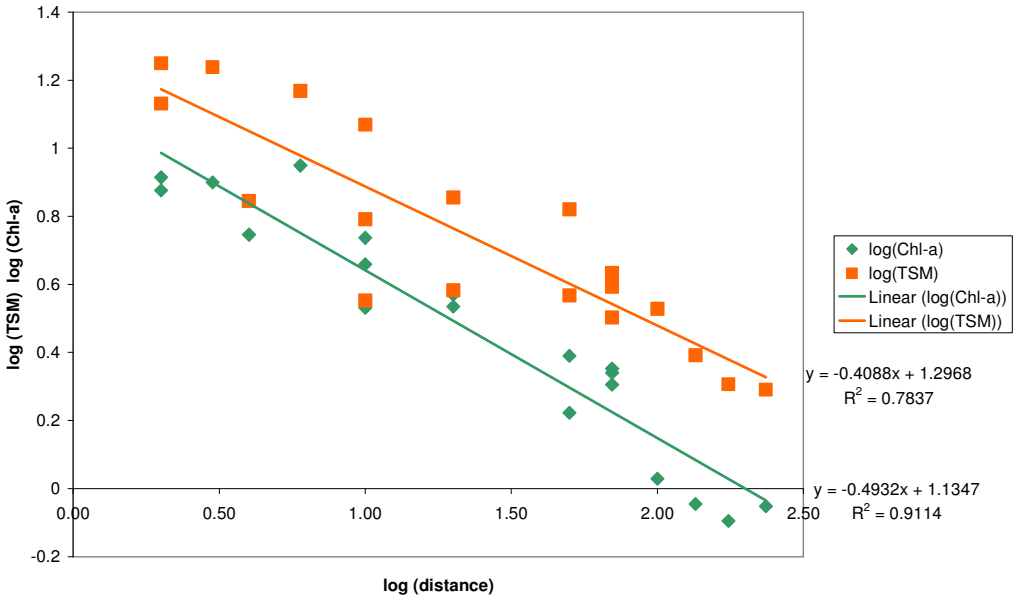


*Figure 7.4 Linear relationships between 4-year mean log(Chl-a), log(TSM) and log(distance)*

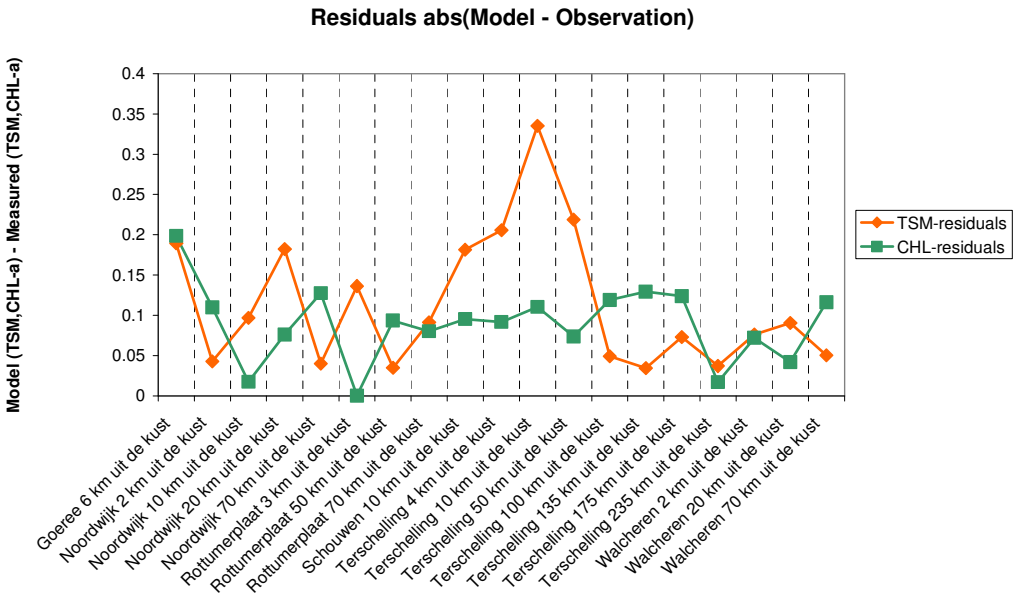


*Figure 7.5 Residuals between MERIS based modelled log(TSM) and log(Chl-a) and MWTL based observed log(TSM) and log(Chl-a) (as 4 years averages)*

## 7.3 Availability of MERIS results per month and per year

The monthly availability of valid MERIS observations is quite variable, mainly related to cloudiness (Figure 7.6). Therefore, it is not surprising to see that the lowest number of observations is in December. The maximum number of valid observations occurs in April and May and not in summer.

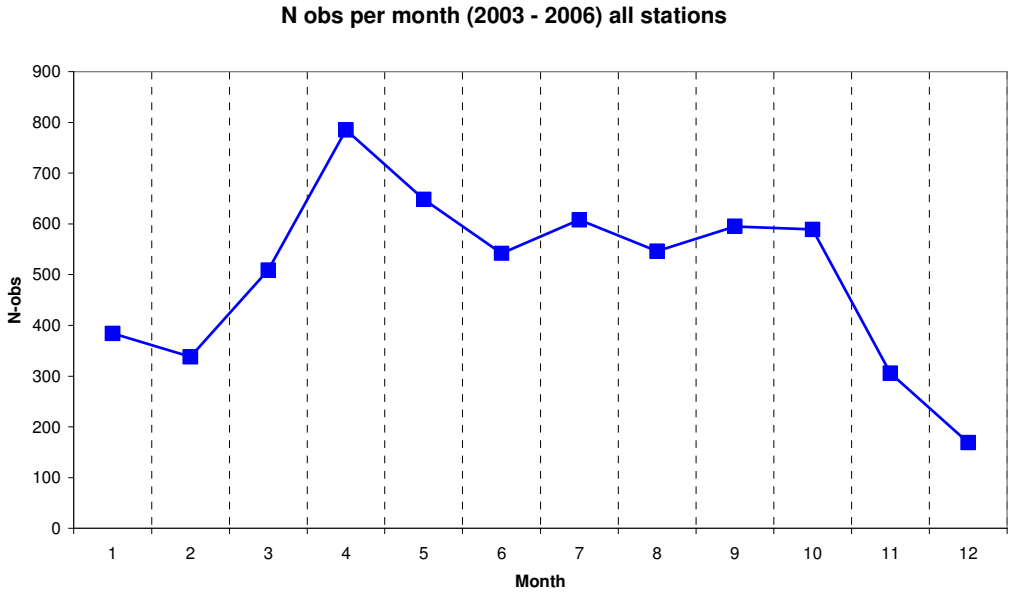


*Figure 7.6 Monthly availability of valid MERIS observations summed over all stations over 4 years*

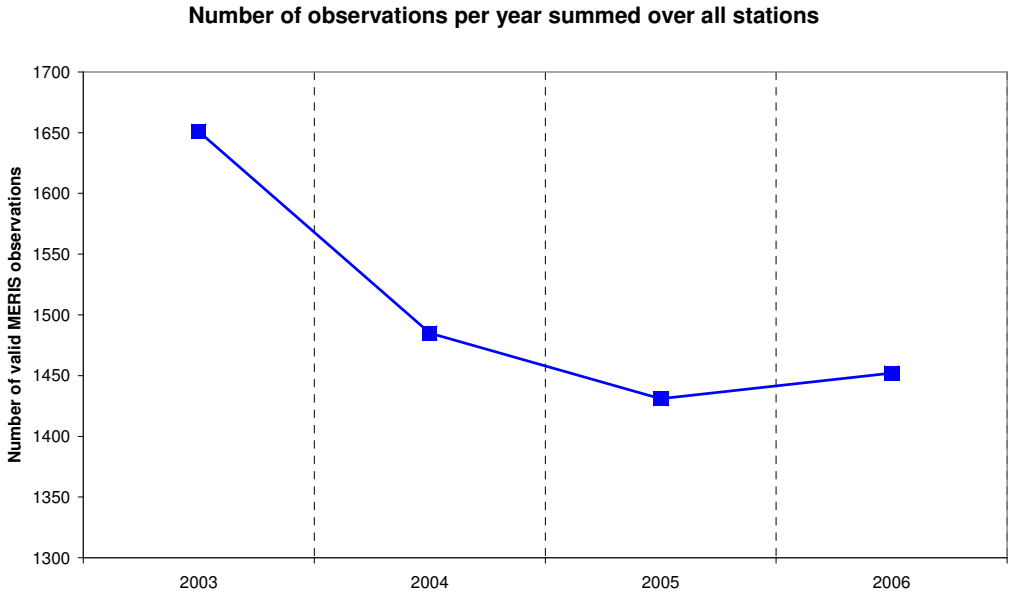


*Figure 7.7 Summation of the number of valid MERIS observations per year over all stations*

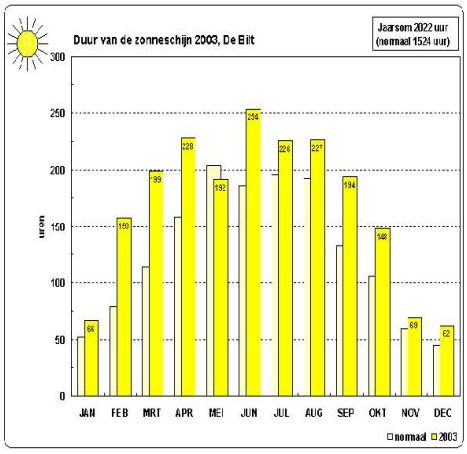


Fig 7.8.1 Monthly insolation in 2003

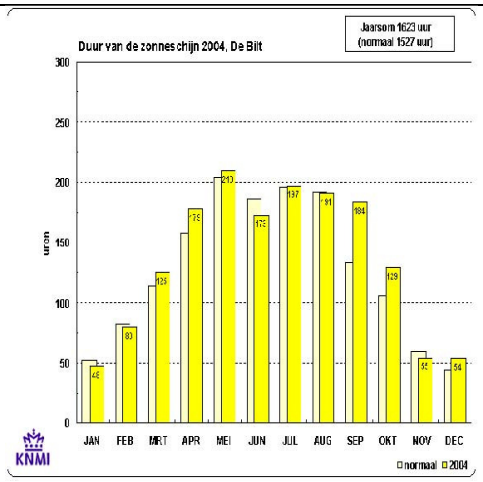


Fig 7.8.2 Monthly insolation in 2004

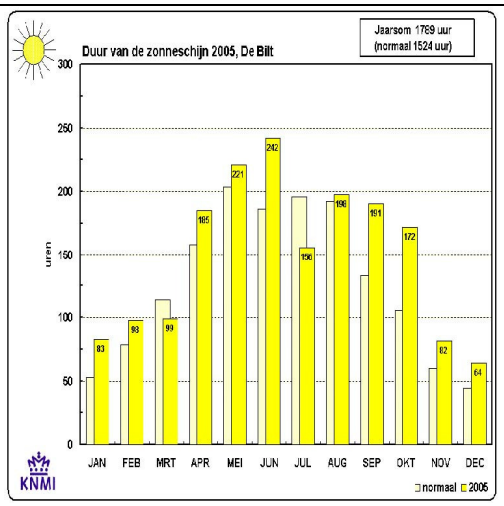


Fig 7.8.3 Monthly insolation in 2005

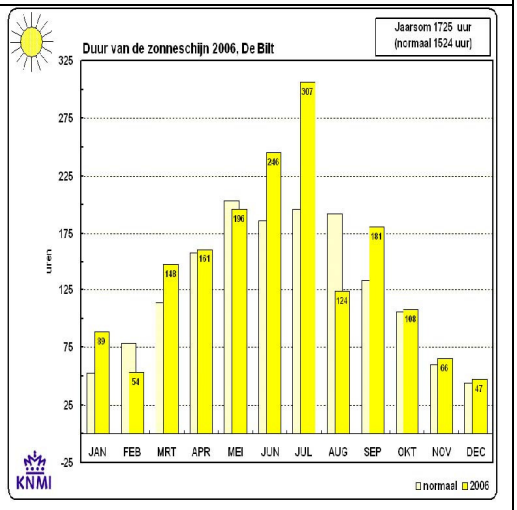


Fig 7.8.4 Monthly insolation in 2006

*Figure 7.8 Monthly insolation (taken from KNMI website) for 2003-2006*

Figure 7.7 shows that the year 2003 featured the highest surface coverage, while the year 2005 has the lowest surface coverage. In order to understand the consequences of surface coverage to the timing and height of the Chlorophyll-a peak in Spring it is illuminating to look at the monthly insolation graphs as published by KNMI (Figure 7.8). Insolation is a measure of solar radiation energy received on a given surface area in a given time. Although it is commonly expressed as average irradiance in watts per square meter ($W/m^2$), the graphs give an approximate number: the total hours of direct sunshine per month.

Figure 7.8.1-4 show that 2003 indeed received far more sunshine per month than the long term means. Since there was a large excess of sunshine in February, March and April, the spring blooms in 2003 started early, had long durations and high peak values. 2004 had a more than normal amount of sunshine in September and October and slightly above normal values in spring leading to low peak values for the spring bloom. The pattern of sunshine in 2005 is similar to 2004, again with excess values of sunshine only in September and October. The year of 2006 was different in the sense that spring sunshine was average to low, resulting in little blooming activities in spring. But the amount of sunshine in June and July was very high, resulting in a relatively large amount of summer data and also in a late, not too high but clearly discernible summer bloom.

Conclusions of the temporal distribution analysis:

- All stations are visible to MERIS with a frequency of about 80 observations per year.
- The lowest availability of MERIS observations is at Noordwijk 2.
- In-situ data are unevenly distributed per station: some stations are under sampled in winter.
- In general the availability of MERIS observations is highest in April and May and lowest in December.
- The year 2003 showed a higher data availability than the other 3 years.
- The temporal distribution of sunshine hours per month is very variable per year leading to large or minute spring blooms and sometimes to summer blooms.

# 8. Optimal calibration for HYDROPT for 2003-2006 for all MWTL stations

## 8.1 General approach

One the most important aims of the OVATIE-2 study is to calculate the optimal calibration for application over longer terms and for the whole of the Dutch EEZ of the North Sea. Given the techniques devised by R. Pasterkamp and outlined in section 3.2, it is possible to calibrate HYDROPT on any reasonably sized subset of in-situ observations. In theory it would be possible to calibrate the algorithm per season, or per month or per event (e.g. a *Phaeocystis* bloom). It would also be possible to calibrate the algorithm for each period (year) separately in order to obtain always the best fit with the in-situ data. This would however compromise the predictive capability of the algorithm since this type of calibrations can only take place on historical data. One other reason not to do this lies with the fact that independent data is required to validate the calibration. Therefore a rather straightforward approach to calibration/validation was chosen, whereby MWTL measurements collected in one calendar year were used to calibrate the algorithm with. The other 3 years, out of the 4 years of data (2003-2006), were used for validation and to test the stability of the calibration.

During the development of the most appropriate calibration validation strategy a number of questions needed to be answered:

- What is the influence of a priori and a posteriori pixel selection during the **calibration** phase; in other words: how is the calibration influenced by allowing only certain pixels in the optimisation process?
- Given a number of possible combinations of flag settings and observation data-subsets: which combination provides the best calibration? In this study we have chosen for a systematic treatment of different selection criteria (flag settings) and 5 different data-subsets: 2003; 2004; 2005; 2006 and the whole period 2003-2006, leading to an analysis of multiple synthetic SIOP datasets.
- Random errors in the remote sensing data will lead to a certain accuracy loss in the estimated CHL and TSM values. Are there ways to discriminate pixels that contain invalid spectra leading to large errors in the concentrations?
- Because of the log-normal distribution of the concentration data (Campbell, 1995; Pasterkamp et al., 2005; Eleveld et al., 2008) the optimisation process compares log normalized annual average values. In preliminary tests it appeared that this might suppress accurate estimations of the more extreme values, thus missing important information on CHL-peaks during blooms and TSM-peaks at e.g. sand-mining locations. Therefore some tests were done to compare the results of 'log-optimisation' with the results of 'lin-optimisation' using the original data.
- What is the influence of a priori and a posteriori pixel selection during the **validation** phase; in other words: how does the calibrated algorithm perform on certain subsets of pixels similar or different from the calibration phase?

- Given two extreme processing schemes: one aimed at providing the highest quality output and one aimed at providing a maximal output at acceptable quality: which flag settings and calibration data subsets (and a choice for linear or log optimisation) provide the best calibration dataset for both processing schemes?
- Ultimately: what is the best algorithm for long term use (the most stable one) for both processing schemes: "high quality" and "high output at acceptable quality"?

## 8.2 Choices in data screening criteria

As already stated in chapter 6, the following pre-selection of data screening criteria seems useful:

### 8.2.1 General a priori data screening criteria

A priori data screening criteria: spectra will be discarded if they contain:

- One or more negative values;
- More than two zero values in wavelengths shorter than 750 nm;
- Saturation, seen as one or more unrealistically high values (>0.3).

### 8.2.2 MERIS and MODIS flags

For MERIS and MODIS there are a multitude of possible a-priori flag settings because the L2 processing provides a number of quality flags (see chapter 6.3). Because our processing chain needs to be as generic as possible, most of these flags cannot be used because they are quite specific for MERIS or MODIS. Still we have chosen to test MERIS flags, because of the following reasons:

- The high glint flag: because of MERIS' nadir looking viewing geometry many images are influenced to some extend by medium or high sun glint. Our experience has shown that high glint situations may seriously affect the retrieval of the water quality parameters. Therefore it is tested as a-priori flag.
- The PCD-1-13 flag: pixels passing this test are guaranteed to be of good quality by ESA. This flag was already used by Pasterkamp et al. (2005) to select pixels for the calibration of the IVM-HYDROPT algorithm.

For both sensors the standard "Land" and "Clouds" flags are used to select eligible water pixels.

### 8.2.3 A posteriori criterion

The $(-\log(P(\chi^2))$ statistic has proved to be (from visual inspection) a very good discriminator between high-quality and low-quality input spectra and results. Therefore this data screening criterion is used in the following analysis. After some experimentation a threshold was set of $-\log(P)>2$ to discriminate unsuitable spectral fits.

A last a posteriori criterion is thresholding. Sometimes the fit between measured and simulated spectrum is realised at unrealistically high concentrations, still giving relatively low error estimates. This may follow from the fact that sometimes multiple solutions are possible (Defoin-Platel & Chami, 2007). Thresholding is the only way to discard these results but should be done with care.

NB: Using these different flag settings complicates the comparison of results because the numbers of observations that pass the flags are variable, resulting in different sizes of the test sets. The most extreme is the PCD-1-13 flag that may omit more than 75% of the MERIS pixels.

In the following sections the optimal calibration is investigated. The prime objective of OVATIE-2 was to do this for MERIS only and to transfer the experience and methods to MODIS processing. Therefore all subsequent tests have been performed on MERIS data, sometimes making use of MERIS specific flags.

### 8.2.4 Flag coding

In the following sections the flags are coded as follows:

1: ALL STATIONS: no a priori or a posteriori selection

2: HG: all selected pixels are not affected by High Glint

3: PCD-1-13: all selected pixels pass the MERIS PCD-1-13 flag

4: BI (Bad Input): all selected pixels pass the $-\log(P)<2$ criterion

To indicate a combination of data screening methods the following a 4 digit Boolean code is used: e.g.:

(ALL STATIONS, HG, PCD-1-13 , BI) = (1000). (All stations, no flagging)

(ALL STATIONS, HG, PCD-1-13 , BI) = (1001). (All stations, minus the stations that are discarded because of the a-priori flag).

## 8.3 Considerations for the comparison of in-situ data and MERIS results

For the whole of the OVATIE-2 study one consistent method was adopted to compare in-situ data to MERIS results. This method is based on internationally accepted methods for validation of remote sensing water quality results (e.g. O'Reilly et al., 1998 and 2000, Peters et al., 2005) and thoroughly discussed with experts from the MARCOAST (Validation Bureau) project. Because one has to compare data that is usually not taken at the same time (often not even at the same day) it is necessary to aggregate both datasets (in-situ data and satellite results) to meaningful values that can be compared. Although the Dutch MWTL dataset can have a very high observation frequency (in summer two samples per month) and spatial density, it still undersamples phenomena like blooms (durations typically between 2 and 3 weeks and moving) and sediment resuspension incidents e.g. during high wind episodes or sand-mining activities. The satellite dataset is typically unevenly distributed throughout the year as a function of cloudless periods, which usually occur in springtime. As a result, algae blooming events are usually sampled in high spatial and temporal detail, because they occur during cloudless episodes. On the other hand, high sediment occurrences are probably under sampled by the satellite because they happen often during bad weather spells in autumn and winter.

In order to have one consistent basic method for validation of remote sensing results the MARCOAST project and its predecessor CoastLooc have adopted an aggregation to yearly means per station (See also Dury et al., 2004). The comparison of in-situ to satel-

lite results is performed in a scatter plot showing the yearly mean values for all valid stations. No requirements are made for the minimum number of in-situ observations.

The performance of the remote sensing results can be expressed as the correlation coefficient ($R^2$), the intercept and the slope of the regression line. It proved to be convenient to take the RMS value as an expression of the combined influence of intercept and slope. In order to prevent adverse effects of extreme values of Chl-a and TSM on the regression and hence on the calibration and validation results, the regression calculations are performed in log-log space. Since the underlying stochastic distribution of Chl-a and TSM is log-normal, it is also convenient to calculate the mean per station as the geometric median value (Campbell, 1995). Because there is no clear independent and dependent variable, the regression is performed as bi-sectoral regression (see also Eleveld et al., 2008).

## 8.4 General findings during the testing phase of the optimization procedure

In an initial step the MWTL data were downloaded from Waterbase and transferred into a suitable format for further analysis. Next the MATLAB optimisation software routines by R. Pasterkamp were reactivated. Because it was already clear from other studies that the PCD-1-13 flag was too strict, it was removed as data screening procedure. After some experimentation alternative data pre-screening algorithms were installed that test for spectra with negative or too many zero-reflectance values and for spectra that saturate. The result of this pre-selection is a set of spectra that qualifies as “good”. This pre-selection was used for all subsequent analysis. Next the procedures for optimisation of the calibration coefficients (the synthetic SIOPs) were carefully analyzed to see if further improvements could be made.

It was not very clear at the beginning which steps would lead to improvement and it took quite some time to address all issues of importance. The most important results during this process were:

1. The High Glint flag is only of minor importance for MERIS data screening (if negative, zero and saturated spectra (Rrs > 0.3) have already been removed). It was therefore not applied in the final analysis.
2. The optimisation procedure itself suffers from a starting value problem: initializing the Levenberg-Marquardt procedure with another SIOP set leads to different results. This was dealt with by taking the most realistic measured dataset as starting point for all analysis: the revamp-median2 dataset.
3. The optimisation procedure is sensitive to local minima. This was found after starting a process of iterative optimisation whereby in each new iteration the results of the prior run were used as initialisation for the next run. A definitive improvement was implemented by adding a small random component to the phytoplankton specific absorption before starting a new optimisation loop. This lead to a highly improved fitting of SIOPs. Each optimisation experiment was executed in sets of 6 iteration loops which proved sufficient to provide a truly realistic SIOP calibration.

In the following step a number of runs were done whereby in each case a certain period (year) is analysed in combination with a certain data screening method. Statistical pa-

rameters are calculated to indicate the quality of TSM and Chl-a after the optimisation. These statistics are first calculated for the year of data on which the optimisation was done. So these numbers may serve for verification and ranking but not for validation since no independent data was used. In the last step a series of cross-validation experiments are done whereby synthetic SIOPs derived from one year are applied to other years and to other data-screenings. From these experiments the overall best, most stable synthetic SIOP set is chosen.

## 8.5 Results from the Optimisation runs (2003-2006; (1000) and (0010)

Table 8.1 compares the calibration results for all "good pixels" whereby the optimisation is performed for all pixels (1000) and separately for all pixels that additionally pass the PCD-1-13 flag (0010). For each calibration case there are 6 iteration loops such as described above at item-3. From each set of 6 runs the best is chosen, based on a combined ranking of all statistics.

This is achieved by first calculating the rank for 8 statistics separately, namely

| | | | |
|---|---|---|---|
| $R^2_{CHL\text{-}a}$, | $RMS_{CHL\text{-}a}$, | $Slope_{CHL\text{-}a}$ | $Intercept_{CHL\text{-}a}$ |
| $R^2_{TSM}$, | $RMS_{TSM}$, | $Slope_{TSM}$ | $Intercept_{TSM}$. |

Next the mean of these ranks is calculated after which the means are ranked again until the final rank is calculated (pink column). The number one of each optimisation run is colour coded in green.

Evidently there is a high correlation between the final rank and the mean RMS (defined as $RMS_{CHL\text{-}a} + RMS_{TSM})/2$ which leads to the conclusion that RMS is a very good indicator of overall optimisation performance.

In general (except 2004) additional data-screening with the PCD-1-13 flag leads to lower RMS error values.

Under the conditions of this experiment the best performing SIOP set is produced for 2003 with PCD-1-13 flagging. Since this is exactly the setting under which historical synthetic SIOP sets for operational use were produced (OVATIE-1, AAN), this result confirms the very good validation results achieved so far.

*Table 8.1 Results of optimisation in log-log space using all available good pixels (no negative reflectances and no saturated reflectances). Additional data-screening is done by applying the PCD-1-13 flag (0010). For both situations optimised SIOPs were calculated. The code 2003-6 refers to optimisation over 4 years of data instead of over 1 year of data*

| Year | All | High Glint | PCD113 | -logP(Chi2) | Iteration | chl-slope | chl-r2 | chl-rms | chl-int | tsm-slope | tsm-r2 | tsm-rms | tsm-int | abs1-slope | rankchl slope | rank chl r2 | rank chl rms | rank chl int | rank tsm slope | rank tsm r2 | rank tsm rms | rank tsm int | mean rank | final rank | mean rms |
|---|---|---|---|---|---|---|---|---|---|---|---|---|---|---|---|---|---|---|---|---|---|---|---|---|---|
| 2003 | 1 | 0 | 0 | 0 | 1 | 0.973 | 0.951 | 0.072 | -0.010 | 1.009 | 0.983 | 0.050 | 0.017 | 0.027 | 1 | 2 | 2 | 1 | 1 | 1 | 4 | 2 | 1.75 | 1 | 0.061 |
| 2003 | 1 | 0 | 0 | 0 | 2 | 0.943 | 0.948 | 0.073 | 0.016 | 1.010 | 0.979 | 0.050 | 0.004 | 0.057 | 4 | 3 | 3 | 3 | 2 | 6 | 6 | 1 | 3.50 | 4 | 0.062 |
| 2003 | 1 | 0 | 0 | 0 | 3 | 0.924 | 0.955 | 0.069 | 0.024 | 0.957 | 0.982 | 0.047 | 0.028 | 0.076 | 6 | 1 | 1 | 5 | 4 | 3 | 2 | 4 | 3.25 | 3 | 0.058 |
| 2003 | 1 | 0 | 0 | 0 | 4 | 0.954 | 0.942 | 0.076 | 0.019 | 0.953 | 0.982 | 0.047 | 0.027 | 0.046 | 2 | 4 | 4 | 4 | 5 | 2 | 1 | 3 | 3.13 | 2 | 0.062 |
| 2003 | 1 | 0 | 0 | 0 | 5 | 0.944 | 0.936 | 0.081 | 0.013 | 0.951 | 0.981 | 0.049 | 0.037 | 0.056 | 3 | 6 | 6 | 2 | 6 | 4 | 3 | 5 | 4.38 | 5 | 0.065 |
| 2003 | 1 | 0 | 0 | 0 | 6 | 0.930 | 0.940 | 0.078 | 0.027 | 0.958 | 0.980 | 0.050 | 0.039 | 0.070 | 5 | 5 | 5 | 6 | 3 | 5 | 5 | 6 | 5.00 | 6 | 0.064 |
| 2003 | 0 | 0 | 1 | 0 | 1 | 0.970 | 0.910 | 0.095 | 0.022 | 0.962 | 0.988 | 0.038 | 0.020 | 0.030 | 2 | 6 | 6 | 5 | 6 | 6 | 6 | 5 | 5.25 | 6 | 0.067 |
| 2003 | 0 | 0 | 1 | 0 | 2 | 0.967 | 0.913 | 0.093 | 0.016 | 0.973 | 0.994 | 0.031 | 0.030 | 0.033 | 4 | 5 | 5 | 4 | 5 | 4 | 4 | 6 | 4.63 | 5 | 0.062 |
| 2003 | 0 | 0 | 1 | 0 | 3 | 0.959 | 0.931 | 0.083 | 0.025 | 1.013 | 0.992 | 0.031 | -0.008 | 0.041 | 5 | 2 | 2 | 6 | 4 | 5 | 5 | 1 | 3.75 | 4 | 0.057 |
| 2003 | 0 | 0 | 1 | 0 | 4 | 0.969 | 0.929 | 0.084 | 0.014 | 0.996 | 0.996 | 0.022 | 0.009 | 0.031 | 3 | 3 | 3 | 2 | 2 | 2 | 1 | 2 | 2.25 | 2 | 0.053 |
| 2003 | 0 | 0 | 1 | 0 | 5 | 0.959 | 0.929 | 0.084 | 0.015 | 1.008 | 0.995 | 0.025 | -0.015 | 0.041 | 6 | 4 | 4 | 3 | 3 | 3 | 3 | 3 | 3.63 | 3 | 0.055 |
| 2003 | 0 | 0 | 1 | 0 | 6 | 0.977 | 0.941 | 0.077 | 0.006 | 1.002 | 0.996 | 0.025 | -0.016 | 0.023 | 1 | 1 | 1 | 1 | 1 | 1 | 2 | 4 | 1.50 | 1 | 0.051 |
| 2004 | 1 | 0 | 0 | 0 | 1 | 0.891 | 0.916 | 0.128 | -0.034 | 1.158 | 0.952 | 0.106 | -0.134 | 0.109 | 3 | 5 | 5 | 6 | 6 | 4 | 5 | 6 | 5.00 | 6 | 0.117 |
| 2004 | 1 | 0 | 0 | 0 | 2 | 0.900 | 0.922 | 0.111 | -0.002 | 1.105 | 0.956 | 0.107 | -0.130 | 0.100 | 2 | 3 | 3 | 1 | 3 | 1 | 6 | 5 | 3.00 | 2 | 0.109 |
| 2004 | 1 | 0 | 0 | 0 | 3 | 0.809 | 0.920 | 0.125 | 0.017 | 1.070 | 0.954 | 0.100 | -0.102 | 0.191 | 6 | 4 | 4 | 4 | 1 | 2 | 1 | 3 | 3.13 | 3 | 0.113 |
| 2004 | 1 | 0 | 0 | 0 | 4 | 0.816 | 0.902 | 0.133 | 0.012 | 1.092 | 0.948 | 0.102 | -0.106 | 0.184 | 5 | 6 | 6 | 3 | 2 | 5 | 3 | 4 | 4.25 | 5 | 0.118 |
| 2004 | 1 | 0 | 0 | 0 | 5 | 0.871 | 0.926 | 0.107 | 0.026 | 1.137 | 0.945 | 0.102 | -0.073 | 0.129 | 4 | 2 | 2 | 5 | 4 | 6 | 2 | 2 | 3.38 | 4 | 0.104 |
| 2004 | 1 | 0 | 0 | 0 | 6 | 0.935 | 0.934 | 0.097 | 0.011 | 1.155 | 0.953 | 0.105 | -0.062 | 0.065 | 1 | 1 | 1 | 2 | 5 | 3 | 4 | 1 | 2.25 | 1 | 0.101 |
| 2004 | 0 | 0 | 1 | 0 | 1 | 0.903 | 0.937 | 0.142 | -0.076 | 1.059 | 0.934 | 0.145 | -0.147 | 0.097 | 4 | 2 | 2 | 6 | 3 | 1 | 5 | 5 | 3.50 | 4 | 0.144 |
| 2004 | 0 | 0 | 1 | 0 | 2 | 0.936 | 0.945 | 0.088 | 0.020 | 1.172 | 0.927 | 0.185 | -0.250 | 0.064 | 2 | 1 | 1 | 3 | 6 | 2 | 6 | 6 | 3.38 | 3 | 0.137 |
| 2004 | 0 | 0 | 1 | 0 | 3 | 0.911 | 0.774 | 0.177 | 0.027 | 0.944 | 0.923 | 0.116 | -0.028 | 0.089 | 3 | 4 | 4 | 4 | 2 | 3 | 2 | 3 | 3.13 | 2 | 0.147 |
| 2004 | 0 | 0 | 1 | 0 | 4 | 0.938 | 0.675 | 0.217 | -0.005 | 0.999 | 0.893 | 0.138 | -0.074 | 0.062 | 1 | 6 | 6 | 1 | 1 | 6 | 4 | 4 | 3.63 | 5 | 0.178 |
| 2004 | 0 | 0 | 1 | 0 | 5 | 0.791 | 0.856 | 0.169 | -0.017 | 0.908 | 0.917 | 0.114 | 0.009 | 0.209 | 5 | 3 | 3 | 2 | 4 | 4 | 1 | 1 | 2.88 | 1 | 0.141 |
| 2004 | 0 | 0 | 1 | 0 | 6 | 0.695 | 0.752 | 0.201 | 0.043 | 0.907 | 0.904 | 0.117 | 0.019 | 0.305 | 6 | 5 | 5 | 5 | 5 | 5 | 3 | 2 | 4.50 | 6 | 0.159 |
| 2005 | 1 | 0 | 0 | 0 | 1 | 1.059 | 0.974 | 0.065 | -0.047 | 0.972 | 0.885 | 0.107 | -0.009 | 0.059 | 5 | 3 | 6 | 6 | 5 | 6 | 6 | 3 | 5.00 | 5 | 0.086 |
| 2005 | 1 | 0 | 0 | 0 | 2 | 1.065 | 0.971 | 0.062 | -0.030 | 1.029 | 0.901 | 0.100 | -0.030 | 0.065 | 6 | 6 | 5 | 4 | 6 | 5 | 5 | 6 | 5.38 | 6 | 0.081 |
| 2005 | 1 | 0 | 0 | 0 | 3 | 1.020 | 0.978 | 0.049 | -0.003 | 1.023 | 0.940 | 0.077 | -0.011 | 0.020 | 2 | 1 | 1 | 1 | 3 | 4 | 4 | 4 | 2.50 | 2 | 0.063 |
| 2005 | 1 | 0 | 0 | 0 | 4 | 0.977 | 0.971 | 0.060 | 0.030 | 1.026 | 0.948 | 0.072 | -0.012 | 0.023 | 3 | 5 | 4 | 5 | 4 | 1 | 1 | 5 | 3.50 | 4 | 0.066 |
| 2005 | 1 | 0 | 0 | 0 | 5 | 0.996 | 0.977 | 0.049 | 0.004 | 1.000 | 0.942 | 0.075 | -0.007 | 0.004 | 1 | 2 | 2 | 2 | 1 | 3 | 3 | 1 | 1.88 | 1 | 0.062 |
| 2005 | 1 | 0 | 0 | 0 | 6 | 0.949 | 0.974 | 0.054 | 0.006 | 1.004 | 0.945 | 0.073 | -0.007 | 0.051 | 4 | 4 | 3 | 3 | 2 | 2 | 2 | 2 | 2.75 | 3 | 0.063 |
| 2005 | 0 | 0 | 1 | 0 | 1 | 1.030 | 0.970 | 0.058 | -0.015 | 1.076 | 0.969 | 0.064 | -0.023 | 0.030 | 2 | 6 | 6 | 5 | 3 | 6 | 6 | 1 | 4.38 | 6 | 0.061 |
| 2005 | 0 | 0 | 1 | 0 | 2 | 1.048 | 0.975 | 0.054 | -0.017 | 1.067 | 0.970 | 0.059 | -0.041 | 0.048 | 6 | 2 | 3 | 6 | 2 | 5 | 2 | 3 | 3.63 | 3 | 0.057 |
| 2005 | 0 | 0 | 1 | 0 | 3 | 1.032 | 0.973 | 0.055 | 0.002 | 1.105 | 0.975 | 0.062 | -0.074 | 0.032 | 4 | 4 | 4 | 1 | 6 | 3 | 5 | 6 | 4.13 | 5 | 0.059 |
| 2005 | 0 | 0 | 1 | 0 | 4 | 1.034 | 0.974 | 0.054 | -0.003 | 1.097 | 0.975 | 0.060 | -0.067 | 0.034 | 5 | 3 | 2 | 2 | 5 | 2 | 3 | 4 | 3.25 | 2 | 0.057 |
| 2005 | 0 | 0 | 1 | 0 | 5 | 1.031 | 0.972 | 0.055 | -0.006 | 1.097 | 0.975 | 0.060 | -0.069 | 0.031 | 3 | 5 | 5 | 3 | 4 | 1 | 4 | 5 | 3.75 | 4 | 0.058 |
| 2005 | 0 | 0 | 1 | 0 | 6 | 0.982 | 0.976 | 0.049 | 0.007 | 1.031 | 0.974 | 0.052 | -0.027 | 0.018 | 1 | 1 | 1 | 4 | 1 | 4 | 1 | 2 | 1.88 | 1 | 0.051 |
| 2006 | 1 | 0 | 0 | 0 | 1 | 0.811 | 0.860 | 0.151 | 0.022 | 0.988 | 0.947 | 0.080 | 0.000 | 0.190 | 1 | 3 | 2 | 3 | 1 | 6 | 5 | 1 | 2.75 | 1 | 0.115 |
| 2006 | 1 | 0 | 0 | 0 | 2 | 0.714 | 0.840 | 0.172 | 0.069 | 1.032 | 0.958 | 0.073 | -0.029 | 0.286 | 6 | 5 | 6 | 6 | 2 | 2 | 2 | 2 | 3.88 | 5 | 0.122 |
| 2006 | 1 | 0 | 0 | 0 | 3 | 0.765 | 0.837 | 0.165 | 0.053 | 1.043 | 0.955 | 0.077 | -0.040 | 0.235 | 3 | 6 | 4 | 5 | 4 | 5 | 4 | 3 | 4.25 | 6 | 0.121 |
| 2006 | 1 | 0 | 0 | 0 | 4 | 0.763 | 0.860 | 0.158 | 0.031 | 1.057 | 0.965 | 0.072 | -0.053 | 0.237 | 4 | 4 | 3 | 4 | 5 | 1 | 1 | 5 | 3.38 | 3 | 0.115 |
| 2006 | 1 | 0 | 0 | 0 | 5 | 0.769 | 0.864 | 0.167 | -0.014 | 1.041 | 0.958 | 0.077 | -0.046 | 0.231 | 2 | 2 | 5 | 2 | 3 | 3 | 3 | 4 | 3.00 | 2 | 0.122 |
| 2006 | 1 | 0 | 0 | 0 | 6 | 0.760 | 0.895 | 0.150 | 0.008 | 1.067 | 0.957 | 0.088 | -0.081 | 0.240 | 5 | 1 | 1 | 1 | 6 | 4 | 6 | 6 | 3.75 | 4 | 0.119 |
| 2006 | 0 | 0 | 1 | 0 | 1 | 0.902 | 0.937 | 0.100 | 0.015 | 1.183 | 0.938 | 0.114 | -0.094 | 0.098 | 5 | 5 | 5 | 6 | 6 | 5 | 6 | 6 | 5.50 | 6 | 0.107 |
| 2006 | 0 | 0 | 1 | 0 | 2 | 0.898 | 0.954 | 0.090 | 0.000 | 1.126 | 0.941 | 0.099 | -0.066 | 0.102 | 6 | 3 | 4 | 1 | 5 | 4 | 5 | 5 | 4.13 | 5 | 0.095 |
| 2006 | 0 | 0 | 1 | 0 | 3 | 0.982 | 0.960 | 0.077 | -0.001 | 1.040 | 0.947 | 0.082 | -0.026 | 0.018 | 1 | 2 | 2 | 2 | 4 | 2 | 2 | 4 | 2.38 | 2 | 0.080 |
| 2006 | 0 | 0 | 1 | 0 | 4 | 0.973 | 0.945 | 0.090 | -0.001 | 0.971 | 0.936 | 0.087 | 0.025 | 0.027 | 3 | 4 | 3 | 3 | 3 | 6 | 4 | 3 | 3.63 | 3 | 0.089 |
| 2006 | 0 | 0 | 1 | 0 | 5 | 0.972 | 0.917 | 0.110 | 0.004 | 1.006 | 0.944 | 0.084 | -0.021 | 0.028 | 4 | 6 | 6 | 4 | 2 | 3 | 3 | 2 | 3.75 | 4 | 0.097 |
| 2006 | 0 | 0 | 1 | 0 | 6 | 1.024 | 0.970 | 0.068 | -0.007 | 0.995 | 0.950 | 0.077 | 0.005 | 0.024 | 2 | 1 | 1 | 5 | 1 | 1 | 1 | 1 | 1.63 | 1 | 0.073 |
| 2003-6 | 1 | 0 | 0 | 0 | 1 | 0.839 | 0.929 | 0.100 | 0.012 | 1.027 | 0.965 | 0.066 | -0.040 | 0.161 | 1 | 2 | 1 | 1 | 5 | 5 | 5 | 6 | 3.25 | 2 | 0.083 |
| 2003-6 | 1 | 0 | 0 | 0 | 2 | 0.788 | 0.920 | 0.107 | 0.044 | 0.990 | 0.965 | 0.061 | -0.012 | 0.213 | 2 | 5 | 2 | 2 | 2 | 2 | 1 | 1 | 2.13 | 1 | 0.084 |
| 2003-6 | 1 | 0 | 0 | 0 | 3 | 0.742 | 0.925 | 0.124 | 0.124 | 0.992 | 0.966 | 0.067 | -0.029 | 0.258 | 5 | 4 | 6 | 5 | 1 | 1 | 6 | 2 | 3.75 | 3 | 0.095 |
| 2003-6 | 1 | 0 | 0 | 0 | 4 | 0.751 | 0.939 | 0.123 | 0.134 | 1.015 | 0.964 | 0.065 | -0.033 | 0.249 | 4 | 1 | 5 | 6 | 3 | 6 | 4 | 5 | 4.25 | 6 | 0.094 |
| 2003-6 | 1 | 0 | 0 | 0 | 5 | 0.742 | 0.928 | 0.118 | 0.113 | 1.018 | 0.965 | 0.063 | -0.030 | 0.258 | 6 | 3 | 4 | 4 | 4 | 4 | 3 | 3 | 3.88 | 5 | 0.091 |
| 2003-6 | 1 | 0 | 0 | 0 | 6 | 0.755 | 0.912 | 0.117 | 0.049 | 1.030 | 0.965 | 0.062 | -0.032 | 0.245 | 3 | 6 | 3 | 3 | 6 | 3 | 2 | 4 | 3.75 | 3 | 0.090 |
| 2003-6 | 0 | 0 | 1 | 0 | 1 | 0.913 | 0.951 | 0.078 | -0.001 | 1.206 | 0.949 | 0.123 | -0.187 | 0.087 | 6 | 5 | 2 | 1 | 6 | 5 | 5 | 5 | 4.38 | 5 | 0.101 |
| 2003-6 | 0 | 0 | 1 | 0 | 2 | 0.929 | 0.950 | 0.081 | -0.015 | 1.193 | 0.945 | 0.147 | -0.216 | 0.071 | 4 | 6 | 3 | 2 | 5 | 6 | 6 | 6 | 4.75 | 6 | 0.114 |
| 2003-6 | 0 | 0 | 1 | 0 | 3 | 0.990 | 0.965 | 0.075 | -0.041 | 1.028 | 0.960 | 0.064 | -0.014 | 0.010 | 1 | 1 | 1 | 3 | 4 | 4 | 4 | 2 | 2.50 | 2 | 0.069 |
| 2003-6 | 0 | 0 | 1 | 0 | 4 | 1.037 | 0.953 | 0.093 | -0.069 | 0.983 | 0.965 | 0.060 | 0.020 | 0.037 | 2 | 4 | 6 | 5 | 2 | 2 | 2 | 3 | 3.25 | 3 | 0.076 |
| 2003-6 | 0 | 0 | 1 | 0 | 5 | 1.039 | 0.956 | 0.085 | -0.058 | 0.996 | 0.967 | 0.057 | 0.003 | 0.039 | 3 | 3 | 4 | 4 | 1 | 1 | 1 | 1 | 2.25 | 1 | 0.071 |
| 2003-6 | 0 | 0 | 1 | 0 | 6 | 1.081 | 0.959 | 0.090 | -0.076 | 1.017 | 0.963 | 0.063 | -0.023 | 0.081 | 5 | 2 | 5 | 6 | 3 | 3 | 3 | 4 | 3.88 | 4 | 0.076 |

## 8.6 Results from the Optimisation runs (2003-2006; (1001) and (0011)

Table 8.2 compares the calibration results for all "good pixels" whereby the optimisation is performed for all pixels that also pass the a posteriori criterion -log(P($\chi$2))<=2. (1001) and separately for all pixels that additionally pass the PCD-1-13 flag (0011).

Like in the previous table, there are for each calibration case 6 iteration loops such as described above at item-3. From each set of 6 runs the best is chosen based on a combined ranking of all statistics.

This is achieved by first calculating the rank for 8 statistics separately, namely

| | | | |
|---|---|---|---|
| $R^2_{CHL\text{-}a}$, | $RMS_{CHL\text{-}a}$, | $Slope_{CHL\text{-}a}$ | $Intercept_{CHL\text{-}a}$ |
| $R^2_{TSM}$, | $RMS_{TSM}$, | $Slope_{TSM}$ | $Intercept_{TSM}$. |

Next the mean of these ranks is calculated after which the means are ranked again until the final rank is calculated (pink column). The number one of each optimisation run is colour coded in green.

Evidently there is again a high correlation between the final rank and the mean RMS (defined as $RMS_{CHL\text{-}a} + RMS_{TSM})/2$ which leads to the conclusion that RMS is a very good indicator of overall optimisation performance.

In general, (except 2003) additional data-screening with the PCD-1-13 flag leads to lower RMS error values.

Under the conditions of this experiment the best performing SIOP set is produced for 2005 with a posteriori and PCD-1-13 flagging. With these data-screening options, slightly higher RMS values are found than the previous table.

*Table 8.2 Results of optimisation in log-log space using all available good pixels (no negative reflectances and no saturated reflectances) that pass also the -logP(χ2)<=2 test. Further selection is done by applying the PCD-1-13 flag (0010). For both situations optimised SIOPs were calculated.*

| LOG BI>2 | All | HG | PCD113 | -logP(chi2) | iteration | chl-slope | chl-r2 | chl-rms | chl-int | tsm-slope | tsm-r2 | tsm-rms | tsm-int | rankslope | rank chlr2 | rank chl rms | rank chl int | rankslope | rank tsm2 | rank tsm rms | rank tsm int | mean rank | final rank | mean RMS |
|---|---|---|---|---|---|---|---|---|---|---|---|---|---|---|---|---|---|---|---|---|---|---|---|---|
| 2003 | 1 | 0 | 0 | 1 | 1 | 1.001 | 0.928 | 0.085 | 0.003 | 0.895 | 0.987 | 0.055 | 0.086 | 1 | 6 | 6 | 1 | 6 | 6 | 6 | 6 | 4.75 | 6 | 0.070 |
| 2003 | 1 | 0 | 0 | 1 | 2 | 0.921 | 0.937 | 0.081 | 0.035 | 0.902 | 0.989 | 0.049 | 0.074 | 2 | 5 | 3 | 3 | 5 | 4 | 5 | 5 | 4.00 | 4 | 0.065 |
| 2003 | 1 | 0 | 0 | 1 | 3 | 0.912 | 0.939 | 0.081 | 0.047 | 0.924 | 0.988 | 0.045 | 0.053 | 3 | 4 | 4 | 6 | 4 | 5 | 3 | 3 | 4.00 | 4 | 0.063 |
| 2003 | 1 | 0 | 0 | 1 | 4 | 0.883 | 0.943 | 0.080 | 0.042 | 0.940 | 0.991 | 0.040 | 0.051 | 5 | 2 | 2 | 4 | 3 | 2 | 2 | 2 | 2.75 | 2 | 0.060 |
| 2003 | 1 | 0 | 0 | 1 | 5 | 0.902 | 0.949 | 0.075 | 0.044 | 0.952 | 0.990 | 0.046 | 0.056 | 4 | 1 | 1 | 5 | 2 | 3 | 4 | 4 | 3.00 | 3 | 0.060 |
| 2003 | 1 | 0 | 0 | 1 | 6 | 0.875 | 0.941 | 0.084 | 0.033 | 0.965 | 0.993 | 0.032 | 0.034 | 6 | 3 | 5 | 2 | 1 | 1 | 1 | 1 | 2.50 | 1 | 0.058 |
| 2003 | 0 | 0 | 1 | 1 | 1 | 1.077 | 0.888 | 0.125 | -0.080 | 0.965 | 0.972 | 0.059 | 0.035 | 6 | 6 | 6 | 6 | 2 | 4 | 4 | 3 | 4.63 | 5 | 0.092 |
| 2003 | 0 | 0 | 1 | 1 | 2 | 0.955 | 0.905 | 0.098 | 0.030 | 0.942 | 0.971 | 0.061 | 0.048 | 5 | 5 | 5 | 5 | 6 | 6 | 6 | 6 | 5.50 | 6 | 0.079 |
| 2003 | 0 | 0 | 1 | 1 | 3 | 0.998 | 0.938 | 0.082 | -0.020 | 0.954 | 0.972 | 0.059 | 0.044 | 1 | 1 | 2 | 3 | 5 | 3 | 5 | 5 | 3.13 | 3 | 0.070 |
| 2003 | 0 | 0 | 1 | 1 | 4 | 0.977 | 0.918 | 0.092 | -0.006 | 0.966 | 0.977 | 0.052 | 0.023 | 3 | 4 | 4 | 2 | 1 | 2 | 2 | 1 | 2.38 | 2 | 0.072 |
| 2003 | 0 | 0 | 1 | 1 | 5 | 1.023 | 0.937 | 0.082 | -0.024 | 0.960 | 0.971 | 0.058 | 0.033 | 4 | 2 | 3 | 4 | 3 | 5 | 3 | 2 | 3.25 | 4 | 0.070 |
| 2003 | 0 | 0 | 1 | 1 | 6 | 0.995 | 0.935 | 0.081 | 0.003 | 0.957 | 0.984 | 0.047 | 0.042 | 2 | 3 | 1 | 1 | 4 | 1 | 1 | 4 | 2.13 | 1 | 0.064 |
| 2004 | 1 | 0 | 0 | 1 | 1 | 0.971 | 0.936 | 0.095 | -0.002 | 1.093 | 0.926 | 0.230 | -0.263 | 1 | 1 | 1 | 1 | 5 | 6 | 6 | 6 | 3.38 | 3 | 0.162 |
| 2004 | 1 | 0 | 0 | 1 | 2 | 0.739 | 0.920 | 0.140 | 0.120 | 1.069 | 0.933 | 0.106 | -0.002 | 6 | 2 | 2 | 6 | 3 | 4 | 4 | 1 | 3.50 | 4 | 0.123 |
| 2004 | 1 | 0 | 0 | 1 | 3 | 0.755 | 0.852 | 0.158 | 0.094 | 1.042 | 0.939 | 0.093 | -0.048 | 4 | 4 | 4 | 4 | 1 | 1 | 1 | 2 | 2.63 | 1 | 0.125 |
| 2004 | 1 | 0 | 0 | 1 | 4 | 0.743 | 0.839 | 0.163 | 0.094 | 1.060 | 0.928 | 0.115 | -0.095 | 5 | 5 | 5 | 5 | 2 | 5 | 5 | 5 | 4.63 | 6 | 0.139 |
| 2004 | 1 | 0 | 0 | 1 | 5 | 0.796 | 0.793 | 0.184 | -0.003 | 1.086 | 0.935 | 0.101 | -0.075 | 3 | 6 | 6 | 2 | 4 | 3 | 3 | 4 | 3.88 | 5 | 0.142 |
| 2004 | 1 | 0 | 0 | 1 | 6 | 0.831 | 0.868 | 0.143 | 0.079 | 1.099 | 0.939 | 0.098 | -0.059 | 2 | 3 | 3 | 3 | 6 | 2 | 2 | 3 | 3.00 | 2 | 0.121 |
| 2004 | 0 | 0 | 1 | 1 | 1 | 1.089 | 0.952 | 0.095 | -0.049 | 1.091 | 0.941 | 0.120 | -0.131 | 4 | 2 | 3 | 6 | 4 | 1 | 6 | 6 | 4.00 | 5 | 0.108 |
| 2004 | 0 | 0 | 1 | 1 | 2 | 0.854 | 0.898 | 0.126 | 0.021 | 1.075 | 0.937 | 0.097 | -0.061 | 6 | 6 | 6 | 4 | 2 | 2 | 1 | 2 | 3.63 | 2 | 0.111 |
| 2004 | 0 | 0 | 1 | 1 | 3 | 0.866 | 0.933 | 0.107 | 0.011 | 1.091 | 0.931 | 0.105 | -0.083 | 5 | 4 | 4 | 3 | 3 | 4 | 3 | 4 | 3.75 | 3 | 0.106 |
| 2004 | 0 | 0 | 1 | 1 | 4 | 0.918 | 0.915 | 0.109 | 0.028 | 1.099 | 0.925 | 0.109 | -0.076 | 3 | 5 | 5 | 5 | 5 | 5 | 4 | 3 | 4.38 | 6 | 0.109 |
| 2004 | 0 | 0 | 1 | 1 | 5 | 0.940 | 0.958 | 0.079 | 0.002 | 1.072 | 0.933 | 0.098 | -0.051 | 2 | 1 | 1 | 1 | 1 | 3 | 2 | 1 | 1.50 | 1 | 0.089 |
| 2004 | 0 | 0 | 1 | 1 | 6 | 0.946 | 0.947 | 0.087 | 0.005 | 1.125 | 0.924 | 0.114 | -0.095 | 1 | 3 | 2 | 2 | 6 | 6 | 5 | 5 | 3.75 | 3 | 0.100 |
| 2005 | 1 | 0 | 0 | 1 | 1 | 1.080 | 0.913 | 0.105 | -0.042 | 1.030 | 0.896 | 0.104 | -0.039 | 1 | 5 | 3 | 6 | 2 | 6 | 2 | 1 | 3.25 | 2 | 0.105 |
| 2005 | 1 | 0 | 0 | 1 | 2 | 0.884 | 0.952 | 0.083 | -0.008 | 1.146 | 0.918 | 0.114 | -0.127 | 3 | 1 | 1 | 2 | 6 | 5 | 3 | 5 | 3.25 | 2 | 0.098 |
| 2005 | 1 | 0 | 0 | 1 | 3 | 0.886 | 0.925 | 0.091 | 0.025 | 1.111 | 0.928 | 0.094 | -0.066 | 2 | 4 | 2 | 4 | 5 | 2 | 1 | 2 | 2.75 | 1 | 0.092 |
| 2005 | 1 | 0 | 0 | 1 | 4 | 0.800 | 0.929 | 0.107 | 0.006 | 1.060 | 0.926 | 0.124 | -0.121 | 4 | 3 | 4 | 1 | 4 | 3 | 4 | 4 | 3.38 | 4 | 0.115 |
| 2005 | 1 | 0 | 0 | 1 | 5 | 0.752 | 0.930 | 0.117 | 0.011 | 1.031 | 0.923 | 0.142 | -0.130 | 5 | 2 | 5 | 3 | 3 | 4 | 6 | 6 | 4.25 | 6 | 0.130 |
| 2005 | 1 | 0 | 0 | 1 | 6 | 0.731 | 0.874 | 0.134 | 0.030 | 1.020 | 0.931 | 0.134 | -0.118 | 6 | 6 | 6 | 5 | 1 | 1 | 5 | 3 | 4.13 | 5 | 0.134 |
| 2005 | 0 | 0 | 1 | 1 | 1 | 1.042 | 0.977 | 0.052 | 0.000 | 1.173 | 0.935 | 0.101 | -0.106 | 5 | 1 | 3 | 1 | 6 | 5 | 6 | 6 | 4.13 | 6 | 0.076 |
| 2005 | 0 | 0 | 1 | 1 | 2 | 1.005 | 0.977 | 0.049 | 0.004 | 1.029 | 0.926 | 0.086 | -0.018 | 1 | 2 | 1 | 2 | 2 | 6 | 5 | 3 | 2.75 | 1 | 0.068 |
| 2005 | 0 | 0 | 1 | 1 | 3 | 0.952 | 0.976 | 0.052 | 0.021 | 0.993 | 0.958 | 0.063 | 0.000 | 6 | 3 | 2 | 6 | 1 | 4 | 3 | 1 | 3.25 | 2 | 0.057 |
| 2005 | 0 | 0 | 1 | 1 | 4 | 0.963 | 0.966 | 0.060 | 0.009 | 1.101 | 0.968 | 0.066 | -0.048 | 4 | 4 | 4 | 3 | 5 | 3 | 4 | 4 | 3.88 | 5 | 0.063 |
| 2005 | 0 | 0 | 1 | 1 | 5 | 0.990 | 0.962 | 0.063 | 0.013 | 1.094 | 0.980 | 0.054 | -0.060 | 2 | 6 | 6 | 4 | 4 | 1 | 1 | 5 | 3.63 | 4 | 0.059 |
| 2005 | 0 | 0 | 1 | 1 | 6 | 0.969 | 0.963 | 0.063 | 0.020 | 1.030 | 0.971 | 0.054 | -0.012 | 3 | 5 | 5 | 5 | 3 | 2 | 2 | 2 | 3.38 | 3 | 0.059 |
| 2006 | 1 | 0 | 0 | 1 | 1 | 0.787 | 0.885 | 0.147 | 0.009 | 1.057 | 0.958 | 0.079 | -0.056 | 1 | 6 | 2 | 1 | 1 | 5 | 4 | 3 | 2.88 | 2 | 0.113 |
| 2006 | 1 | 0 | 0 | 1 | 2 | 0.746 | 0.905 | 0.142 | 0.065 | 1.067 | 0.965 | 0.073 | -0.060 | 2 | 3 | 1 | 3 | 2 | 2 | 1 | 4 | 2.25 | 1 | 0.108 |
| 2006 | 1 | 0 | 0 | 1 | 3 | 0.709 | 0.897 | 0.153 | 0.073 | 1.086 | 0.966 | 0.085 | -0.095 | 3 | 5 | 4 | 5 | 5 | 1 | 6 | 6 | 4.38 | 5 | 0.119 |
| 2006 | 1 | 0 | 0 | 1 | 4 | 0.687 | 0.908 | 0.155 | 0.086 | 1.087 | 0.960 | 0.078 | -0.048 | 5 | 2 | 5 | 6 | 6 | 3 | 3 | 1 | 3.88 | 4 | 0.116 |
| 2006 | 1 | 0 | 0 | 1 | 5 | 0.701 | 0.903 | 0.153 | 0.067 | 1.072 | 0.960 | 0.076 | -0.051 | 4 | 4 | 3 | 4 | 3 | 4 | 2 | 2 | 3.25 | 3 | 0.114 |
| 2006 | 1 | 0 | 0 | 1 | 6 | 0.676 | 0.913 | 0.158 | 0.045 | 1.083 | 0.956 | 0.082 | -0.063 | 6 | 1 | 6 | 2 | 4 | 6 | 5 | 5 | 4.38 | 5 | 0.120 |
| 2006 | 0 | 0 | 1 | 1 | 1 | 0.906 | 0.938 | 0.098 | 0.020 | 1.169 | 0.931 | 0.118 | -0.068 | 6 | 6 | 5 | 4 | 6 | 6 | 6 | 6 | 5.63 | 6 | 0.108 |
| 2006 | 0 | 0 | 1 | 1 | 2 | 0.974 | 0.964 | 0.105 | -0.069 | 1.155 | 0.938 | 0.110 | -0.065 | 3 | 4 | 6 | 6 | 5 | 4 | 5 | 5 | 4.75 | 5 | 0.107 |
| 2006 | 0 | 0 | 1 | 1 | 3 | 1.045 | 0.956 | 0.085 | -0.014 | 1.013 | 0.938 | 0.087 | -0.006 | 4 | 5 | 4 | 3 | 2 | 5 | 3 | 1 | 3.38 | 4 | 0.086 |
| 2006 | 0 | 0 | 1 | 1 | 4 | 1.085 | 0.969 | 0.078 | -0.030 | 1.011 | 0.939 | 0.087 | -0.014 | 5 | 2 | 3 | 5 | 1 | 3 | 2 | 2 | 2.88 | 3 | 0.082 |
| 2006 | 0 | 0 | 1 | 1 | 5 | 1.026 | 0.968 | 0.070 | -0.008 | 1.027 | 0.946 | 0.082 | -0.016 | 2 | 3 | 2 | 2 | 3 | 1 | 1 | 3 | 2.13 | 1 | 0.076 |
| 2006 | 0 | 0 | 1 | 1 | 6 | 1.006 | 0.970 | 0.067 | 0.003 | 1.046 | 0.940 | 0.088 | -0.026 | 1 | 1 | 1 | 1 | 4 | 2 | 4 | 4 | 2.25 | 2 | 0.077 |
| 2007 | 1 | 0 | 0 | 1 | 1 | 0.975 | 0.931 | 0.085 | 0.010 | 1.058 | 0.962 | 0.091 | -0.096 | 2 | 1 | 1 | 2 | 6 | 6 | 5 | 6 | 3.63 | 4 | 0.088 |
| 2007 | 1 | 0 | 0 | 1 | 2 | 0.997 | 0.898 | 0.104 | 0.000 | 1.018 | 0.965 | 0.064 | -0.033 | 1 | 5 | 4 | 1 | 3 | 4 | 1 | 1 | 2.50 | 2 | 0.084 |
| 2007 | 1 | 0 | 0 | 1 | 3 | 0.934 | 0.905 | 0.100 | 0.026 | 1.018 | 0.967 | 0.077 | -0.060 | 3 | 4 | 2 | 4 | 4 | 2 | 3 | 3 | 3.13 | 3 | 0.088 |
| 2007 | 1 | 0 | 0 | 1 | 4 | 0.863 | 0.912 | 0.102 | 0.018 | 1.007 | 0.969 | 0.065 | -0.037 | 5 | 2 | 3 | 3 | 1 | 1 | 2 | 2 | 2.38 | 1 | 0.083 |
| 2007 | 1 | 0 | 0 | 1 | 5 | 0.881 | 0.909 | 0.107 | 0.073 | 1.017 | 0.967 | 0.079 | -0.063 | 4 | 3 | 5 | 6 | 2 | 3 | 4 | 4 | 3.88 | 5 | 0.093 |
| 2007 | 1 | 0 | 0 | 1 | 6 | 0.820 | 0.871 | 0.121 | 0.047 | 1.030 | 0.965 | 0.095 | -0.090 | 6 | 6 | 6 | 5 | 5 | 5 | 6 | 5 | 5.50 | 6 | 0.108 |
| 2007 | 0 | 0 | 1 | 1 | 1 | 0.784 | 0.965 | 0.088 | 0.056 | 1.130 | 0.947 | 0.098 | -0.117 | 6 | 1 | 5 | 6 | 6 | 6 | 6 | 6 | 5.25 | 6 | 0.093 |
| 2007 | 0 | 0 | 1 | 1 | 2 | 1.012 | 0.928 | 0.093 | -0.036 | 1.066 | 0.949 | 0.080 | -0.014 | 2 | 6 | 6 | 4 | 2 | 4 | 4 | 1 | 3.63 | 4 | 0.087 |
| 2007 | 0 | 0 | 1 | 1 | 3 | 1.071 | 0.949 | 0.080 | -0.029 | 1.100 | 0.949 | 0.085 | -0.032 | 5 | 5 | 4 | 2 | 5 | 3 | 5 | 2 | 3.88 | 5 | 0.082 |
| 2007 | 0 | 0 | 1 | 1 | 4 | 0.986 | 0.957 | 0.077 | -0.033 | 1.067 | 0.948 | 0.078 | -0.032 | 3 | 4 | 2 | 3 | 3 | 5 | 3 | 3 | 3.25 | 3 | 0.077 |
| 2007 | 0 | 0 | 1 | 1 | 5 | 1.034 | 0.963 | 0.065 | -0.022 | 1.065 | 0.953 | 0.074 | -0.037 | 4 | 2 | 1 | 1 | 1 | 2 | 1 | 4 | 2.00 | 1 | 0.070 |
| 2007 | 0 | 0 | 1 | 1 | 6 | 1.011 | 0.957 | 0.079 | -0.044 | 1.081 | 0.953 | 0.075 | -0.043 | 1 | 3 | 3 | 5 | 4 | 1 | 2 | 5 | 3.00 | 2 | 0.077 |

## 8.7 Results from the Optimisation runs (2003-2006; lin-lin space; (1000) and (0010)

In order to test if extreme values do affect the optimisation significantly, the runs were repeated in linear space, but the resulting TSM and Chl-a were converted to log values to be able to calculated comparable statistics.

Table 8.3 compares the calibration results in linear space for all "good pixels" whereby the optimisation is performed for all pixels (1000) and separately for all pixels that additionally pass the PCD-1-13 flag (0010).

For each calibration case there are 6 iteration loops such as described above at item-3. From each set of 6 runs the best is chosen based on a combined ranking of all statistics.

This is achieved by first calculating the rank for 8 statistics separately, namely

| | | | |
|---|---|---|---|
| $R^2_{CHL\text{-}a}$, | $RMS_{CHL\text{-}a}$, | $Slope_{CHL\text{-}a}$ | $Intercept_{CHL\text{-}a}$ |
| $R^2_{TSM}$, | $RMS_{TSM}$, | $Slope_{TSM}$ | $Intercept_{TSM}$. |

Next the mean of these ranks is calculated after which the means are ranked again until the final rank is calculated (pink column). The number one of each optimisation run is colour coded in green.

In general, (except 2005) additional data-screening with the PCD-1-13 flag does **NOT** lead to lower RMS error values.

It is interesting to observe that the year that is likely to have produced the highest extreme values (2003) is also the year that has the largest increase in RMS values which confirms that the optimisation should be performed in log-log space.

Under the conditions of this experiment the best performing SIOP set is produced for 2005 with PCD-1-13 flagging. In linear space, slightly higher RMS values are found as compared to the same analysis in log-log space.

*Table 8.3 Results of optimisation in lin-lin space using all available good pixels (no negative reflectances and no saturated reflectances). Further selection is done by applying the PCD-1-13 flag (0010). For both situations optimised SIOPs were calculated*

| lin-bi>2 | All | HG | PCD113 | -logP(chi2) | iteration | chl-slope | chl-r2 | chl-rms | chl-int | tsm-slope | tsm-r2 | tsm-rms | tsm-int | rankslope | rank chlr2 | rank chl rms | rank chl int | rankslope | rank tsm2 | rank tsm rms | rank tsm int | mean rank | final rank | |
|---|---|---|---|---|---|---|---|---|---|---|---|---|---|---|---|---|---|---|---|---|---|---|---|---|
| 2003 | 1 | 0 | 0 | 1 | 1 | 1.134 | 0.861 | 0.149 | -0.114 | 0.917 | 0.936 | 0.113 | 0.122 | 5 | 5 | 5 | 6 | 5 | 6 | 6 | 6 | 5.50 | 6 | 0.131 |
| 2003 | 1 | 0 | 0 | 1 | 2 | 1.130 | 0.840 | 0.157 | -0.113 | 1.035 | 0.967 | 0.066 | -0.003 | 4 | 6 | 6 | 5 | 2 | 5 | 3 | 2 | 4.13 | 5 | 0.111 |
| 2003 | 1 | 0 | 0 | 1 | 3 | 0.997 | 0.906 | 0.111 | -0.052 | 1.103 | 0.983 | 0.058 | -0.071 | 1 | 3 | 3 | 3 | 6 | 2 | 2 | 4 | 3.00 | 2 | 0.085 |
| 2003 | 1 | 0 | 0 | 1 | 4 | 1.052 | 0.901 | 0.107 | 0.006 | 1.055 | 0.983 | 0.093 | -0.113 | 2 | 4 | 2 | 1 | 4 | 1 | 5 | 5 | 3.00 | 2 | 0.100 |
| 2003 | 1 | 0 | 0 | 1 | 5 | 0.696 | 0.910 | 0.125 | 0.109 | 1.011 | 0.982 | 0.057 | 0.027 | 6 | 2 | 4 | 4 | 1 | 3 | 1 | 3 | 3.00 | 2 | 0.091 |
| 2003 | 1 | 0 | 0 | 1 | 6 | 0.878 | 0.937 | 0.084 | 0.050 | 1.052 | 0.975 | 0.067 | 0.002 | 3 | 1 | 1 | 2 | 3 | 4 | 4 | 1 | 2.38 | 1 | 0.075 |
| 2003 | 0 | 0 | 1 | 1 | 1 | 1.090 | 0.917 | 0.105 | -0.066 | 1.121 | 0.977 | 0.071 | -0.094 | 2 | 1 | 1 | 2 | 6 | 2 | 2 | 3 | 2.38 | 1 | 0.088 |
| 2003 | 0 | 0 | 1 | 1 | 2 | 1.230 | 0.915 | 0.131 | -0.122 | 1.091 | 0.976 | 0.110 | -0.146 | 4 | 2 | 3 | 5 | 3 | 3 | 5 | 5 | 3.75 | 4 | 0.121 |
| 2003 | 0 | 0 | 1 | 1 | 3 | 1.278 | 0.875 | 0.156 | -0.113 | 1.064 | 0.969 | 0.129 | -0.150 | 5 | 3 | 5 | 3 | 1 | 4 | 6 | 6 | 4.13 | 5 | 0.142 |
| 2003 | 0 | 0 | 1 | 1 | 4 | 1.424 | 0.848 | 0.236 | -0.280 | 1.089 | 0.961 | 0.096 | -0.112 | 6 | 6 | 6 | 6 | 2 | 5 | 4 | 4 | 4.88 | 6 | 0.166 |
| 2003 | 0 | 0 | 1 | 1 | 5 | 1.035 | 0.874 | 0.118 | -0.031 | 1.115 | 0.946 | 0.093 | -0.056 | 1 | 4 | 2 | 1 | 5 | 6 | 3 | 1 | 2.88 | 2 | 0.105 |
| 2003 | 0 | 0 | 1 | 1 | 6 | 1.092 | 0.869 | 0.149 | -0.115 | 1.107 | 0.983 | 0.059 | -0.072 | 3 | 5 | 4 | 4 | 4 | 1 | 1 | 2 | 3.00 | 3 | 0.104 |
| 2004 | 1 | 0 | 0 | 1 | 1 | 1.023 | 0.968 | 0.073 | -0.033 | 1.190 | 0.935 | 0.152 | -0.216 | 1 | 1 | 1 | 3 | 3 | 3 | 4 | 4 | 2.50 | 1 | 0.113 |
| 2004 | 1 | 0 | 0 | 1 | 2 | 0.940 | 0.923 | 0.108 | -0.014 | 1.219 | 0.934 | 0.172 | -0.255 | 3 | 3 | 3 | 1 | 5 | 5 | 5 | 5 | 3.75 | 4 | 0.140 |
| 2004 | 1 | 0 | 0 | 1 | 3 | 0.964 | 0.919 | 0.106 | 0.014 | 1.236 | 0.915 | 0.220 | -0.319 | 2 | 4 | 2 | 2 | 6 | 6 | 6 | 6 | 4.25 | 5 | 0.163 |
| 2004 | 1 | 0 | 0 | 1 | 4 | 0.779 | 0.879 | 0.142 | 0.054 | 1.201 | 0.936 | 0.141 | -0.201 | 6 | 5 | 6 | 5 | 4 | 2 | 3 | 3 | 4.25 | 5 | 0.142 |
| 2004 | 1 | 0 | 0 | 1 | 5 | 0.826 | 0.923 | 0.114 | 0.046 | 1.168 | 0.935 | 0.124 | -0.154 | 4 | 2 | 4 | 4 | 2 | 4 | 2 | 2 | 3.00 | 2 | 0.119 |
| 2004 | 1 | 0 | 0 | 1 | 6 | 0.825 | 0.874 | 0.138 | 0.060 | 1.153 | 0.940 | 0.116 | -0.140 | 5 | 6 | 5 | 6 | 1 | 1 | 1 | 1 | 3.25 | 3 | 0.127 |
| 2004 | 0 | 0 | 1 | 1 | 1 | 1.038 | 0.943 | 0.136 | -0.111 | 1.190 | 0.932 | 0.142 | -0.195 | 3 | 4 | 4 | 4 | 1 | 2 | 1 | 1 | 2.50 | 1 | 0.139 |
| 2004 | 0 | 0 | 1 | 1 | 2 | 1.203 | 0.961 | 0.173 | -0.193 | 1.238 | 0.935 | 0.159 | -0.242 | 6 | 1 | 6 | 6 | 2 | 1 | 3 | 4 | 3.63 | 4 | 0.166 |
| 2004 | 0 | 0 | 1 | 1 | 3 | 1.127 | 0.957 | 0.119 | -0.110 | 1.240 | 0.925 | 0.156 | -0.226 | 5 | 2 | 1 | 3 | 3 | 3 | 2 | 2 | 2.63 | 2 | 0.138 |
| 2004 | 0 | 0 | 1 | 1 | 4 | 1.030 | 0.930 | 0.132 | -0.093 | 1.265 | 0.917 | 0.163 | -0.238 | 2 | 6 | 3 | 1 | 5 | 4 | 4 | 3 | 3.50 | 3 | 0.148 |
| 2004 | 0 | 0 | 1 | 1 | 5 | 1.029 | 0.951 | 0.122 | -0.097 | 1.263 | 0.904 | 0.183 | -0.265 | 1 | 3 | 2 | 2 | 4 | 5 | 6 | 6 | 3.63 | 4 | 0.152 |
| 2004 | 0 | 0 | 1 | 1 | 6 | 1.076 | 0.931 | 0.141 | -0.116 | 1.270 | 0.901 | 0.177 | -0.252 | 4 | 5 | 5 | 5 | 6 | 6 | 5 | 5 | 5.13 | 6 | 0.159 |
| 2005 | 1 | 0 | 0 | 1 | 1 | 1.104 | 0.966 | 0.078 | -0.055 | 1.108 | 0.902 | 0.127 | -0.129 | 2 | 1 | 1 | 5 | 1 | 6 | 4 | 3 | 2.88 | 3 | 0.102 |
| 2005 | 1 | 0 | 0 | 1 | 2 | 1.170 | 0.932 | 0.121 | -0.096 | 1.188 | 0.919 | 0.129 | -0.171 | 6 | 3 | 6 | 6 | 5 | 4 | 6 | 5 | 5.13 | 6 | 0.125 |
| 2005 | 1 | 0 | 0 | 1 | 3 | 0.963 | 0.932 | 0.090 | -0.025 | 1.215 | 0.938 | 0.128 | -0.193 | 1 | 4 | 3 | 2 | 6 | 1 | 5 | 6 | 3.50 | 4 | 0.109 |
| 2005 | 1 | 0 | 0 | 1 | 4 | 0.853 | 0.931 | 0.095 | 0.005 | 1.120 | 0.932 | 0.094 | -0.084 | 4 | 5 | 5 | 1 | 2 | 3 | 1 | 1 | 2.75 | 2 | 0.095 |
| 2005 | 1 | 0 | 0 | 1 | 5 | 0.855 | 0.944 | 0.084 | 0.034 | 1.143 | 0.938 | 0.102 | -0.122 | 3 | 2 | 2 | 3 | 3 | 2 | 2 | 2 | 2.38 | 1 | 0.093 |
| 2005 | 1 | 0 | 0 | 1 | 6 | 0.853 | 0.927 | 0.093 | 0.037 | 1.187 | 0.911 | 0.122 | -0.144 | 5 | 6 | 4 | 4 | 4 | 5 | 3 | 4 | 4.38 | 5 | 0.108 |
| 2005 | 0 | 0 | 1 | 1 | 1 | 1.074 | 0.961 | 0.074 | -0.041 | 1.149 | 0.937 | 0.100 | -0.118 | 2 | 6 | 3 | 2 | 6 | 6 | 6 | 6 | 4.63 | 6 | 0.087 |
| 2005 | 0 | 0 | 1 | 1 | 2 | 1.010 | 0.977 | 0.049 | 0.000 | 1.116 | 0.956 | 0.082 | -0.095 | 1 | 1 | 1 | 1 | 5 | 5 | 5 | 5 | 3.00 | 2 | 0.066 |
| 2005 | 0 | 0 | 1 | 1 | 3 | 0.855 | 0.968 | 0.072 | 0.050 | 1.048 | 0.975 | 0.053 | -0.037 | 3 | 4 | 2 | 3 | 1 | 2 | 1 | 1 | 2.13 | 1 | 0.063 |
| 2005 | 0 | 0 | 1 | 1 | 4 | 0.837 | 0.969 | 0.086 | 0.080 | 1.065 | 0.965 | 0.064 | -0.051 | 6 | 3 | 6 | 6 | 3 | 4 | 4 | 3 | 4.38 | 5 | 0.075 |
| 2005 | 0 | 0 | 1 | 1 | 5 | 0.841 | 0.971 | 0.081 | 0.074 | 1.055 | 0.971 | 0.059 | -0.047 | 5 | 2 | 5 | 5 | 2 | 3 | 2 | 2 | 3.25 | 3 | 0.070 |
| 2005 | 0 | 0 | 1 | 1 | 6 | 0.848 | 0.967 | 0.074 | 0.052 | 1.079 | 0.975 | 0.061 | -0.070 | 4 | 5 | 4 | 4 | 4 | 1 | 3 | 4 | 3.63 | 4 | 0.068 |
| 2006 | 1 | 0 | 0 | 1 | 1 | 0.853 | 0.952 | 0.100 | 0.060 | 1.129 | 0.956 | 0.107 | -0.135 | 1 | 6 | 2 | 1 | 6 | 6 | 6 | 6 | 4.25 | 5 | 0.103 |
| 2006 | 1 | 0 | 0 | 1 | 2 | 0.820 | 0.972 | 0.097 | 0.075 | 1.098 | 0.963 | 0.083 | -0.089 | 2 | 1 | 1 | 2 | 4 | 5 | 4 | 4 | 2.88 | 2 | 0.090 |
| 2006 | 1 | 0 | 0 | 1 | 3 | 0.783 | 0.958 | 0.120 | 0.099 | 1.109 | 0.963 | 0.098 | -0.122 | 6 | 5 | 5 | 4 | 5 | 4 | 5 | 5 | 4.88 | 6 | 0.109 |
| 2006 | 1 | 0 | 0 | 1 | 4 | 0.812 | 0.971 | 0.103 | 0.085 | 1.071 | 0.973 | 0.069 | -0.068 | 3 | 2 | 3 | 3 | 3 | 1 | 2 | 3 | 2.50 | 1 | 0.086 |
| 2006 | 1 | 0 | 0 | 1 | 5 | 0.800 | 0.967 | 0.117 | 0.107 | 1.063 | 0.972 | 0.068 | -0.060 | 4 | 4 | 4 | 5 | 2 | 2 | 1 | 2 | 3.00 | 3 | 0.092 |
| 2006 | 1 | 0 | 0 | 1 | 6 | 0.786 | 0.967 | 0.129 | 0.126 | 1.058 | 0.966 | 0.073 | -0.058 | 5 | 3 | 6 | 6 | 1 | 3 | 3 | 1 | 3.50 | 4 | 0.101 |
| 2006 | 0 | 0 | 1 | 1 | 1 | 0.927 | 0.899 | 0.123 | 0.029 | 1.083 | 0.938 | 0.094 | -0.060 | 6 | 4 | 4 | 6 | 6 | 6 | 6 | 4 | 5.25 | 6 | 0.109 |
| 2006 | 0 | 0 | 1 | 1 | 2 | 1.027 | 0.888 | 0.132 | -0.017 | 1.082 | 0.950 | 0.088 | -0.070 | 3 | 5 | 5 | 3 | 5 | 5 | 5 | 6 | 4.63 | 5 | 0.110 |
| 2006 | 0 | 0 | 1 | 1 | 3 | 1.046 | 0.866 | 0.147 | -0.019 | 1.059 | 0.952 | 0.083 | -0.056 | 4 | 6 | 6 | 4 | 3 | 3 | 3 | 3 | 4.00 | 4 | 0.115 |
| 2006 | 0 | 0 | 1 | 1 | 4 | 1.055 | 0.918 | 0.116 | -0.021 | 1.021 | 0.950 | 0.079 | -0.023 | 5 | 2 | 2 | 5 | 2 | 4 | 2 | 2 | 3.00 | 3 | 0.097 |
| 2006 | 0 | 0 | 1 | 1 | 5 | 0.983 | 0.905 | 0.119 | 0.008 | 1.073 | 0.954 | 0.084 | -0.064 | 2 | 3 | 3 | 1 | 4 | 1 | 4 | 5 | 2.88 | 2 | 0.101 |
| 2006 | 0 | 0 | 1 | 1 | 6 | 1.017 | 0.949 | 0.088 | -0.010 | 1.016 | 0.953 | 0.076 | -0.014 | 1 | 1 | 1 | 2 | 1 | 2 | 1 | 1 | 1.25 | 1 | 0.082 |
| 2007 | 1 | 0 | 0 | 1 | 1 | 1.012 | 0.969 | 0.105 | -0.092 | 1.145 | 0.966 | 0.096 | -0.140 | 2 | 2 | 6 | 6 | 1 | 6 | 1 | 1 | 3.13 | 3 | 0.101 |
| 2007 | 1 | 0 | 0 | 1 | 2 | 0.994 | 0.967 | 0.080 | -0.054 | 1.157 | 0.969 | 0.104 | -0.159 | 1 | 3 | 5 | 5 | 2 | 2 | 2 | 2 | 2.75 | 2 | 0.092 |
| 2007 | 1 | 0 | 0 | 1 | 3 | 0.944 | 0.973 | 0.061 | -0.012 | 1.193 | 0.970 | 0.121 | -0.195 | 3 | 1 | 1 | 3 | 4 | 1 | 4 | 4 | 2.63 | 1 | 0.091 |
| 2007 | 1 | 0 | 0 | 1 | 4 | 0.924 | 0.965 | 0.069 | -0.007 | 1.197 | 0.969 | 0.124 | -0.200 | 5 | 4 | 2 | 2 | 5 | 3 | 5 | 5 | 3.88 | 4 | 0.097 |
| 2007 | 1 | 0 | 0 | 1 | 5 | 0.933 | 0.958 | 0.071 | -0.002 | 1.203 | 0.967 | 0.126 | -0.203 | 4 | 5 | 3 | 1 | 6 | 5 | 6 | 6 | 4.50 | 6 | 0.098 |
| 2007 | 1 | 0 | 0 | 1 | 6 | 0.883 | 0.956 | 0.074 | 0.026 | 1.174 | 0.968 | 0.112 | -0.175 | 6 | 6 | 4 | 4 | 3 | 4 | 3 | 3 | 4.13 | 5 | 0.093 |
| 2007 | 0 | 0 | 1 | 1 | 1 | 0.893 | 0.976 | 0.058 | 0.036 | 1.157 | 0.952 | 0.099 | -0.132 | 5 | 1 | 1 | 3 | 6 | 6 | 6 | 6 | 4.25 | 4 | 0.079 |
| 2007 | 0 | 0 | 1 | 1 | 2 | 0.882 | 0.964 | 0.070 | 0.047 | 1.095 | 0.960 | 0.076 | -0.077 | 6 | 2 | 3 | 6 | 5 | 5 | 5 | 5 | 4.63 | 5 | 0.073 |
| 2007 | 0 | 0 | 1 | 1 | 3 | 0.920 | 0.957 | 0.069 | 0.023 | 1.071 | 0.969 | 0.064 | -0.058 | 1 | 3 | 2 | 1 | 3 | 3 | 3 | 3 | 2.38 | 1 | 0.067 |
| 2007 | 0 | 0 | 1 | 1 | 4 | 0.894 | 0.937 | 0.085 | 0.041 | 1.090 | 0.964 | 0.071 | -0.072 | 4 | 6 | 6 | 5 | 4 | 4 | 4 | 4 | 4.63 | 5 | 0.078 |
| 2007 | 0 | 0 | 1 | 1 | 5 | 0.897 | 0.943 | 0.080 | 0.032 | 1.047 | 0.972 | 0.056 | -0.033 | 3 | 5 | 5 | 2 | 1 | 1 | 1 | 1 | 2.38 | 1 | 0.068 |
| 2007 | 0 | 0 | 1 | 1 | 6 | 0.901 | 0.950 | 0.076 | 0.038 | 1.049 | 0.971 | 0.057 | -0.036 | 2 | 4 | 4 | 4 | 2 | 2 | 2 | 2 | 2.75 | 3 | 0.067 |

## 8.8 Summary of calibration results

Table 8.4 summarises the results of Table 8.1, Table 8.2 and Table 8.3. Best overall calibration results are obtained in log-log space when using the PCD-1-13 flag in combination with the –log(P) criterion, although the differences are very small.

It was therefore decided to test those 5 SIOP-sets (2003, 2004, 2005, 2006 and 2003-6) for stability.

Note that in table 8.4 "2007" is mentioned. This is not an actual year but an acronym that refers to testing for the whole 2003-2006 period at once.

*Table 8.4 Combination of optimisation results. For each of the 3 test cases (log-all; log all--logP>2 and lin-all the results are shown after optimisation.*

| | | | | | | | | | | | | | | | SUM RMS | |
|---|---|---|---|---|---|---|---|---|---|---|---|---|---|---|---|---|
| lin-bi>2 | All | HG | PCD113 | -logP(Chi2) | chl-slope | chl-r2 | chl-rms | chl-int | tsm-slope | tsm-r2 | tsm-rms | tsm-int | sum rms | | 1001 | 0011 |
| 2003 | 1 | 0 | 0 | 1 | 0.87825 | 0.93714 | 0.08419 | 0.050289 | 1.0523 | 0.97505 | 0.066746 | 0.002301 | 0.150936 | | 0.150936 | |
| 2003 | 0 | 0 | 1 | 1 | 1.0895 | 0.9165 | 0.10543 | -0.06584 | 1.1214 | 0.97682 | 0.070827 | -0.09364 | 0.176257 | | | 0.176257 |
| 2004 | 1 | 0 | 0 | 1 | 1.0225 | 0.96801 | 0.07303 | -0.0334 | 1.1904 | 0.93498 | 0.15207 | -0.21574 | 0.2251 | | 0.2251 | |
| 2004 | 0 | 0 | 1 | 1 | 1.0379 | 0.94325 | 0.13575 | -0.11107 | 1.1897 | 0.93189 | 0.14184 | -0.19491 | 0.27759 | | | 0.27759 |
| 2005 | 1 | 0 | 0 | 1 | 0.85512 | 0.94422 | 0.084162 | 0.034449 | 1.1431 | 0.93774 | 0.10152 | -0.12168 | 0.185682 | | 0.185682 | |
| 2005 | 0 | 0 | 1 | 1 | 0.85545 | 0.96846 | 0.07219 | 0.049907 | 1.0482 | 0.97495 | 0.052832 | -0.0372 | 0.125022 | | | 0.125022 |
| 2006 | 1 | 0 | 0 | 1 | 0.81213 | 0.97095 | 0.10259 | 0.084742 | 1.0713 | 0.97296 | 0.06858 | -0.06765 | 0.17117 | | 0.17117 | |
| 2006 | 0 | 0 | 1 | 1 | 1.0171 | 0.94895 | 0.088179 | -0.00972 | 1.0156 | 0.9527 | 0.0761 | -0.01376 | 0.164279 | | | 0.164279 |
| 2007 | 1 | 0 | 0 | 1 | 0.94437 | 0.97297 | 0.061083 | -0.01182 | 1.1925 | 0.9702 | 0.12071 | -0.19543 | 0.181793 | | 0.181793 | |
| 2007 | 0 | 0 | 1 | 1 | 0.91973 | 0.95662 | 0.069436 | 0.022872 | 1.0714 | 0.9687 | 0.064107 | -0.05766 | 0.133543 | | | 0.133543 |
| | | | | | Mean CHL RMS | | 0.087604 | | Mean TSM RMS | | 0.091533 | | | | 0.182936 | 0.175338 |

| | | | | | | | | | | | | | | | | |
|---|---|---|---|---|---|---|---|---|---|---|---|---|---|---|---|---|
| logBI>2 | All | HG | PCD113 | -logP(Chi2) | chl-slope | chl-r2 | chl-rms | chl-int | tsm-slope | tsm-r2 | tsm-rms | tsm-int | | | 1001 | 0011 |
| 2003 | 1 | 0 | 0 | 1 | 0.87534 | 0.94054 | 0.083651 | 0.032626 | 0.96494 | 0.99348 | 0.032009 | 0.034475 | 0.11566 | | 0.11566 | |
| 2003 | 0 | 0 | 1 | 1 | 0.99476 | 0.93474 | 0.0811 | 0.003467 | 0.95699 | 0.98415 | 0.046721 | 0.042041 | 0.127821 | | | 0.127821 |
| 2004 | 1 | 0 | 0 | 1 | 0.75524 | 0.8519 | 0.1575 | 0.093812 | 1.0423 | 0.93928 | 0.0926 | -0.04762 | 0.2501 | | 0.2501 | |
| 2004 | 0 | 0 | 1 | 1 | 0.9402 | 0.95776 | 0.079246 | 0.001518 | 1.0716 | 0.93302 | 0.098329 | -0.05125 | 0.177575 | | | 0.177575 |
| 2005 | 1 | 0 | 0 | 1 | 0.88628 | 0.9248 | 0.090856 | 0.024687 | 1.1106 | 0.92791 | 0.093868 | -0.06639 | 0.184724 | | 0.184724 | |
| 2005 | 0 | 0 | 1 | 1 | 1.0045 | 0.97685 | 0.049125 | 0.00393 | 1.0294 | 0.92581 | 0.085934 | -0.01758 | 0.135059 | | | 0.135059 |
| 2006 | 1 | 0 | 0 | 1 | 0.74617 | 0.90524 | 0.1419 | 0.065272 | 1.0673 | 0.96499 | 0.073438 | -0.05977 | 0.215338 | | 0.215338 | |
| 2006 | 0 | 0 | 1 | 1 | 1.026 | 0.96805 | 0.070266 | -0.00759 | 1.0271 | 0.94574 | 0.082216 | -0.01577 | 0.152482 | | | 0.152482 |
| 2007 | 1 | 0 | 0 | 1 | 0.86258 | 0.91215 | 0.1018 | 0.018463 | 1.0074 | 0.96851 | 0.065147 | -0.03742 | 0.166947 | | 0.166947 | |
| 2007 | 0 | 0 | 1 | 1 | 1.0337 | 0.96268 | 0.06543 | -0.02183 | 1.0646 | 0.95258 | 0.073624 | -0.03665 | 0.139054 | | | 0.139054 |
| | | | | | Mean CHL RMS | | 0.092087 | | Mean TSM RMS | | 0.074389 | | | | 0.186554 | 0.146398 |

| | | | | | | | | | | | | | | | | |
|---|---|---|---|---|---|---|---|---|---|---|---|---|---|---|---|---|
| log-all | All | HG | PCD113 | -logP(Chi2) | chl-slope | chl-r2 | chl-rms | chl-int | tsm-slope | tsm-r2 | tsm-rms | tsm-int | | | 1000 | 0010 |
| 2003 | 1 | 0 | 0 | 0 | 0.97257 | 0.95143 | 0.072338 | -0.00971 | 1.009 | 0.9827 | 0.049956 | 0.017042 | 0.122294 | | 0.122294 | |
| 2003 | 0 | 0 | 1 | 0 | 0.97717 | 0.94062 | 0.076974 | 0.005729 | 1.0017 | 0.9963 | 0.025183 | -0.01567 | 0.102157 | | | 0.102157 |
| 2004 | 1 | 0 | 0 | 0 | 0.9354 | 0.93366 | 0.096624 | 0.010942 | 1.1546 | 0.95325 | 0.10497 | -0.06189 | 0.201594 | | 0.201594 | |
| 2004 | 0 | 0 | 1 | 0 | 0.7909 | 0.85622 | 0.1686 | -0.01692 | 0.90764 | 0.91732 | 0.11375 | 0.009438 | 0.28235 | | | 0.28235 |
| 2005 | 1 | 0 | 0 | 0 | 0.99559 | 0.97686 | 0.048738 | 0.004008 | 0.99963 | 0.94194 | 0.074713 | -0.00727 | 0.123451 | | 0.123451 | |
| 2005 | 0 | 0 | 1 | 0 | 0.98172 | 0.97612 | 0.049493 | 0.007146 | 1.031 | 0.97366 | 0.052381 | -0.02713 | 0.101874 | | | 0.101874 |
| 2006 | 1 | 0 | 0 | 0 | 0.8105 | 0.86044 | 0.15111 | 0.02192 | 0.98798 | 0.94674 | 0.079813 | -0.00035 | 0.230923 | | 0.230923 | |
| 2006 | 0 | 0 | 1 | 0 | 1.024 | 0.96968 | 0.068301 | -0.00689 | 0.99461 | 0.94976 | 0.077356 | 0.00525 | 0.145657 | | | 0.145657 |
| 2007 | 1 | 0 | 0 | 0 | 0.7875 | 0.9204 | 0.10742 | 0.043532 | 0.99003 | 0.96542 | 0.06083 | -0.01174 | 0.16825 | | 0.16825 | |
| 2007 | 0 | 0 | 1 | 0 | 1.0387 | 0.95575 | 0.084522 | -0.05791 | 0.99554 | 0.96704 | 0.056991 | 0.002934 | 0.141513 | | | 0.141513 |
| | | | | | Mean CHL RMS | | 0.092412 | | Mean TSM RMS | | 0.069594 | | | | 0.169302 | 0.15471 |

## 8.9 Stability tests: selection of the final best synthetic SIOP set

Table 8.5 and Table 8.6 show the results of stability tests. In this test, the synthetic SIOPs that were derived for each year with certain data screening options are applied to MERIS observations of the other years with similar or other data screening options. In this analysis the mean RMS value is used as criterion to select the best overall performing synthetic SIOP set.

**Overall best performance is obtained with the dataset from the calibration with 2006 PCD_1_13 (code 0011) data. This dataset is selected as the final best calibration dataset.**

*Table 8.5 Stability test results for cases where SIOPs were calculated with (0011) data screening and validated also with (0011) data screening. This is the most optimal case to obtain high quality results; for operational use this is less interesting option since the PCD-1-13 flag discards too many data points of still reasonable quality.*

| SIOPS determined at 0011 | | | | | | Validation at 0011 | | | | | | | | | | Mean RMS (CHL + TSM) | | | | |
|---|---|---|---|---|---|---|---|---|---|---|---|---|---|---|---|---|---|---|---|---|
| Calibration-year | validation year | all | HG | PCD113 | -logP(Chi2) | chl-slope | cht-r2 | chl-rms | chl-int | chl-int-1 | tsm-slope | tsm-r2 | tsm-rms | tsm-int | tsm-int-1 | 2003 | 2004 | 2005 | 2006 | 2007 |
| 2003 | 2003 | 0 | 0 | 1 | 1 | 0.995 | 0.935 | 0.081 | 0.003 | 0.002 | 0.957 | 0.984 | 0.047 | 0.042 | 0.016 | 0.064 | | | | |
| 2004 | 2003 | 0 | 0 | 1 | 1 | 0.887 | 0.962 | 0.086 | 0.094 | 0.052 | 0.978 | 0.947 | 0.146 | 0.137 | 0.124 | | 0.116 | | | |
| 2005 | 2003 | 0 | 0 | 1 | 1 | 1.053 | 0.929 | 0.089 | -0.026 | -0.007 | 0.790 | 0.972 | 0.127 | 0.220 | 0.092 | | | 0.108 | | |
| 2006 | 2003 | 0 | 0 | 1 | 1 | 1.134 | 0.943 | 0.098 | -0.014 | 0.036 | 0.791 | 0.960 | 0.104 | 0.174 | 0.047 | | | | 0.049 | |
| 2003-6 | 2003 | 0 | 0 | 1 | 1 | 1.247 | 0.911 | 0.137 | -0.056 | 0.036 | 0.976 | 0.983 | 0.105 | 0.110 | 0.095 | | | | | 0.121 |
| 2003 | 2004 | 0 | 0 | 1 | 1 | 0.816 | 0.898 | 0.131 | 0.029 | -0.025 | 1.045 | 0.938 | 0.143 | -0.139 | -0.110 | 0.137 | | | | |
| 2004 | 2004 | 0 | 0 | 1 | 1 | 0.940 | 0.958 | 0.079 | 0.002 | -0.016 | 1.072 | 0.933 | 0.098 | -0.051 | -0.006 | | 0.089 | | | |
| 2005 | 2004 | 0 | 0 | 1 | 1 | 0.962 | 0.920 | 0.120 | -0.047 | -0.058 | 0.951 | 0.943 | 0.086 | 0.014 | -0.017 | | | 0.103 | | |
| 2006 | 2004 | 0 | 0 | 1 | 1 | 1.013 | 0.924 | 0.104 | -0.011 | -0.007 | 0.935 | 0.941 | 0.089 | 0.019 | -0.022 | | | | 0.052 | |
| 2003-6 | 2004 | 0 | 0 | 1 | 1 | 1.076 | 0.928 | 0.110 | -0.045 | -0.023 | 1.015 | 0.924 | 0.105 | -0.046 | -0.037 | | | | | 0.108 |
| 2003 | 2005 | 0 | 0 | 1 | 1 | 0.966 | 0.947 | 0.075 | 0.019 | 0.012 | 1.130 | 0.933 | 0.140 | -0.178 | -0.104 | 0.107 | | | | |
| 2004 | 2005 | 0 | 0 | 1 | 1 | 0.963 | 0.905 | 0.101 | 0.032 | 0.024 | 1.210 | 0.919 | 0.121 | -0.152 | -0.032 | | 0.111 | | | |
| 2005 | 2005 | 0 | 0 | 1 | 1 | 1.005 | 0.977 | 0.049 | 0.004 | 0.005 | 1.029 | 0.926 | 0.086 | -0.018 | -0.001 | | | 0.068 | | |
| 2006 | 2005 | 0 | 0 | 1 | 1 | 1.108 | 0.978 | 0.073 | 0.015 | 0.040 | 0.958 | 0.951 | 0.071 | 0.004 | -0.020 | | | | 0.036 | |
| 2003-6 | 2005 | 0 | 0 | 1 | 1 | 1.067 | 0.939 | 0.086 | -0.030 | -0.015 | 1.102 | 0.915 | 0.104 | -0.088 | -0.029 | | | | | 0.095 |
| 2003 | 2006 | 0 | 0 | 1 | 1 | 0.840 | 0.925 | 0.127 | -0.019 | -0.054 | 1.125 | 0.952 | 0.131 | -0.169 | -0.095 | 0.129 | | | | |
| 2004 | 2006 | 0 | 0 | 1 | 1 | 0.816 | 0.929 | 0.117 | 0.029 | -0.012 | 1.188 | 0.922 | 0.127 | -0.138 | -0.027 | | 0.122 | | | |
| 2005 | 2006 | 0 | 0 | 1 | 1 | 0.941 | 0.961 | 0.095 | -0.041 | -0.055 | 1.035 | 0.949 | 0.080 | -0.025 | -0.005 | | | 0.087 | | |
| 2006 | 2006 | 0 | 0 | 1 | 1 | 1.026 | 0.968 | 0.070 | -0.008 | -0.002 | 1.027 | 0.946 | 0.082 | -0.016 | 0.000 | | | | 0.035 | |
| 2003-6 | 2006 | 0 | 0 | 1 | 1 | 0.769 | 0.901 | 0.145 | 0.008 | -0.043 | 1.131 | 0.930 | 0.114 | -0.117 | -0.039 | | | | | 0.130 |
| | | | | | | | | | | | | | | | Mean RMS per year | 0.109 | 0.109 | 0.091 | **0.043** | 0.113 |

*Table 8.6 Stability test results for cases where SIOPs were calculated with (0011) data screening and validated also with (1001) data screening. This is the operational case without PCD-1-13 flagging.*

| SIOPS determined at 0011 | | | | | | Validation at 1001 | | | | | | | | | | Mean RMS (CHL + TSM) | | | | |
|---|---|---|---|---|---|---|---|---|---|---|---|---|---|---|---|---|---|---|---|---|
| Calibration-year | validation year | all | HG | PCD113 | BI | chl-slope | cht-r2 | chl-rms | chl-int | chl-int-1 | tsm-slope | tsm-r2 | tsm-rms | tsm-int | tsm-int-1 | 2003 | 2004 | 2005 | 2006 | 2007 |
| 2003 | 2003 | 1 | 0 | 0 | 1 | 0.924 | 0.934 | 0.087 | 0.001 | -0.027 | 0.938 | 0.988 | 0.058 | -0.003 | -0.041 | 0.073 | | | | |
| 2004 | 2003 | 1 | 0 | 0 | 1 | 0.803 | 0.950 | 0.101 | 0.120 | 0.046 | 0.924 | 0.972 | 0.112 | 0.141 | 0.095 | | 0.106 | | | |
| 2005 | 2003 | 1 | 0 | 0 | 1 | 0.990 | 0.944 | 0.085 | -0.037 | -0.040 | 0.782 | 0.988 | 0.100 | 0.192 | 0.060 | | | 0.093 | | |
| 2006 | 2003 | 1 | 0 | 0 | 1 | 1.070 | 0.948 | 0.078 | -0.026 | 0.000 | 0.800 | 0.983 | 0.078 | 0.124 | 0.003 | | | | 0.078 | |
| 2003-6 | 2003 | 1 | 0 | 0 | 1 | 1.068 | 0.939 | 0.094 | 0.018 | 0.043 | 0.931 | 0.989 | 0.064 | 0.092 | 0.050 | | | | | 0.079 |
| 2003 | 2004 | 1 | 0 | 0 | 1 | 0.741 | 0.894 | 0.150 | 0.030 | -0.046 | 1.066 | 0.942 | 0.168 | -0.183 | -0.142 | 0.159 | | | | |
| 2004 | 2004 | 1 | 0 | 0 | 1 | 0.719 | 0.926 | 0.137 | 0.104 | 0.022 | 1.034 | 0.951 | 0.080 | -0.025 | -0.003 | | 0.109 | | | |
| 2005 | 2004 | 1 | 0 | 0 | 1 | 0.818 | 0.904 | 0.136 | 0.001 | -0.052 | 0.936 | 0.956 | 0.078 | 0.019 | -0.021 | | | 0.107 | | |
| 2006 | 2004 | 1 | 0 | 0 | 1 | 0.930 | 0.885 | 0.127 | 0.002 | -0.018 | 1.056 | 0.936 | 0.107 | -0.086 | -0.050 | | | | 0.117 | |
| 2003-6 | 2004 | 1 | 0 | 0 | 1 | 0.857 | 0.888 | 0.130 | 0.019 | -0.023 | 1.027 | 0.939 | 0.105 | -0.072 | -0.055 | | | | | 0.117 |
| 2003 | 2005 | 1 | 0 | 0 | 1 | 0.887 | 0.944 | 0.081 | 0.025 | 0.000 | 1.053 | 0.958 | 0.162 | -0.178 | -0.148 | 0.121 | | | | |
| 2004 | 2005 | 1 | 0 | 0 | 1 | 0.843 | 0.942 | 0.098 | 0.080 | 0.045 | 1.096 | 0.935 | 0.096 | -0.094 | -0.039 | | 0.097 | | | |
| 2005 | 2005 | 1 | 0 | 0 | 1 | 0.930 | 0.959 | 0.067 | 0.013 | -0.003 | 0.915 | 0.946 | 0.078 | 0.020 | -0.028 | | | 0.073 | | |
| 2006 | 2005 | 1 | 0 | 0 | 1 | 1.042 | 0.946 | 0.079 | 0.005 | 0.015 | 0.956 | 0.930 | 0.106 | -0.043 | -0.068 | | | | 0.093 | |
| 2003-6 | 2005 | 1 | 0 | 0 | 1 | 1.033 | 0.959 | 0.076 | 0.028 | 0.035 | 1.068 | 0.918 | 0.122 | -0.117 | -0.078 | | | | | 0.099 |
| 2003 | 2006 | 1 | 0 | 0 | 1 | 0.737 | 0.961 | 0.138 | -0.009 | -0.067 | 0.972 | 0.969 | 0.174 | -0.147 | -0.163 | 0.156 | | | | |
| 2004 | 2006 | 1 | 0 | 0 | 1 | 0.734 | 0.951 | 0.125 | 0.053 | -0.005 | 1.070 | 0.966 | 0.082 | -0.084 | -0.043 | | 0.104 | | | |
| 2005 | 2006 | 1 | 0 | 0 | 1 | 0.844 | 0.979 | 0.105 | -0.036 | -0.070 | 0.913 | 0.969 | 0.076 | 0.012 | -0.039 | | | 0.091 | | |
| 2006 | 2006 | 1 | 0 | 0 | 1 | 0.919 | 0.978 | 0.074 | -0.022 | -0.040 | 0.907 | 0.949 | 0.107 | -0.016 | -0.071 | | | | 0.091 | |
| 2003-6 | 2006 | 1 | 0 | 0 | 1 | 0.755 | 0.939 | 0.139 | -0.007 | -0.061 | 1.006 | 0.958 | 0.114 | -0.092 | -0.089 | | | | | 0.127 |
| | | | | | | | | | | | | | | | average RMS per calibration year | 0.127 | 0.104 | **0.091** | 0.095 | 0.106 |

# 9. Validation of the 2006-0011 calibration

## 9.1 Analysis of yearly average data for 2003, 2004 and 2005

A graphical representation of the validation results of the best calibration dataset (2006 – 0011 screening) is given in Figure 9.1 to 9.5. These results can be compared to the earlier results, as presented in Chapters 3 and 4.

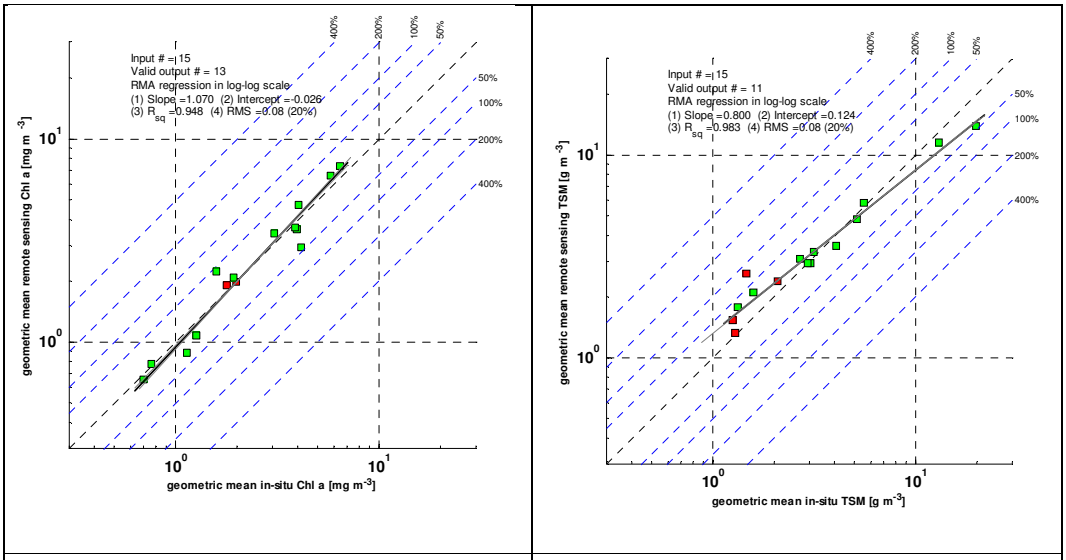


| | |
|---|---|
| SIOP: Best-2006-0011<br>Parameter: CHL<br>Year: 2003 flag settings: 1001 | SIOP: Best-2006-0011<br>Parameter: TSM<br>Year: 2003 flag settings: 1001 |

*Figure 9.1 Comparison of 2003 annual geometric mean values of Chl-a and TSM as observed in-situ on MWTL monitoring stations and derived from HYDROPT MERIS observations at MWTL locations*

Figure 9.1 shows that in 2003 the 2006-calibrated SIOPs perform very well for Chl-a and TSM retrievals. The TSM slope slightly deviates from the 1:1 line leading to small underestimations of high TSM values and small overestimations of low TSM values.

Figure 9.2 (below) shows that in 2004 the 2006-calibrated SIOPs perform very well for Chl-a and TSM although the RMS values are higher as compared to 2003, probably due to the fact that no clear spring peak was witnessed during this year. Yearly geometric mean Chl-a values are in general lower in 2004 than in 2003. TSM values seem to be higher in 2004.

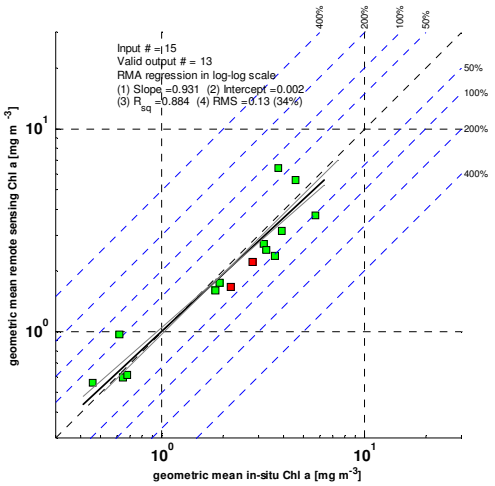


SIOP: Best-2006-0011

Parameter: CHL

Year: 2004 flag settings: 1001

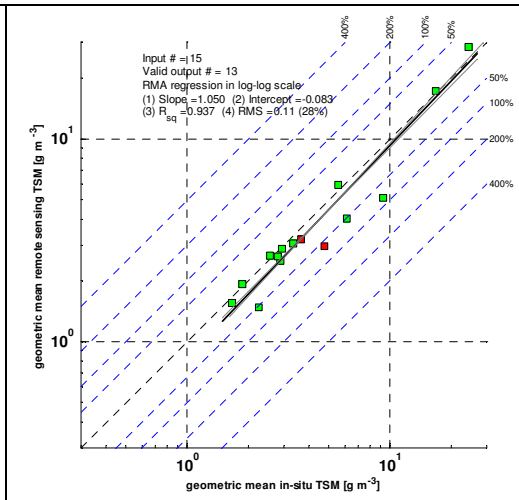


SIOP: Best-2006-0011

Parameter: TSM

Year: 2004 flag settings: 1001

*Figure 9.2 Comparison of 2004 annual geometric mean values of Chl-a and TSM as observed in-situ on MWTL monitoring stations and derived from HYDROPT MERIS observations at MWTL locations*

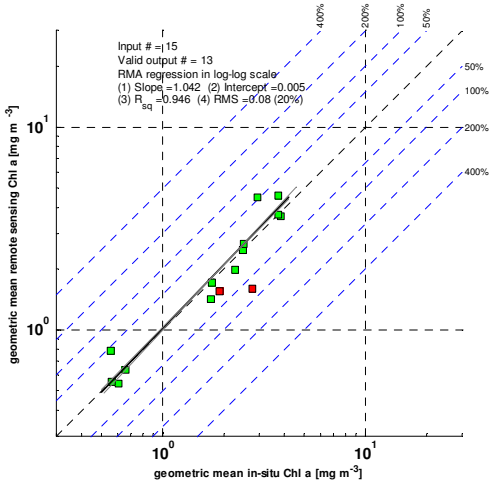


SIOP: Best-2006-0011

Parameter: CHL

Year: 2005 flag settings: 1001

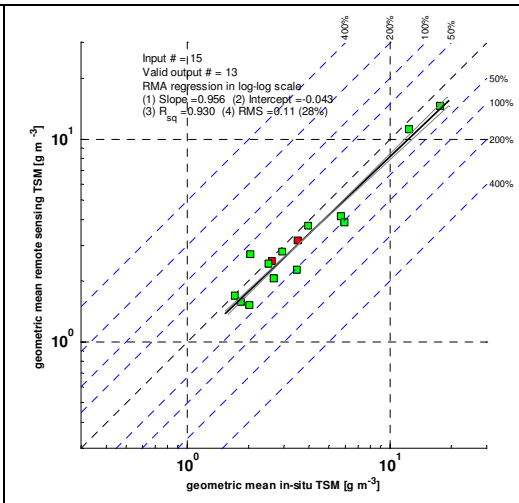


SIOP: Best-2006-0011

Parameter: TSM

Year: 2005 flag settings: 1001

*Figure 9.3 Comparison of 2005 annual geometric mean values of Chl-a and TSM as observed in-situ on MWTL monitoring stations and derived from HYDROPT MERIS observations at MWTL locations*

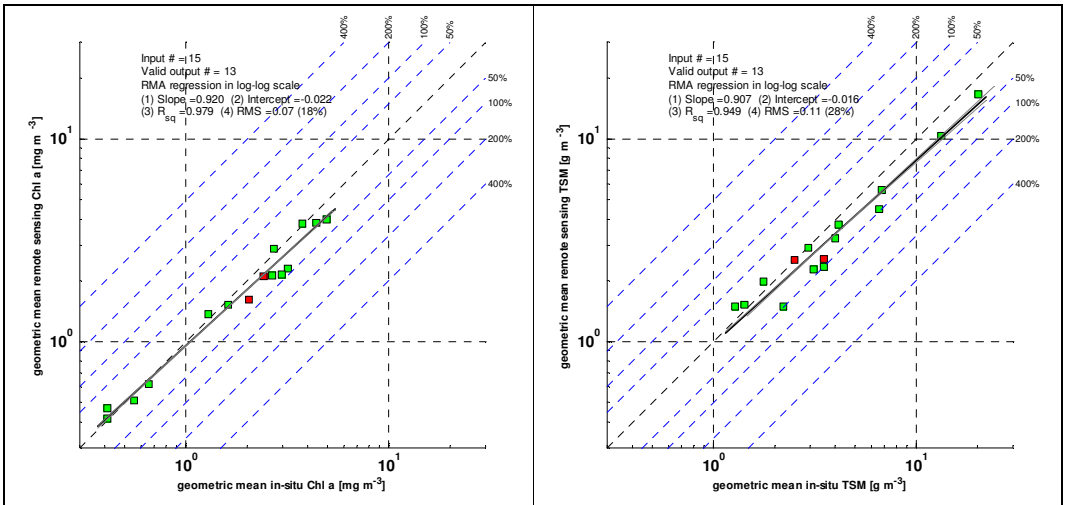


| | |
|---|---|
| SIOP: Best-2006-0011<br>Parameter: CHL<br>Year: 2006 flag settings: 1001 | SIOP: Best-2006-0011<br>Parameter: TSM<br>Year: 2006 flag settings: 1001 |

*Figure 9.4 Comparison of 2006 annual geometric mean values of Chl-a and TSM as observed in-situ on MWTL monitoring stations and derived from HYDROPT MERIS observations at MWTL locations*

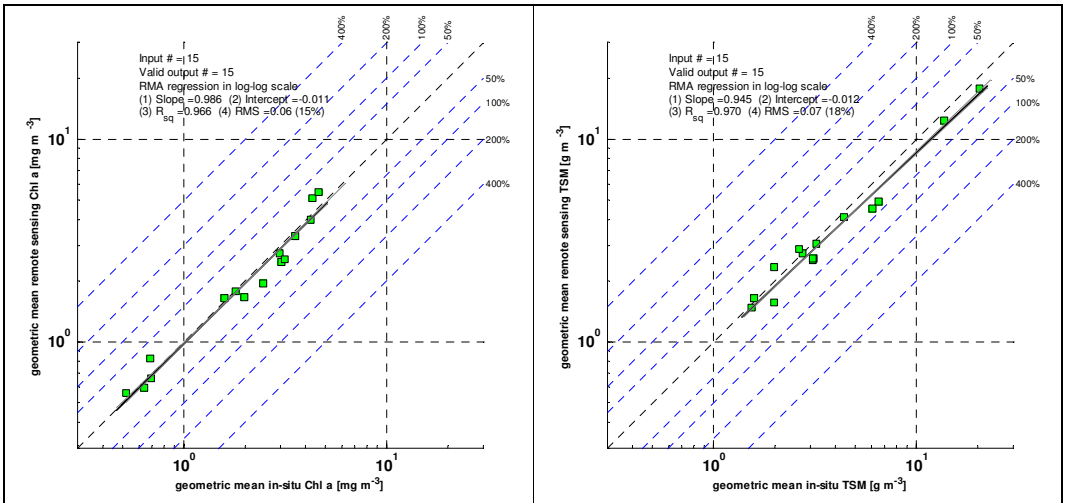


| | |
|---|---|
| SIOP: Best-2006-0011<br>Parameter: CHL<br>Year: 2003-2006 flag settings: 1001 | SIOP: Best-2006-0011<br>Parameter: TSM<br>Year: 2003-2006 flag settings: 1001 |

*Figure 9.5 Comparison of 2003-2006 4-year geometric mean values of Chl-a and TSM as observed in-situ on MWTL monitoring stations and derived from HYDROPT MERIS observations at MWTL locations*

Figure 9.3 shows that in 2005 the 2006-calibrated SIOPs perform very well for Chl-a and TSM although the RMS values for TSM are slightly higher as compared to 2003, probably due to the fact that no clear spring peak was witnessed during this year. Again, yearly geometric mean Chl-a values are in general lower in 2004 than in 2003, but comparable to 2006.

Figure 9.4 shows the verification of the 2006-calibrated SIOPs. The calibrated algorithm has very low RMS values for Chl-a and low RMS values for TSM. One should keep in mind that the algorithm is calibrated on PCD-1-13 and $-\log(P(\chi 2))$ filtered data. In Figure 8.4 the calibrated algorithm is applied to a much larger dataset of only $-\log(P(\chi 2))$ filtered data. Therefore the calibration and validation datasets are partly dependent.

Figure 9.5 shows the performance of the calibrated algorithm for all spectra at MWTL locations in the years 2003-2006 that pass the $-\log(P(\chi 2))$ data screening. At each point the 4 year geometric mean is calculated of MERIS and MWTL observations. The Chl-a regression line is almost perfectly on the 1:1 line; the TSM regression line has a very small deviation. RMS values are extremely low. This graph actually confirms that the procedure of selecting the best and most stable SIOP set has actually given a very good result.

## 9.2 Analysis of time series of HYDROPT MERIS results at MWTL stations

In order to have better understanding of the local – regional validity of the calibrated HYDROPT MERIS algorithm (using the best-2006-0011 SIOP dataset) an analysis was made of the results per MWTL station. In the Figures 9.6 and 9.7 the ratio of median Chl-a and TSM from MWTL and from MERIS for every year are plotted per MWTL station. This ratio provides direct insight in the performance of the algorithm at a certain location. Unfortunately, the number of in-situ samples is not always the same for each location and (because of under sampling) there is not always sufficient data to allow for a representative and robust comparison. In appendix 1 a complete overview is given of all time-series results for Chl-a and TSM at the MWTL locations.

Although it was not analysed in detail in this report, the number of in-situ samples also influences the results of the HYDROPT calibration. If e.g. winter storms prevent the RWS ship from sampling, it may have as result that the performance of the calibrated HYDROPT algorithm is affected for periods of resuspension during and after storms.

In general the ratios behave quite similar per station over the years. Therefore Figure 9.8 (depicting the ratios for the summed 4 year period) is used to illustrate the differences per station. These plots can be summarized as follows:

- TSM is systematically underestimated by MERIS at stations Walcheren 2 and Goeree 6. TSM is overestimated by the satellite at Noordwijk 20, Terschelling 100 and the Rottumerplaat stations 50 and 70.
- Chl-a is most seriously overestimated by MERIS at Goeree 6. This salinity measurements at this station show that it is regularly influenced by the fresh water outflow from the Haringvliet and Nieuwe Waterweg, which might influence the SIOP values.
- There is no correlation between TSM and Chl-a deviations over all stations over the 4 year period which is an argument for the stability of the HYDROPT calibration.

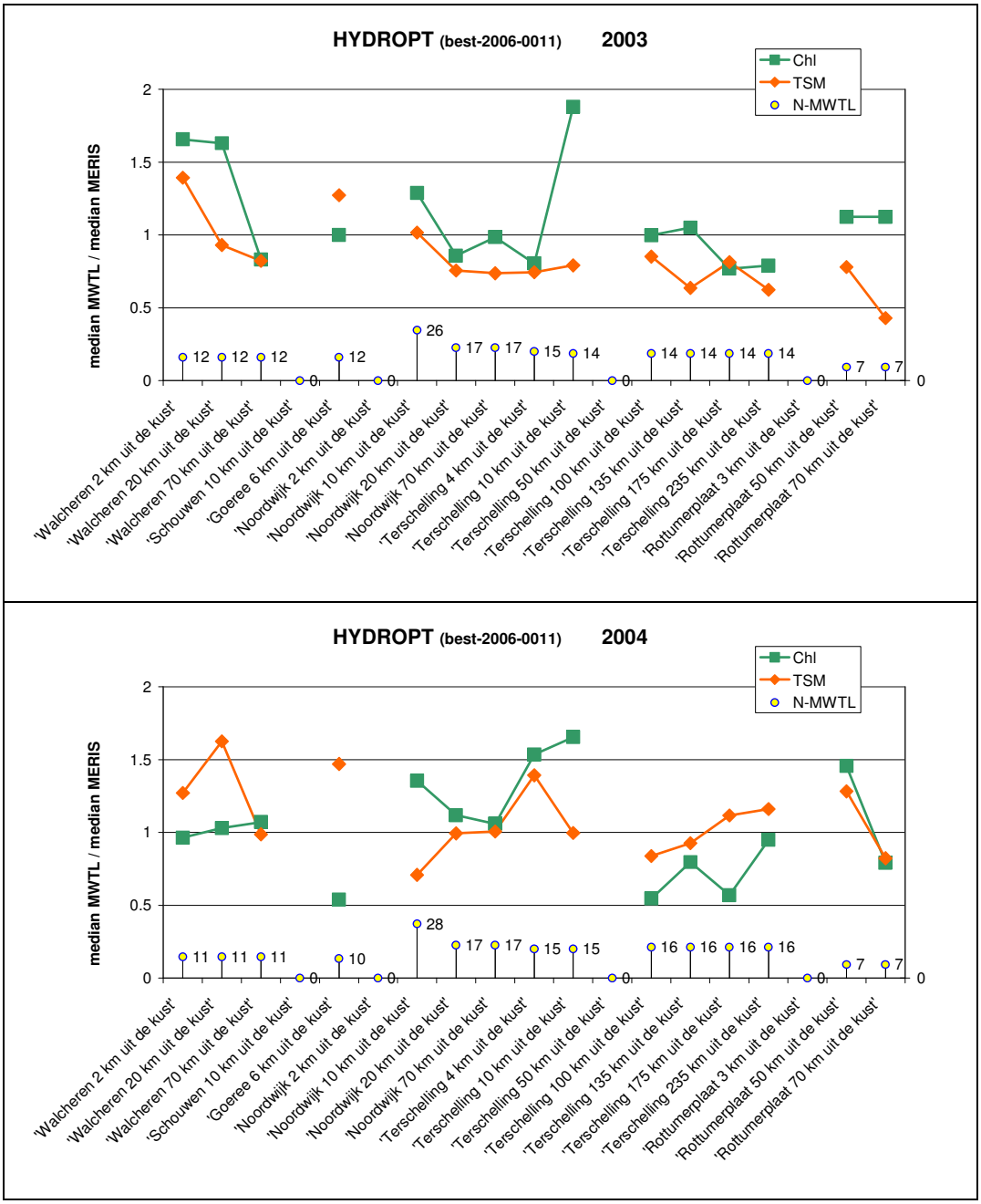


*Figure 9.6 Ratio of yearly median Chl-a and TSM per station for 2003 and 2004. Yellow circles indicate the number of in-situ samples taken at the MWTL station*

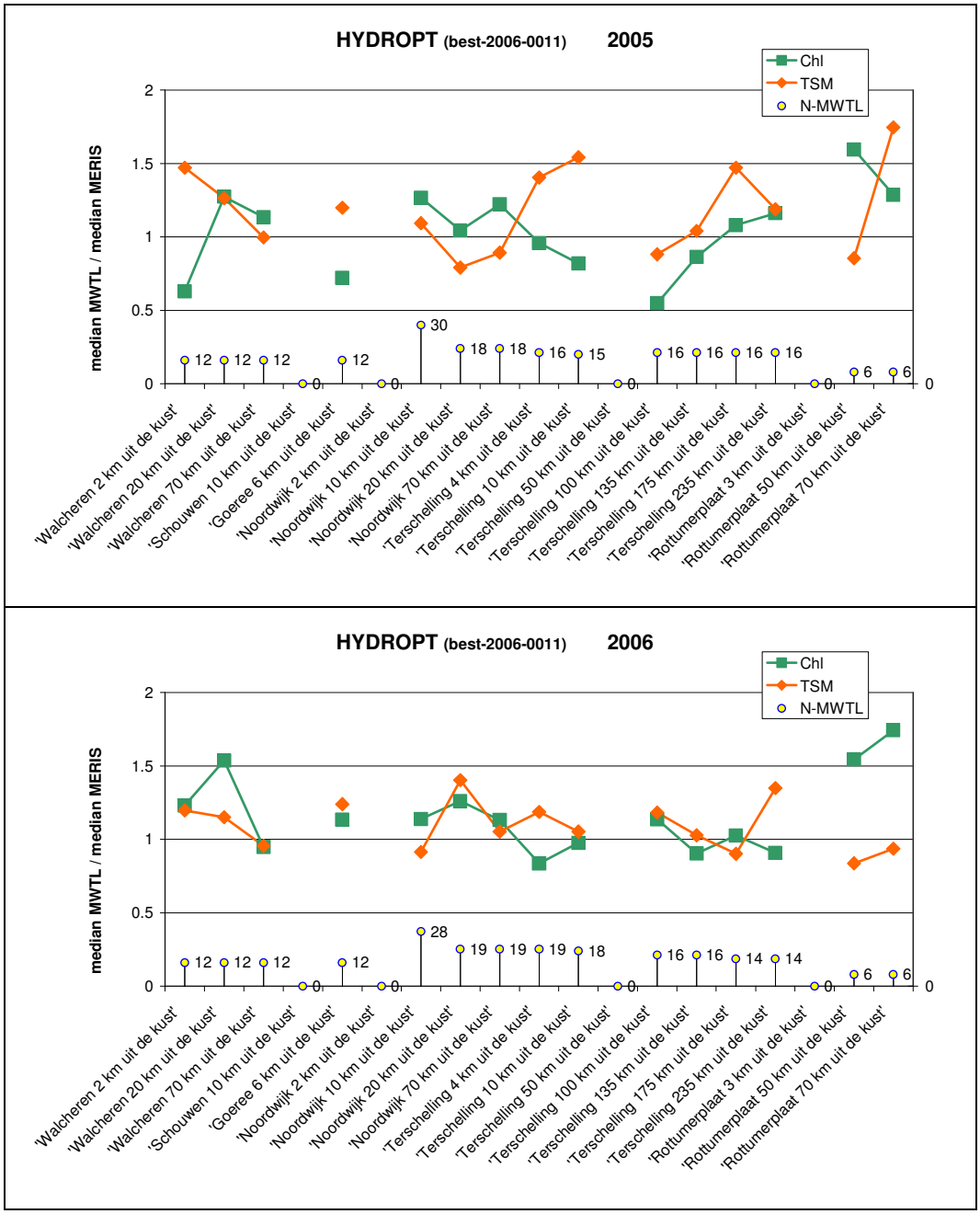


*Figure 9.7 Ratio of yearly median Chl-a and TSM per station for 2005 and 2006. Yellow circles indicate the number of in-situ samples taken at the MWTL station.*

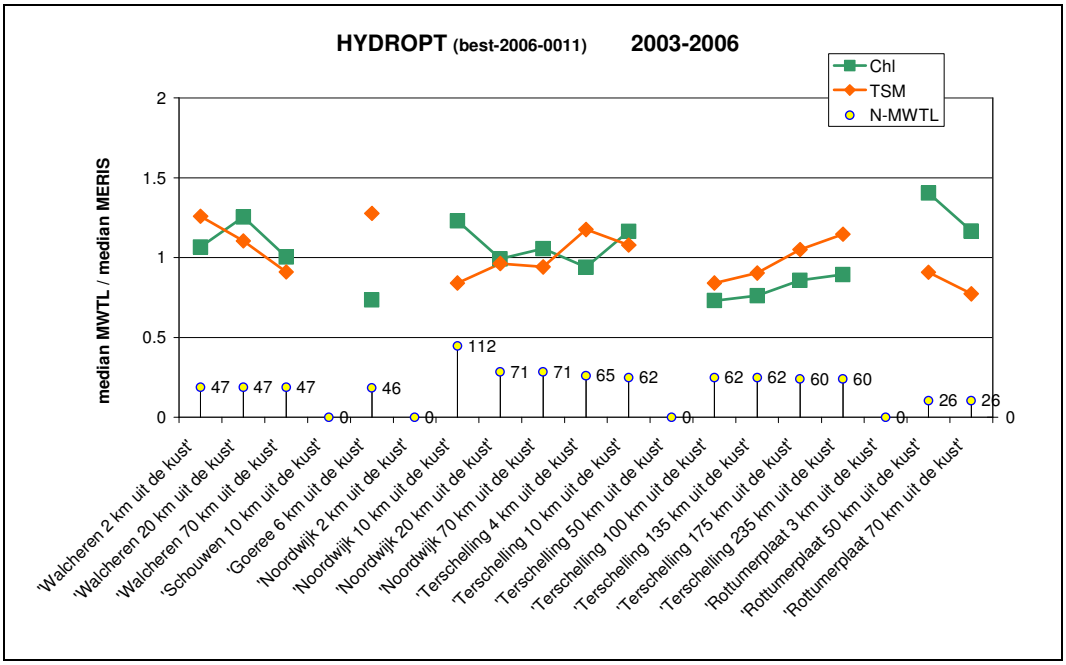


*Figure 9.8 Ratio of 4-yearly median Chl-a and TSM per station for the period 2003-2006. Yellow circles indicate the number of in-situ samples taken at the MWTL station*

- Rottumerplaat stations are less reliable because the stations are not sampled during wintertime. The Walcheren stations are probably also less reliable per year because the frequency of sampling is about once per month.
- The Noordwijk and Terschelling stations have relatively high sampling frequencies and a good correspondence between in-situ and satellite observations.
- When looking at the 2003 results (Figure 9.6) under estimation of blooms by the sparse in-situ data is probably the cause of the large relative errors in Chl-a at some stations.
- From the Figure 9.6 to Figure 9.8 and also the time series plots per station (see Appendix 1), it can be derived that the conclusion by Van der Woerd & Pasterkamp (2008) that HYDROPT is less suitable for case 1 waters is not confirmed for Dutch clear water stations.

Based on Figure 9.8 it is probably realistic to state that the relative accuracy of the satellite observations (both TSM and Chl-a) are well within 25% for all stations over 4 years. If calculated as Σ abs(1-median(MWTL)/median(MERIS))/N (over all stations; 4 years period) then the overall relative accuracy of MERIS Chl-a would be 16% and MERIS TSM would be 13%. If the frequency of in-situ sampling would increase, it is likely that this measurement of the relative accuracy of the HYDROPT MERIS results could improve maybe to around 10%. The good results for TSM are remarkable, especially in view of the fact that at individual stations the temporal variability can be very high. Still, the trend in TSM per year is captured very well by the satellite, evidently.

# 10. Comparison of SIOP results

In this chapter the final synthetic SIOP sets are compared to historic results (MAT-OPT-MEGS74 from the OVATIE-1 study) and field measurements (the REVAMP MEDIAN2 set from the REVAMP and AAN projects). In Figure 10.1, Figure 10.2, Figure 10.3 and Figure 10.4 the SIOP results are shown for the 5 selected sets that were tested for stability.

The selected dataset (best2006-0011 in brown) shows some typical deviations from the reference datasets (REVAMP-MEDIAN-2). In all wavelengths, but especially at 440 and 667 nm the phytoplankton absorption is much higher than the REVAMP measurements. This may be due to the fact that REVAMP measurements in the German, Dutch and Belgian waters were dominated by *Phaeocystis* blooms during 2003, while the other years showed a larger diversity of phytoplankton species. The $a^*_{NAP}$ (NAP= Non-algal Particles) of the optimised dataset is similar to the REVAMP measurements, albeit that the overall values are lower.

The most striking difference between the optimised SIOP set and the REVAMP measurements lies with the CDOM values, which are significantly higher in the optimised dataset. The cause of this difference is unclear. CDOM is a conservative parameter in the optimisation. The optimisation of the CDOM absorption slope is not restricted by CDOM measurements. In order to understand the sensitivity of the Chl-a and TSM retrieval for shifts in the CDOM absorption it would be necessary to re-evaluate the results of the optimised algorithm with different settings of the CDOM absorption slope. In the meanwhile one might postulate that the deviation in the optimised CDOM absorption is caused by inaccuracies in the atmospheric correction of MERIS. Especially in the blue region, large differences between in-situ measured water leaving reflectance and satellite observed reflectance have been reported by e.g. Peters, 2006. Optimised specific scattering generally is of the same value as the REVAMP data (which was derived from the publication by Babin et al., 2003).

The most pronounced effect of the optimisation on the scattering curve is a spectral differentiation. Specific scattering around 620, 665 are higher and the specific scattering around 709 nm is lower than the REVAMP measurements. It should be noted that in the REVAMP dataset measurements at 620 and 705 nm are under-represented because SIOP measurement systems like the AC-9 are programmed for SeaWiFS bands only. It is possible that the increase of 665 nm specific scattering is a compensation for the increase in phytoplankton absorption in the same spectral band. The most logical next step to understand the results of the SIOP optimisation would be to study time series of reflectance measurements at fixed location(s) or from ships together with match-ups of MERIS observations and to study CDOM absorption at MWTL locations.

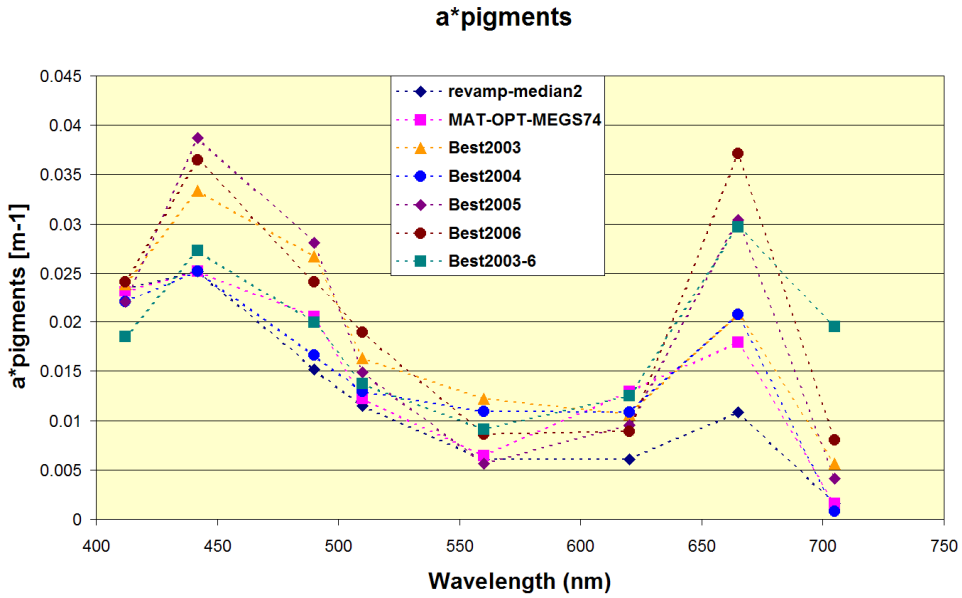


*Figure 10.1 Optimised specific phytoplankton absorption for Dutch MWTL stations. Presented are the results for MERIS bands for the algorithms that were obtained after optimisation with good pixels passing also the PCD-1-13 flag. Reference values (REVAMP median 2 and MAT-OPT-MEGS74 are also shown)*

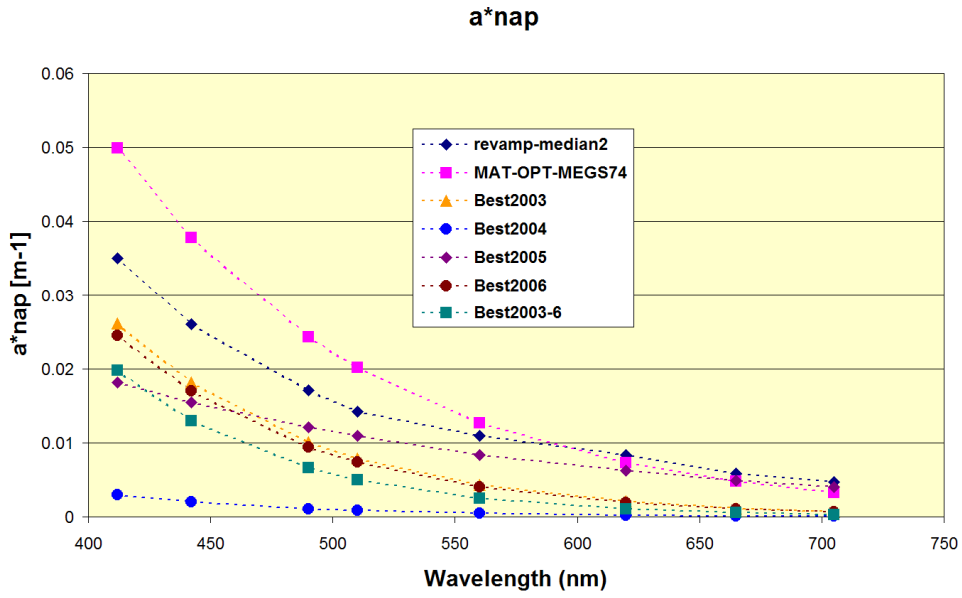


*Figure 10.2 Optimised specific tripton absorption for Dutch MWTL stations. Presented are the results for MERIS bands for the algorithms that were obtained after optimisation with good pixels passing also the PCD-1-13 flag. Reference values (REVAMP median 2 and MAT-OPT-MEGS74 are also shown)*

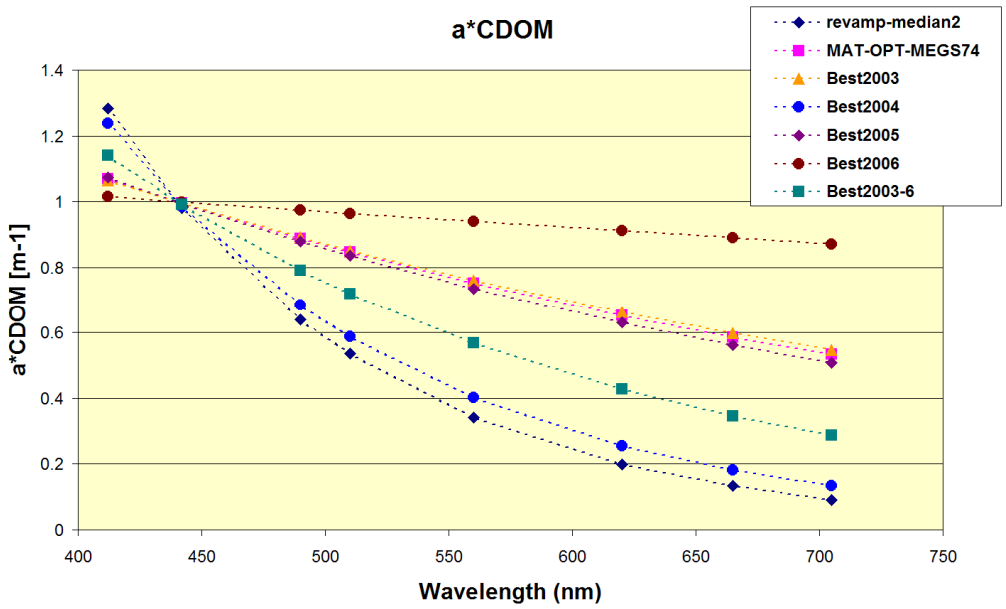


*Figure 10.3 Optimised normalised CDOM absorption for Dutch MWTL stations. Presented are the results for MERIS bands for the algorithms that were obtained after optimisation with good pixels passing also the PCD-1-13 flag. Reference values (REVAMP median 2 and MAT-OPT-MEGS74 are also shown)*

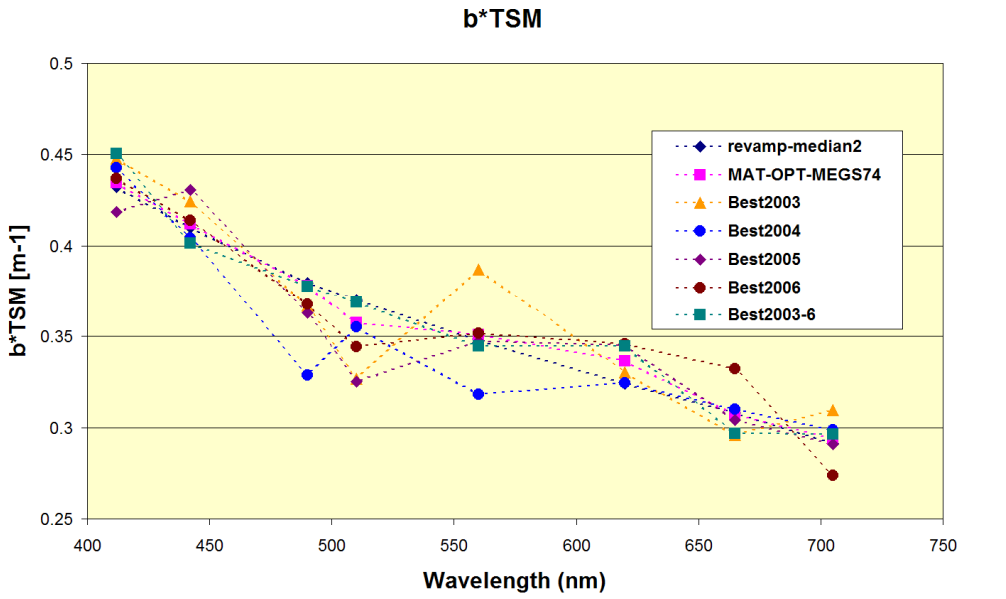


*Figure 10.4 Optimised specific TSM scattering for Dutch MWTL stations. Presented are the results for MERIS bands for the algorithms that were obtained after optimisation with good pixels passing also the PCD-1-13 flag. Reference values (REVAMP median 2 and MAT-OPT-MEGS74 are also shown)*

# 11. HYDROPT for MODIS-Aqua: customising and calibration results

## 11.1 Background

HYDROPT was developed for MERIS. Extension to other Ocean Colour sensors was anticipated in the programming approach of the HYDROPT software libraries, but was not implemented yet.

## 11.2 Using HYDROPT for MODIS processing

Whilst MERIS is a sensor on a European (ESA) satellite that has band-settings specifically targeted for good retrieval of CHL in coastal waters, NASA's MODIS-Aqua has different characteristics that are more in line with its predecessor SeaWiFS. These differences comprise, a.o., hardware (sensors), band settings, flags, viewing angles, data formats and processing software compliance. The following section shows how these differences were dealt with, so that HYDROPT could also be applied to MODIS data. This stepwise procedure was carefully implemented, checking results after each major alteration. The following steps were taken to enable the use of the HYDROPT algorithm for MODIS processing.

### Information collection

1. From the MERIS and MODIS specifications, differences in band settings in detector averaged centre wavelength were investigated. This is important for input SIOPS.
2. Information about MERIS and MODIS L2 file structure and flag coding was retrieved (Chapter 6 in this report, ESA, 2002; NASA, 2007b).
3. Subsequently HydroLight settings (Mobley, 1998) for HYDROPT (Pasterkamp et al., 2005; Van der Woerd & Pasterkamp, 2008) were investigated.

### Checking HydroLight settings for MERIS (consolidation of the existing software):

1. First HydroLight was run to recreate the lookup table with reflectances at MERIS wavelengths. The new output LUT version 20 and original LUT version 16 were compared.
2. Then a polynomial fit for the LUT was calculated and exported to allow fast Java processing (Van der Woerd & Pasterkamp, 2008).
3. The algorithm was run with standard SIOP settings (i.e., optimised with in situ 2003 data for MEGS 7.4 atmospherically corrected products) with LUT 16 and 20 and results were compared.

### MODIS LUT creation

1. Atmospherically corrected data with MUMM extension (Ruddick et al., 2000) were collected.
2. HydroLight was run to generate a lookup table with reflectances for the MODIS ban settings. Pure water absorption and scattering at MODIS wavelengths were estab-

lished, and approximations of absorption and scattering for other optical constituents were derived from the REVAMP median SIOP dataset for MERIS.
3. A polynomial fit for the LUT was calculated and exported to allow fast Java processing (Van der Woerd & Pasterkamp, 2008).

General adaptations to the HYDROPT software to read MODIS files:

1. Adapt the module to read satellite images from ENVISAT .N1 format to MODIS HDF5 format.
2. Translation the MODIS normalised water leaving radiances observations to HYDROPT required reflectances.
3. Accommodate differences in definitions of viewing geometry parameters between MERIS and MODIS
4. Adaptations to read the MODIS instead of the MERIS flags (in the case of MODIS the flags ATMFAIL or LAND or CLDICE are normally used to select water pixels with sufficient surface visibility and of which the atmospheric correction seems correct.

The new LUT and polynomial coefficients-table were extensively tested by comparing results of processed MERIS and MODIS images for the same day using the same SIOP dataset.

One important difference between MERIS and MODIS is the lack of a 620 and a 708 nm band in the MODIS configuration (see Table 6.1). Since HYDROPT essentially operates on consecutive band differences, this means that the most important band to determine Chl-a absorption in case-2 waters (the band around 667 nm) is now subtracted from the two nearest MODIS bands (547 and 747). It is expected that these differences affect the Chl-a retrieval of MODIS in case-2 waters to some extent.

## 11.3 Optimising the HYDROPT calibration for MODIS

Using the procedures outlined in Pasterkamp et al. (2005) and in this report a calibration of HYDROPT on MWTL data was performed to obtain the optimal SIOP set for this sensor for Dutch coastal waters.

Since it was requested by RWS to produce MODIS results on MWTL points and for the coastal waters for 2003 and 2004 it was deemed unnecessary in this stage to repeat the stability tests as executed for the MERIS 2003 – 2006 observations. As an alternative, the MODIS 2003 dataset was used to find the optimal SIOPs after which these were applied to the 2004 dataset without further adaptations.

As a result of this work, two datasets were finally transferred to RWS:

1. MODIS HYDROPT results on MWTL points for 2003 and 2004
2. Processing results of all available MODIS images

Here we will present the results as standard annual geometric mean scatter plots to compare the results of MODIS processing on MWTL points with MERIS results for 2003 and 2004.

## 11.4 Data screening for MODIS images

Unfortunately there was little time available in the project to investigate in depth the quality of the MODIS spectra and the reason why many MODIS spectra show negative values of zero values at lower wavelengths. During the calibration phase it appeared that many MODIS spectra are probably too low, resulting in invalid reflectance values. It was speculated that this might be a result of automated application of the MUMM atmospheric correction algorithm where tuning per image maybe should have been performed. On the other hand it cannot be excluded that standard SeaDAS atmospheric correction or image calibration already results in too low observations.

As a result, the basic data screening methods as designed for MERIS in this study were too strict which would corrupt the "maximum yield" strategy as formulated by RWS. Since the HYDROPT algorithm is designed to compensate for offset errors, it was attempted to widen the data screening criteria so that sufficient spectra of still acceptable quality pass the screening.

After some experimentation it was found that reasonable results can still be achieved with a maximum number of zero observations of 1 and a maximum of negative observations of 2.

Since the band with the longest wavelength (750 nm) features very high water absorption, it can be expected that (given the radiometric resolution of the sensor) in clear waters the values in this band approach zero. Contrary to the MERIS processing system, SEADAS produces negative reflectances. This is because the Neural Network underlying the MERIS processing always finds a positive answer from the training set, while SeaDAS removes atmospheric influences with a physical model. In this model erroneous aerosol characterisations may easily lead to offsets in the observed spectra.

Since MODIS does not feature a PCD-1-13 type flag, further data screening was performed using the HYDROPT $-\log(P(\chi 2))$ flag as described in this report.

## 11.5 Results of the HYDROPT MODIS calibration

Using the above outlined approach toward data screening and the extracted MODIS spectra at MWTL locations, an optimal SIOP set was calculated for all observations of 2003. The results are given in Figure 11.1.

Figure 11.1 and Figure 11.2 illustrate the somewhat reduced capability of MODIS (as compared to MERIS) to resolve Chl-a in Dutch coastal waters. In 2003 MODIS Chl-a is a bit biased (negative intercept with a slope that is very close to unity). In 2004 (with lower data availability due to cloudiness) the spread in the Chl-a results is rather large. This is possibly also a result of the wider data screening criteria (allowing 1 zero value and/or 2 negative values). On the other hand, MODIS provides very convincing results for TSM with low RMS values in both years.

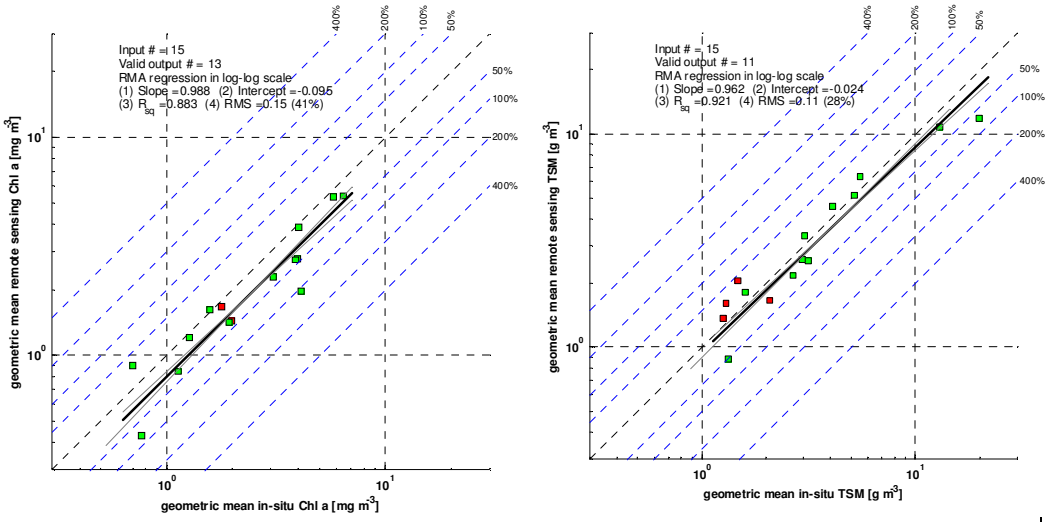


| | |
|---|---|
| SIOP: MODIS 2003 optimized<br>Parameter: CHL<br>Year: 2003 | SIOP: MODIS 2003 optimized<br>Parameter: TSM<br>Year: 2003 |

*Figure 11.1 Results of HYDROPT calibration for MODIS on MWTL observations of 2003. Shown are annual geometric mean Chl-a and TSM for valid MWTL stations*

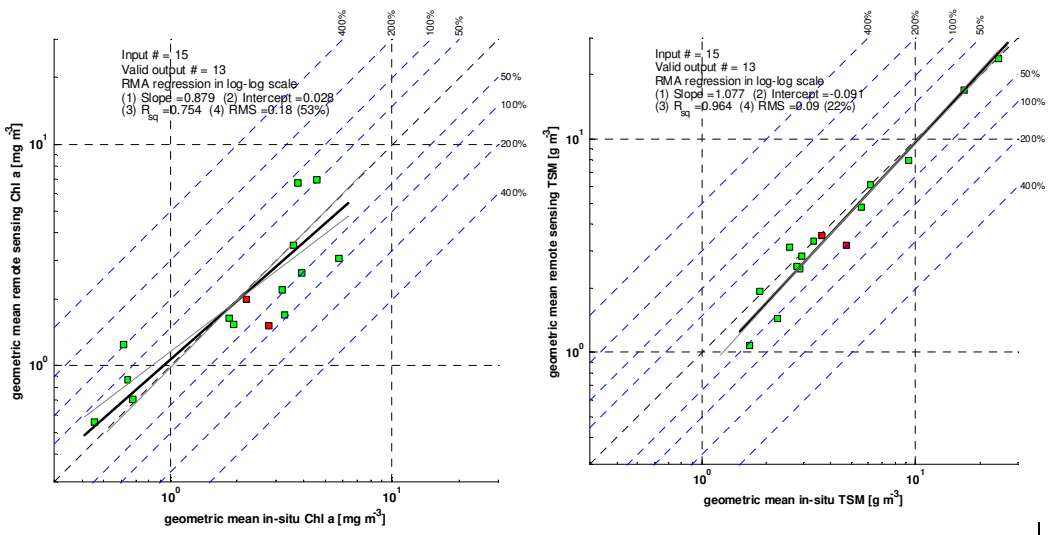


| | |
|---|---|
| SIOP: MODIS 2003 optimized<br>Parameter: CHL<br>Year: 2004 | SIOP: MODIS 2003 optimized<br>Parameter: TSM<br>Year: 2004 |

*Figure 11.2 Results of HYDROPT calibration for MODIS on MWTL observations of 2004. Shown are annual geometric mean Chl-a and TSM for valid MWTL stations.*

From this analysis we may conclude that HYDROPT MODIS TSM images for turbidity studies should be quite valuable, while HYDROPT MODIS Chl-a images should be used with caution. Comparative analysis of MODIS Chl-a results to simultaneous MERIS images could provide an insight in the consequences for MODIS Chl-a maps. It may very well be that MODIS Chl-a maps provide good insight in the spatial patterns of algae blooms, but with significantly more noise than similar MERIS maps. It may also be that MODIS Chl-a maps feature different patterns due to regional aerosol characterisation failures which would make the Chl-a maps less usable for operational purposes. In any case, further research is required to better characterize and possibly improve the MODIS Chl-a product for case-2 waters. Attention should be given to improved tuning of the atmospheric correction to avoid negative reflectances. It is also recommended to expand the MODIS validation dataset to 2005 and 2006, and possibly also to 2007 and 2008 and to obtain the most stable SIOP dataset for a longer period according to the methods outlined in this report.

# 12. Conclusions and recommendations

In this study the HYDROPT algorithm was calibrated for optimal performance in Dutch coastal waters. To do so, synthetic (optimized) SIOPs were calculated based on a fit of MERIS derived TSM and Chl-a values to MWTL observed TSM and Chl-a values for the years 2003-2006. First, the optimisations were done per year with various permutations of a priori and a posteriori data screening methods. Based on requirements by RWS three main data screening strategies were designed:

1. The flags=1000 case. Basic screening for obvious erroneous spectra. This involves the screening for negative values, zero values at lower wavelengths and high (saturation) values. Although this screening is done for MERIS by ESA by means of the PCD-1-13 flag, it was implemented separately for HYDROPT. The main reason for this is that the PCD-1-13 flag is not available for other sensors and the flag is reportedly too strict (possibly because it is partly based on the High Glint Flag which is too strict).
2. The flags=0011 case. Highest quality data: this strategy uses a combination of the ESA PCD-1-13 flag and the HYDROPT (-log(P($\chi$2)) flag in order to select suitable pixels. Using the PCD-1-13 flag results in a large omission of data. Analysis indicates that mainly the High-glint component of the PCD-1-13 flag is too strict.
3. The flags=1001 case. Highest yield with reasonable quality data: this strategy uses only the HYDROPT (-log(P($\chi$2)) flag in order to select suitable pixels.

The second strategy can be applied to MERIS only since there is no PCD-1-13 equivalent flag for MODIS or other sensors. The first and third strategy can be applied to any sensor. During the analysis it was found that after removal of negative, zero and saturated spectra, the ESA High Glint flag is only of minor importance for MERIS data screening. It was therefore not applied in the final analysis.

Next, the best calibration result for each year for data screening strategy 1) and 3) was applied to all other years in order to test the stability of the calibration files for the period 2003-2006. As a result it was found that the SIOP set that was derived for 2006, using the highest quality data screening, performed best for all years (using both data screening strategies). Therefore it has been adopted as the best calibration for operational processing and for further validation studies.

MERIS results at MWTL locations for 2003-2006 based on this calibration were delivered to RWS for validation by an independent Institute, of which the results were published by Uhlig et al. (2007).

Also as a result of this project all available MERIS images of 2003-2006 were processed with the optimally calibrated HYDROPT algorithm. The results of this processing were delivered on portable HD to RWS/DID.

In the process of determining the best calibration it was found that the optimisation procedure suffers from a starting value problem: initializing the Levenberg-Marquardt procedure with another SIOP set leads to different results. This was dealt with by taking the most realistic measured dataset as starting point for all analysis: the revamp-median2

dataset. An additional step was implemented whereby the optimisation was executed in a number of consecutive loops. Each loop was started by initialising the optimisation procedure with the SIOP result of the previous loop. This resulted in incremental improvements for each loop for some runs. Other runs showed little improvements after the first or second run. In order to test if the optimisation is sensitive to local minima, a small random component was added to the phytoplankton specific absorption before starting a new optimisation loop. As a result, most optimisation runs now showed a highly increased accuracy. From each set of 6 iteration loops the SIOPs of the best performing loop were selected for stability testing.

Stability testing was performed by validating HYDROPT results calibrated with the best SIOP sets for each year and data screening strategy with MWTL results of other years. Because the MWTL and the MERIS results are unevenly distributed over stations and in time an analysis was made of the availability of the data. It was found that:

- All stations are visible to MERIS with a frequency of about 80 observations per year
- The lowest availability of MERIS observations is at Noordwijk 2 (50 per year) and the highest availability is at Walcheren 20 (90 per year).
- In-situ data are unevenly distributed per station: some stations are not sampled or under sampled in winter
- In general the availability of MERIS observations is highest in April and May and lowest in December
- The year 2003 showed a higher data availability than the other 3 years
- The temporal distribution of Sunshine hours per month is very variable per year leading to variation bloom timing and intensity.

The fact that the stability analysis has selected 2006 as the best calibration year raises the suspicion that 2003 featured anomalous algae blooms (with respect to 2004-2006) that might have influenced the vicarious calibration. Indeed, 2003 was a year with extremely high *Phaeocystis* blooms which occurred to a much lesser extent in the following years. Since years with extreme blooms are relatively sparse (yet) the adoption of the 2006 calibration for longer term periods seems a good choice, but evidence from other extreme bloom years should be collected to verify this. E.g. 2007 would be a suitable year to do this.

For the calibration and validation runs one consistent method was used to calculate the statistics to underpin the selection of a best SIOP set. Use was made of yearly geometric mean data per station (MERIS and MWTL) to compensate for data availability differences. The yearly geometric means per station were plotted in log-log space in a scatter plot and regression parameters were calculated, assuming a linear relationship in log-log space for both Chl-a and TSM. It appeared that the Root Mean Square error was sufficiently discriminating to base selection of SIOPs on. Additional tests showed that optimisation in lin-lin space provided significantly worse results.

Also an analysis was made of the performance of the optimized algorithm for the individual MWTL stations. From the comparison per station of yearly MWTL and MERIS results very good results were achieved:

- Based on Figure 9.8 it is probably realistic to state that the relative accuracy of the satellite observations (both TSM and Chl-a) are well within 25% for all stations over 4 years. If calculated as Σ abs(1-median(MWTL)/median(MERIS))/N (over all stations; 4 years period) then the overall relative accuracy of MERIS Chl-a would be 16% and MERIS TSM would be 13%. If the frequency of in-situ sampling would increase, it is likely that this measurement of the relative accuracy of the HYDROPT MERIS results could improve maybe to around 10%. The good results for TSM are remarkable, especially in view of the fact that at individual stations the temporal variability can be very high. Still, the trend in TSM per year is captured very well by the satellite, evidently.
- There is no correlation between TSM and Chl-a deviations over all stations over the 4 year period which is an argument for the stability of the HYDROPT calibration.
- From the Figure 9.6 to 9.8 and also from the time series plots per station (see appendix 1), it can be derived that the conclusion by Van der Woerd and Pasterkamp (2008) that HYDROPT is less suitable for case 1 waters is not confirmed for Dutch clear water stations.
- The Noordwijk and Terschelling transect stations have relatively high sampling frequencies and a good correspondence between in-situ and satellite observations.

The station-wise comparison provided some issues that might be resolved in the future:

- TSM is systematically underestimated by MERIS at stations Walcheren 2 and Goeree 6. TSM is overestimated by the satellite at Noordwijk 20, Terschelling 100 and the Rottumerplaat stations 50 and 70.
- Chl-a is seriously overestimated by MERIS at Goeree 6. Interestingly, this station is regularly influenced by the fresh water outflow from the Haringvliet and Nieuwe Waterweg, which might influence the SIOP values.
- Rottumerplaat results are unreliable because the stations are not sampled during wintertime. The Walcheren transect stations are probably also less reliable per year because the frequency of sampling is about once per month.
- When looking at the 2003 results (Figure 9.6) under estimation of blooms by the sparse in-situ data is probably the cause of the large relative errors in Chl-a at some stations.

From the comparison of optimised SIOPs to REVAMP measurements it was concluded that:

- In all wavelengths, but especially at 440 and 667 nm the phytoplankton absorption is much higher than the REVAMP measurements. This may be due to the fact that REVAMP measurements in the German, Dutch and Belgian waters were dominated by *Phaeocystis* blooms during 2003, while the other years showed a larger diversity of phytoplankton species.
- The $a^*_{NAP}$ of the optimised dataset is similar to the REVAMP measurements, albeit that the overall values are lower.

- The most striking difference between the optimised SIOP set and the REVAMP measurements lies with the CDOM values, which are significantly higher in the optimised dataset. The cause of this difference is unclear. CDOM is a conservative parameter in the optimisation; therefore the optimisation of the CDOM absorption slope is not determined by CDOM MWTL measurements. In order to understand the sensitivity of the Chl-a and TSM retrieval for shifts in the CDOM absorption it would be necessary to re-evaluate the results of the optimised algorithm with different settings of the CDOM absorption slope.
- In the meanwhile one might postulate that the deviation in the optimised CDOM absorption is caused by inaccuracies in the atmospheric correction of MERIS. Especially in the blue region, large differences between in-situ measured water leaving reflectance and satellite observed reflectance have been reported by e.g. Peters, 2006.
- Optimised specific scattering generally is of the same value as the REVAMP data (which was derived from the publication by Babin et al. (2003). The most pronounced effect of the optimisation on the scattering curve is a spectral differentiation. Specific scattering around 620, 665 are higher and the specific scattering around 709 nm is lower than the REVAMP measurements. It should be noted that in the REVAMP dataset measurements at 620 and 705 nm are under-represented because SIOP measurement systems like the AC-9 are programmed for SeaWiFS bands only. It is possible that the increase of 665 nm specific scattering is a compensation for the increase in phytoplankton absorption in the same spectral band.
- The most logical next step to understand the results of the SIOP optimisation would be to study time series of reflectance measurements at fixed location(s) or from ships together with match-ups of MERIS observations and to study CDOM absorption at MWTL locations.

From the analysis of MODIS results for 2003 and 2004 it was concluded that:

- HYDROPT MODIS TSM images for turbidity studies should be quite valuable, while for the moment HYDROPT MODIS Chl-a images should be used with caution.
- Comparative analysis of MODIS Chl-a results to simultaneous MERIS images could provide an insight in the consequences for MODIS Chl-a maps
- Further research is required to better characterize and possibly improve the MODIS Chl-a product for case-2 waters. Attention should be given to improve the tuning of the atmospheric correction to avoid negative reflectance values.
- It is recommended to expand the MODIS validation dataset to 2005 and 2006, and possibly also to 2007 and 2008 and to obtain the most stable SIOP dataset for a longer period according to the methods outlined in this report.

## General conclusions

The calibrated HYDROPT algorithm using the best-2006-0011 SIOP set performs very well for TSM and Chl-a retrieval from MERIS in Dutch coastal waters. Validation with data from 2003, 2004 and 2005 confirm this. It is possible to loosen data screening criteria (as compared to the ESA PCD-1-13 flag) to accommodate a 'maximum yield' strategy. HYDROPT was also calibrated for MODIS band settings using MWTL data of 2003. The calibrated algorithm was validated using 2004 data which indicated that MODIS results seem to be less accurate for Chl-a. The results for TSM are very good. Since it is expected that the images of 2007 and 2008 will confirm the results of this study, it is concluded that the current best-2006-0011 SIOP set should be used for operational processing.

## General recommendations

In order to further substantiate the validation results it is recommended to expand the MERIS analysis to the results of 2007 and 2008. For MODIS it is recommended to perform a stability analysis to determine the SIOP set that performs best for multiple years. Therefore an analysis should be made of MODIS images of 2005 and 2006, preferably expanded with images from2007 and 2008.

## Possible follow-up research

From the graphs of time series per MWTL location it is obvious that the peak of the spring bloom is quite variable in time. This was also noticed by Uhlig et al. (2007). This variability affects the outcome of detailed validation according to the method proposed by Van Duin and executed by Uhlig et al. (2007). It is recommended to study the time series per MWTL point and to design methods to accommodate for the inter-annual variability in the Van Duin method of validation.

Since there are unexplained deviations at certain locations between satellite and MWTL results (e.g. at Goeree 6) it is recommended to set-up additional field studies to study the variability of SIOPs at MWTL locations in time. Ideally, the monitoring ship should be instrumented with a package of AC-9, BB6 and TRIOS autonomous measurements systems to collect reliable and representative volumes of SIOP measurements.

# 13. Literature

Babin, M., Stramski, D., Ferrari, G.M., Claustre, H., Bricaud, A., Obolensky, G. & Hoepffner, N. (2003). Variations in the light absorption coefficients of phytoplankton, non-algal particles, and dissolved organic matter in coastal waters around Europe. *Journal of Geophysical Research-Oceans, 108*(3211).

Campbell, J. W. (1995). The log-normal distribution as a model for bio-optical variability in the sea. *J. Geophys. Res., 100*(C7), 13, 237–13,254.

Defoin-Platel, M. & Chami, M. (2007). How ambiguous is the inverse problem of ocean color in coastal waters? *Journal of Geophysical Research 112,* C03004.

Eleveld, M.A., Pasterkamp R., van der Woerd, H.J. & Pietrzak, J. (2008). Remotely sensed seasonality in the spatial distribution of sea-surface suspended particulate matter in the southern North Sea. *Estuarine, Coastal and Shelf Science, 80*, 103–113.

ESA, 2002. MERIS Algorithm Theoretical Basis Documents. Online available at http://envisat.esa.int/instruments/meris/atbd/

Dury, S., Hakvoort, H., Jordans, R., Hesselmans, G. & Slater, M. (2004). *Water quality monitoring in the Southern North Sea by optical remote sensing: validation of satellite data*. AGI report no. 0406GAR001, Delft, Netherlands.

Gons, H. J., Rijkeboer, M. & Ruddick, K. G. (2002). A chlorophyll-retrieval algorithm for satellite imagery (Medium Resolution Imaging Spectrometer) of inland and coastal waters. *Journal of Plankton Research, 24*, 947–951.

Gordon, H. R., Brown, O. B., Evans, R. H., Brown, J. W., Smith, R. C., Baker, K. S., et al. (1988). A semianalytic radiance model of ocean color. *Journal of Geophysical Research-Oceans, 93*, 10 909–10 924.

Hoogenboom, H.J., Dekker, A.G. & de Haan, J.F. (1998). *InveRSion: assessment of water composition from spectral reflectance*: *a feasibility study to the use of the matrix inversion method.* Report number E-98/11 (NRSP-2 report 98-15), IVM, Amsterdam, Netherlands.

Mobley, C.D. (1994). *Light and water; Radiative transfer in natural waters*. London: Academic Press.

Mobley, C.D. (1998). *Hydrolight 4.0 Users' guide*. Sequoia Scientific, Inc., Mercer Island, Washington.

Mobley, C.D., Gentili, B., Gordon, H.R., Jin, Z., Kattawar, G.W., Morel, A., Reinersman, P.H., Stamnes, K. & Stavn, R.H.1(993). Comparison of numerical models for computing underwater light fields. *Appl. Opt., 32*, 7484-7504.

Mobley, C.D., Sundman, L.K. & Boss, E. (2002). Phase function effects on oceanic light fields, *Appl. Opt., 41*(6), 1035-1050.

NASA (2007). MODIS Algorithm Theoretical Basis Documents. Online available at http://modis.gsfc.nasa.gov/data/atbd/ocean_atbd.php

O'Reilly, J. E., Maritorena, S., Mitchell, B. G., Siegel, D. A., Carder, K. L., Garver, S., et al. (1998). Ocean color chlorophyll algorithms for SeaWiFS. *Journal of Geophysical Research-Oceans, 103*, 24937–24953.

O'Reilly, J. E., Maritorena, S., Siegel, D., O'Brien, M., Toole, D., Greg Mitchell, B., et al. (2000). Ocean color chlorophyll a algorithms for SeaWiFS, OC2, and OC4: Version 4. In O'Reilly, J.E. (Ed.), *SeaWiFS Postlaunch Calibration and Validation Analyses, Part 3. NASA NASA Technical Memorandum 2000-206892, Vol. 11*. (pp. 9–23). Greenbelt, Maryland: NASA Goddard Space Flight Center Chapter 2.

Otto, L., Zimmerman, J.T.F., Furnes, G.K., Mork, M., Saetre, R. & Becker, G. (1990). Review of the physical oceanography of the North Sea. Neth. J.*Sea Res., 26*, 161-238.

Pasterkamp, R., van der Woerd, H.J., Roberti, J.R., Peters, S.W.M. & Eleveld, M.A. (2005). *Simultaneous determination of suspended sediment and chlorophyll-a: validation for the North Sea in 2003*. Halifax, Nova Scotia, presented at the Eighth International Conference on Remote Sensing for Marine and Coastal Environments.

Pasterkamp, R. (1999). *Optical modelling of coastal waters*. IVM Report (O-99/06). Institute for Environmental Studies, VU University, Amsterdam.

Peters, S.W.M., Eleveld, M.A., Pasterkamp, R., van der Woerd, H.J., Devolder, M., Jans, S., Park, Y., Ruddick, K.G., Block, T, Brockmann, C., Doerffer, R., Kraseman, H.L., Schönfeld, W., Jørgensen, P.V., Tilstone, G.H., Moore, G.F., Sørensen, K. & Aas, E. (2005). *Atlas of Chlorophyll-a concentration for the North Sea based on MERIS imagery of 2003*. IVM report (R-05/03). Institute for Environmental Studies, VU University, Amsterdam, 117 pp. ISBN 90-5192-026-1.

Peters, S.W.M. (2006). *MERIS Reflectance and Algal-2 validation at the North Sea*. Proceedings ESA- MAVT, Frascati, Rome.

Ruddick, K.G., Ovidio, F. & Rijkeboer, M. (2000). Atmospheric Correction of SeaWIFS Imagery for Turbid Coastal and Inland Waters. *Applied Optics, 39*, 897–912.

Sørensen, K., Grung, M. & Röttgers, R. (2007). An intercomparison of in vitro chlorophyll a determinations for MERIS level 2 data validation. *Int. J. Rem. Sens., 28*(3), 537 — 554.

Tilstone, G. H., Moore, G. F., Sørensen, K., Doerffer, R., Røttgers, R., Ruddick, K. G., Pasterkamp, R. & Jørgensen, P.V. (2004). *Protocols for the validation of MERIS products in Case 2 waters.* Proceedings of the ENVISAT validation workshop, European Space Agency. 6(10):875-889.

Tilstone, G.H. et al. (2008). Variation in absorption properties of the North Sea: Application to case 2 ocean colour satellite algorithms. Submitted to Journal of Geophysical research (in review).

Uhlig, S., Simon, K., Antoni, S. & Kunath, K. (2007). *Incorporation of Remote Sensing Data in Monitoring Programmes*. Report by Quo Data Quality Management and Statistics GmbH, Dresden; under supervision and commission by: Dr. Richard N.M. Duin (Rijkswaterstaat).

van der Woerd, H.J, Pasterkamp, R. (2005). *Chlorofyl atlas van de Nederlandse kustzone*. Management rapport project RIKZ - 1173; Periode 2004-2005. IVM Report (W-05/31). Institute for Environmental Studies, VU University, Amsterdam.

van der Woerd, H.J. & Pasterkamp, R. (2008). HYDROPT: A fast and flexible method to retrieve chlorophyll-a from multispectral satellite observations of optically complex coastal waters. *Remote Sensing of Environment, 112*, 1795-1807.

# Appendix I. Time series graphs of TSM and Chl-a at MWTL stations

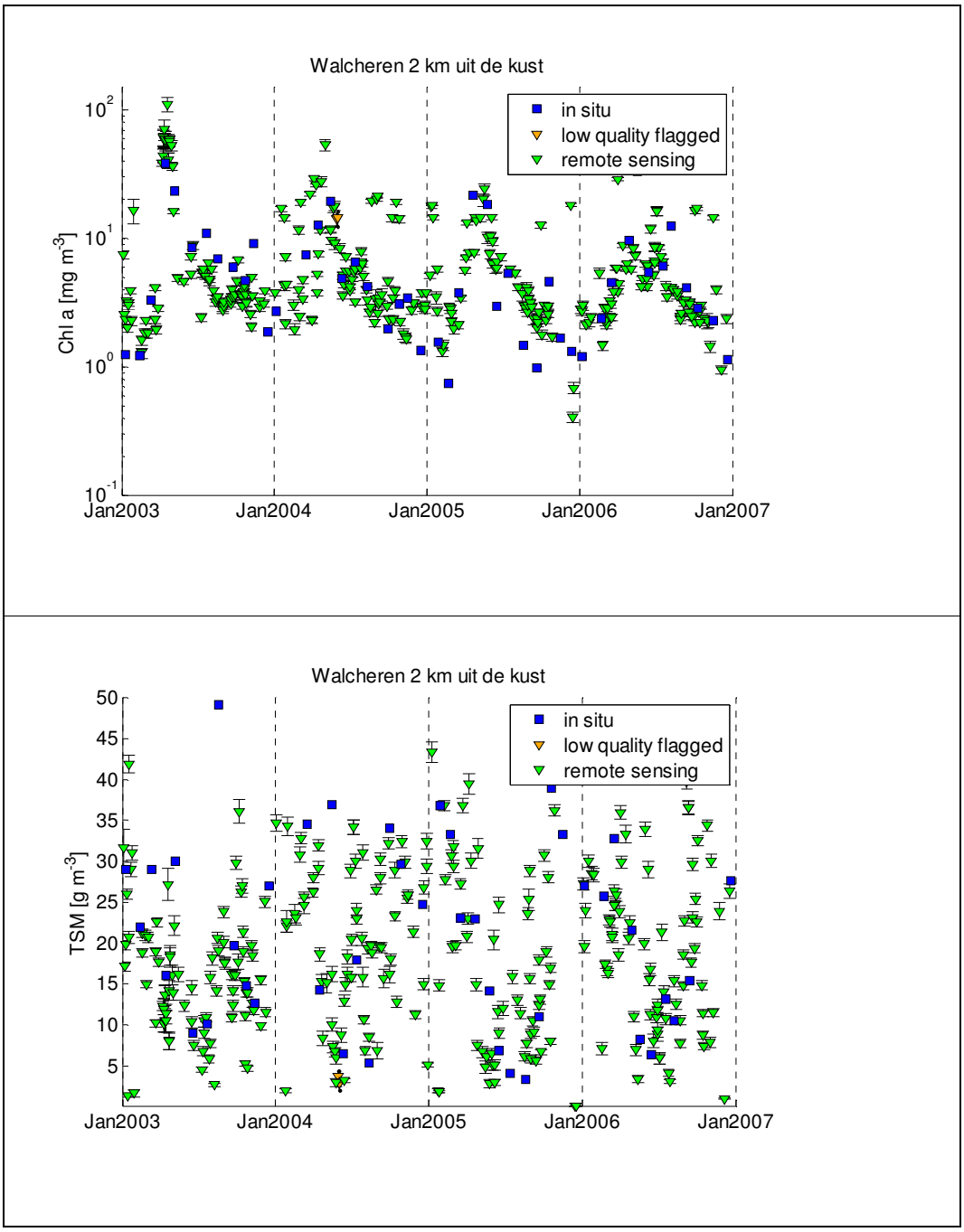


*Figure I.1 Station "Walcheren 2 km uit de kust": Time series of Chl-a and TSM (blue squares = MWTL and green triangles = MERIS-best-2006-0011). Shown are the results for "high yield" data screening.*

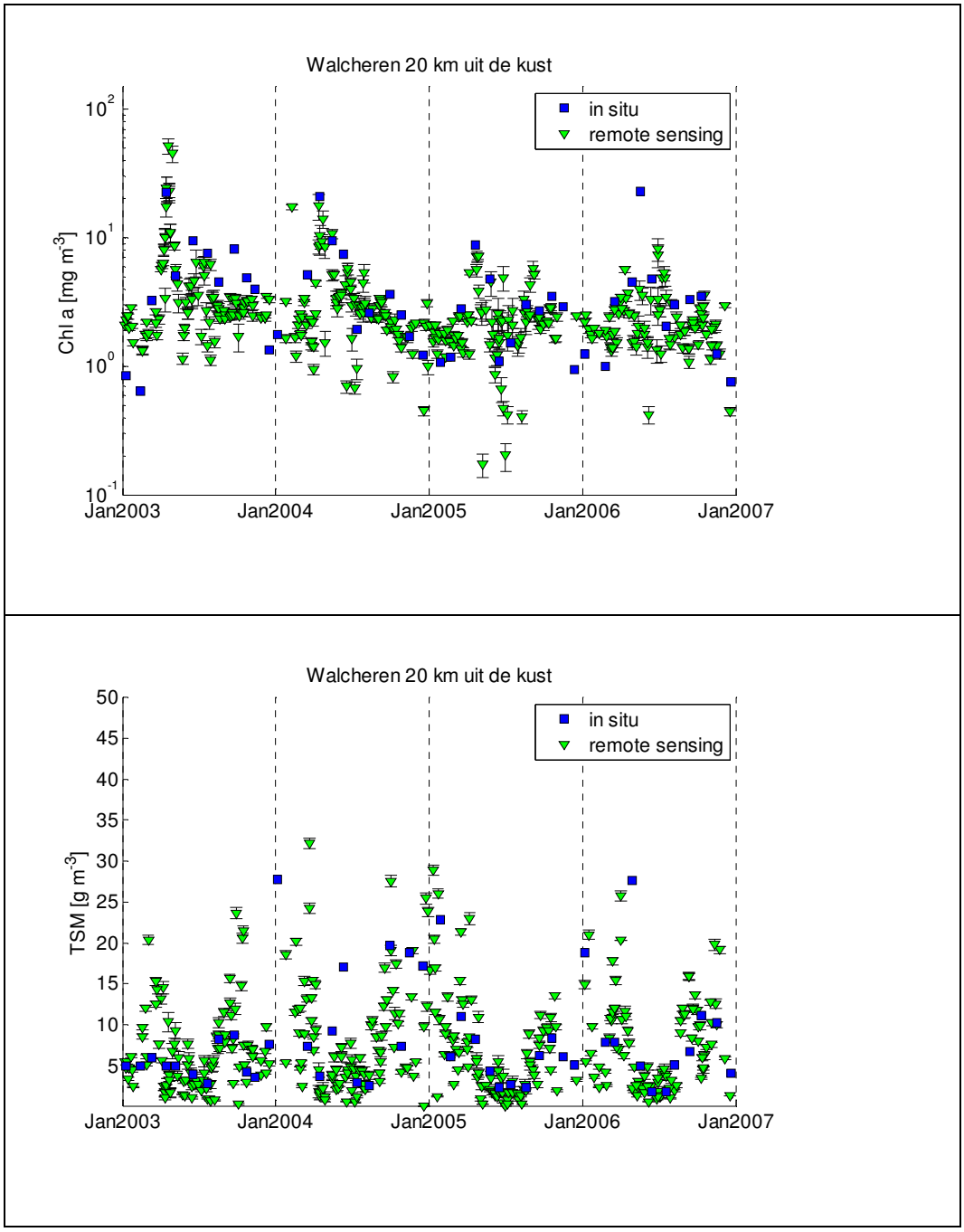


*Figure I.2 Station "Walcheren 20 km uit de kust": Time series of Chl-a and TSM (blue squares = MWTL and green triangles = MERIS-best-2006-0011). Shown are the results for "high yield" data screening.*

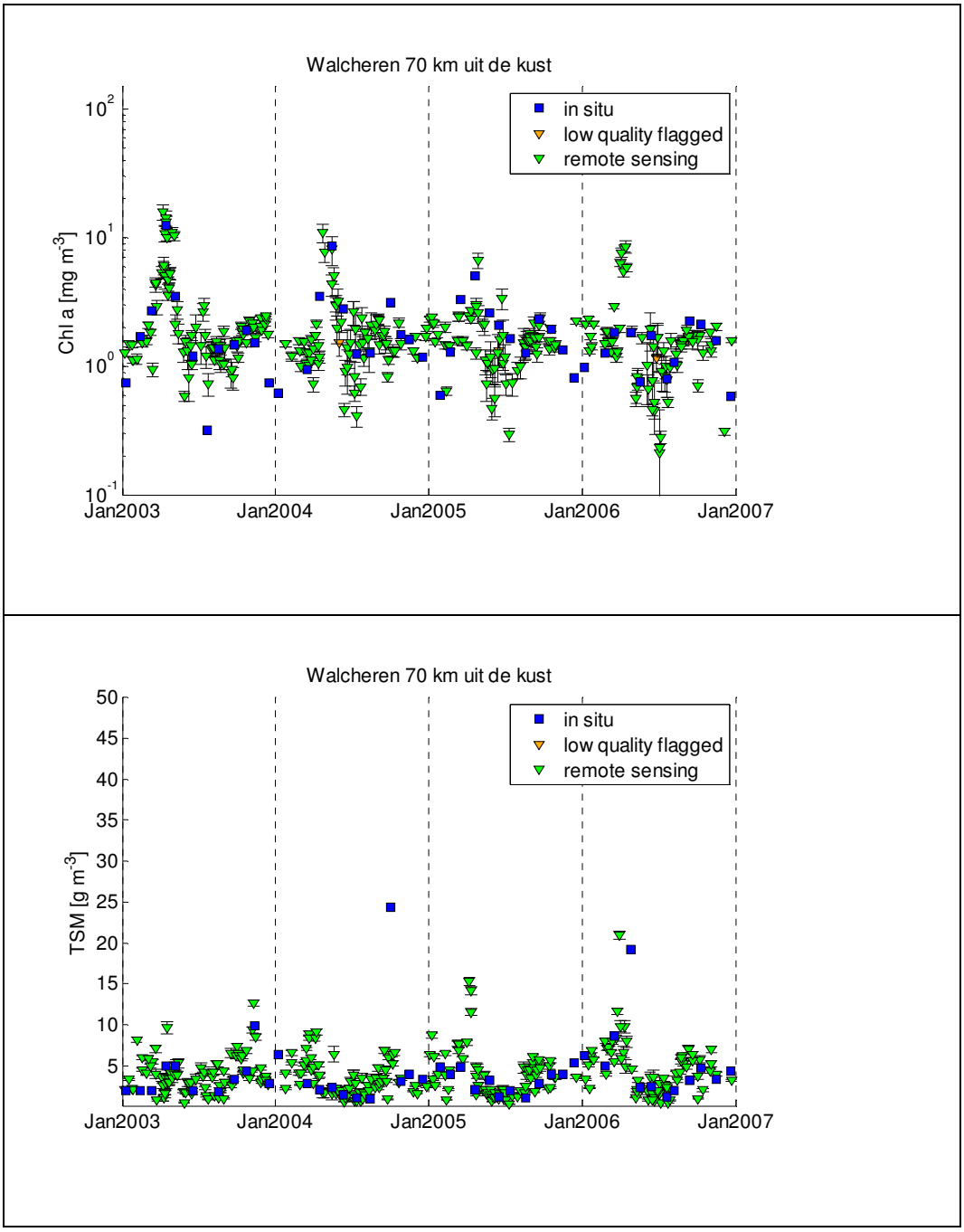


*Figure I.3 Station "Walcheren 70 km uit de kust": Time series of Chl-a and TSM (blue squares = MWTL and green triangles = MERIS-best-2006-0011). Shown are the results for "high yield" data screening.*

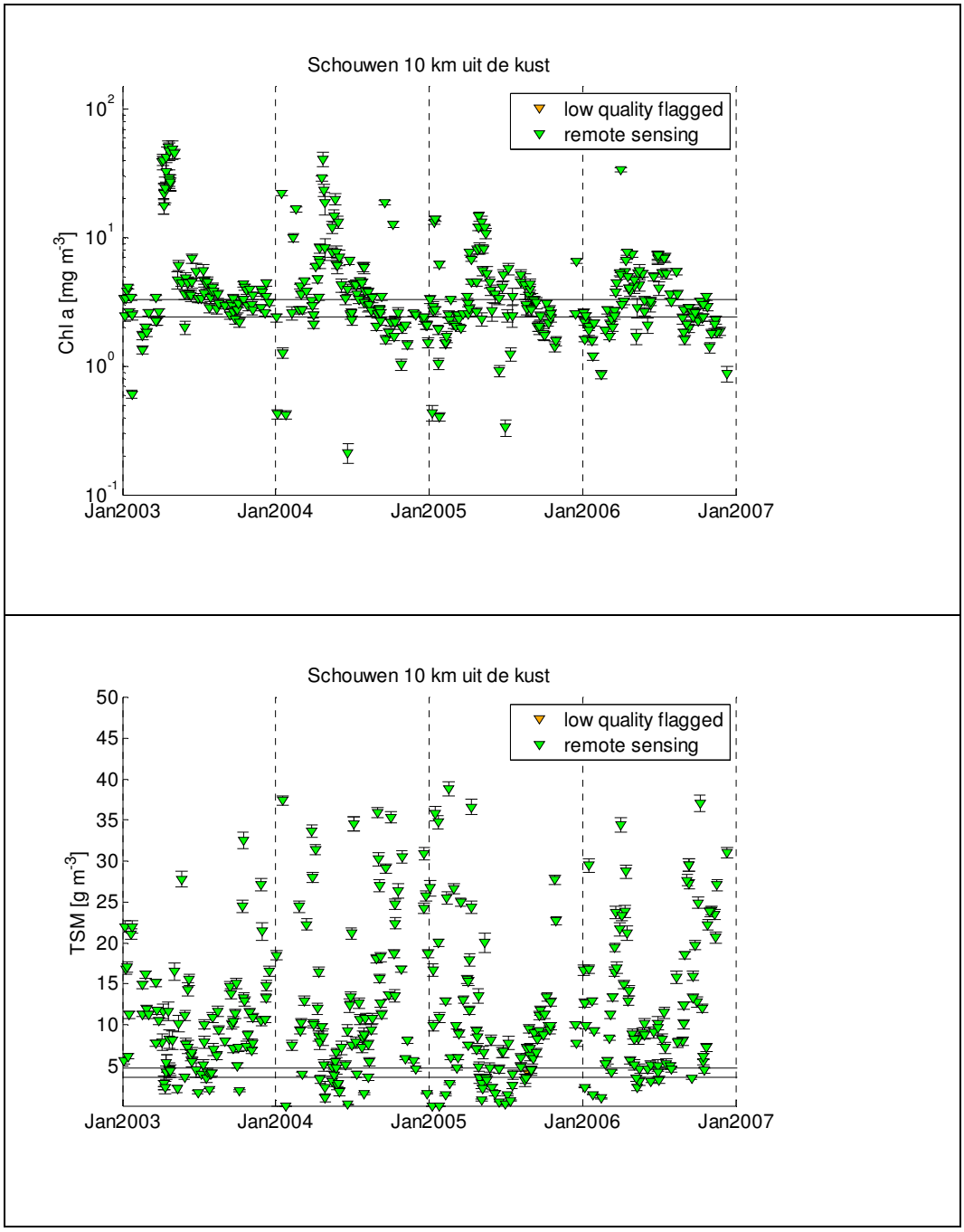


*Figure I.4 Station "Schouwen 10 km uit de kust": Time series of Chl-a and TSM (blue squares = MWTL and green triangles = MERIS-best-2006-0011). Shown are the results for "high yield" data screening.*

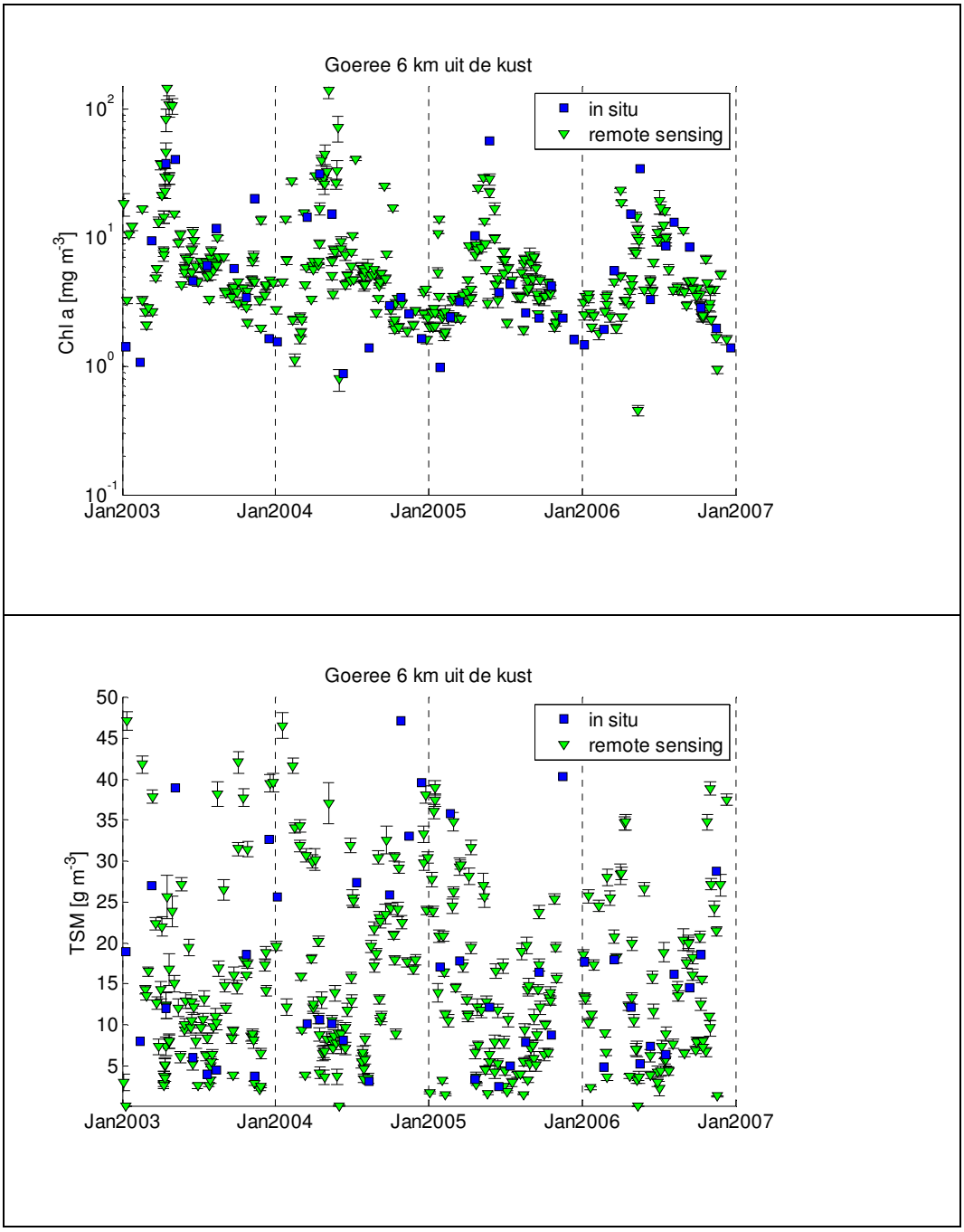


*Figure I.5 Station "Goeree 6 km uit de kust": Time series of Chl-a and TSM (blue squares = MWTL and green triangles = MERIS-best-2006-0011). Shown are the results for "high yield" data screening.*

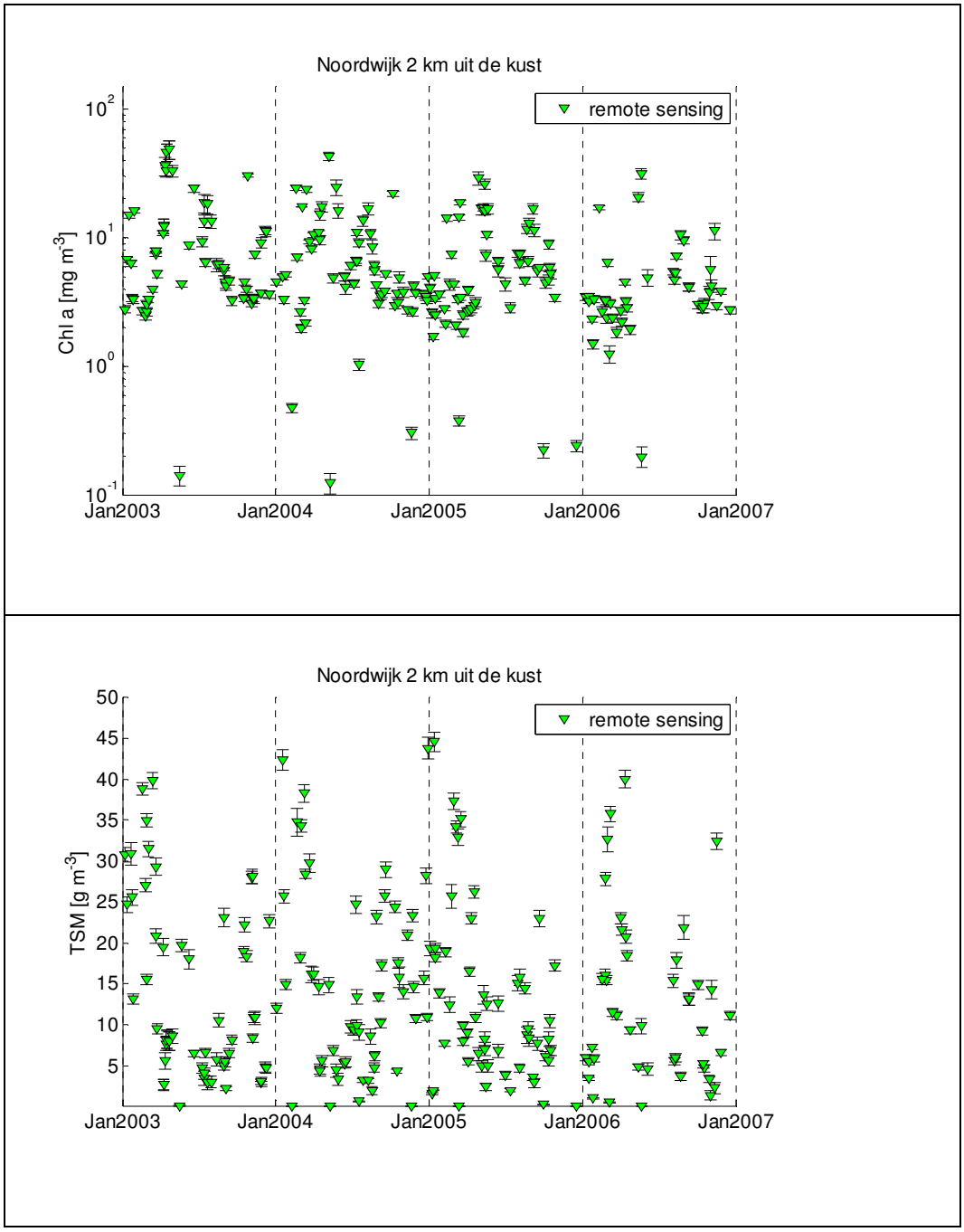


*Figure I.6 Station "Noordwijk 2 km uit de kust": Time series of Chl-a and TSM (blue squares = MWTL and green triangles = MERIS-best-2006-0011). Shown are the results for "high yield" data screening.*

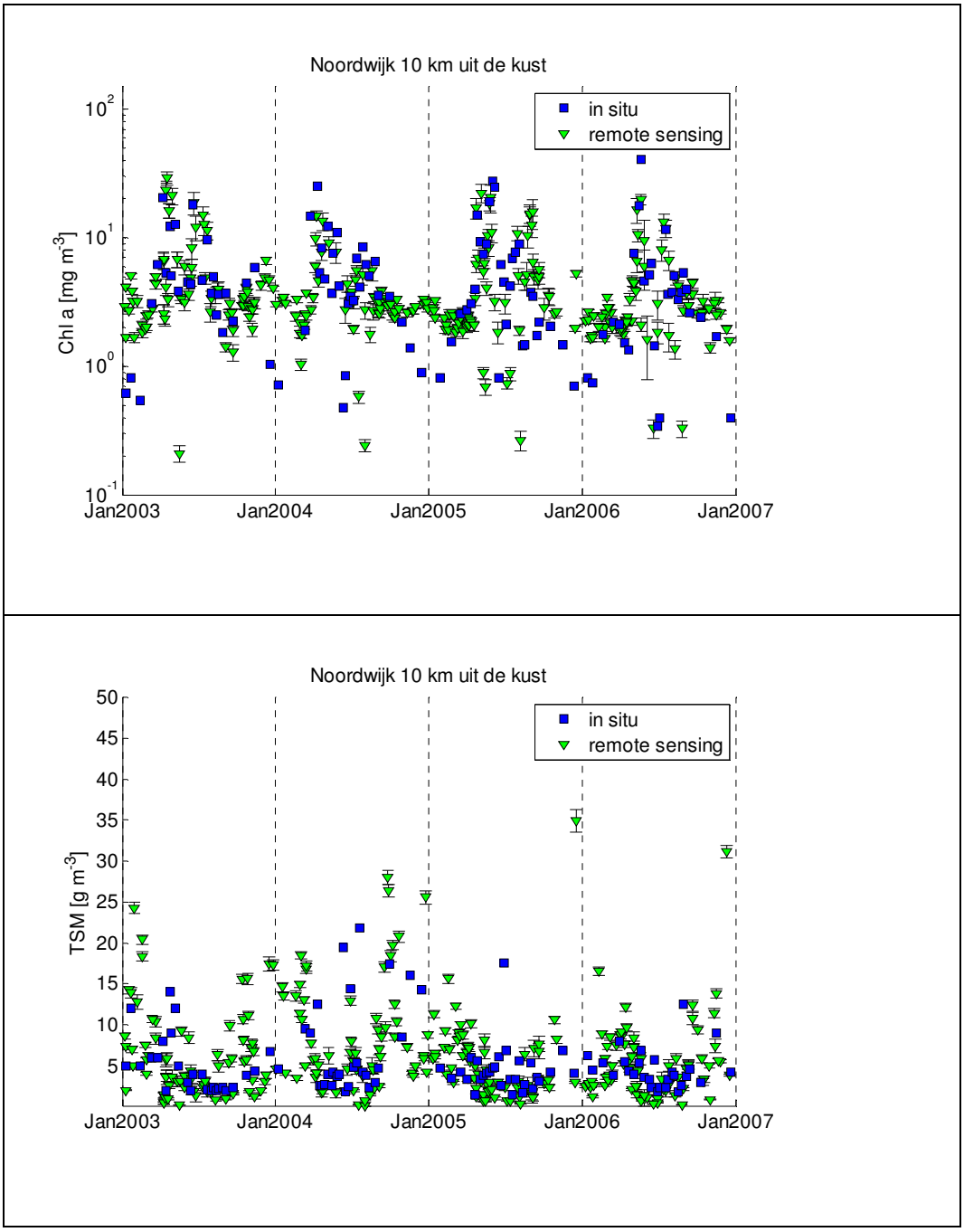


*Figure I.7 Station "Noordwijk 10 km uit de kust": Time series of Chl-a and TSM (blue squares = MWTL and green triangles = MERIS-best-2006-0011). Shown are the results for "high yield" data screening.*

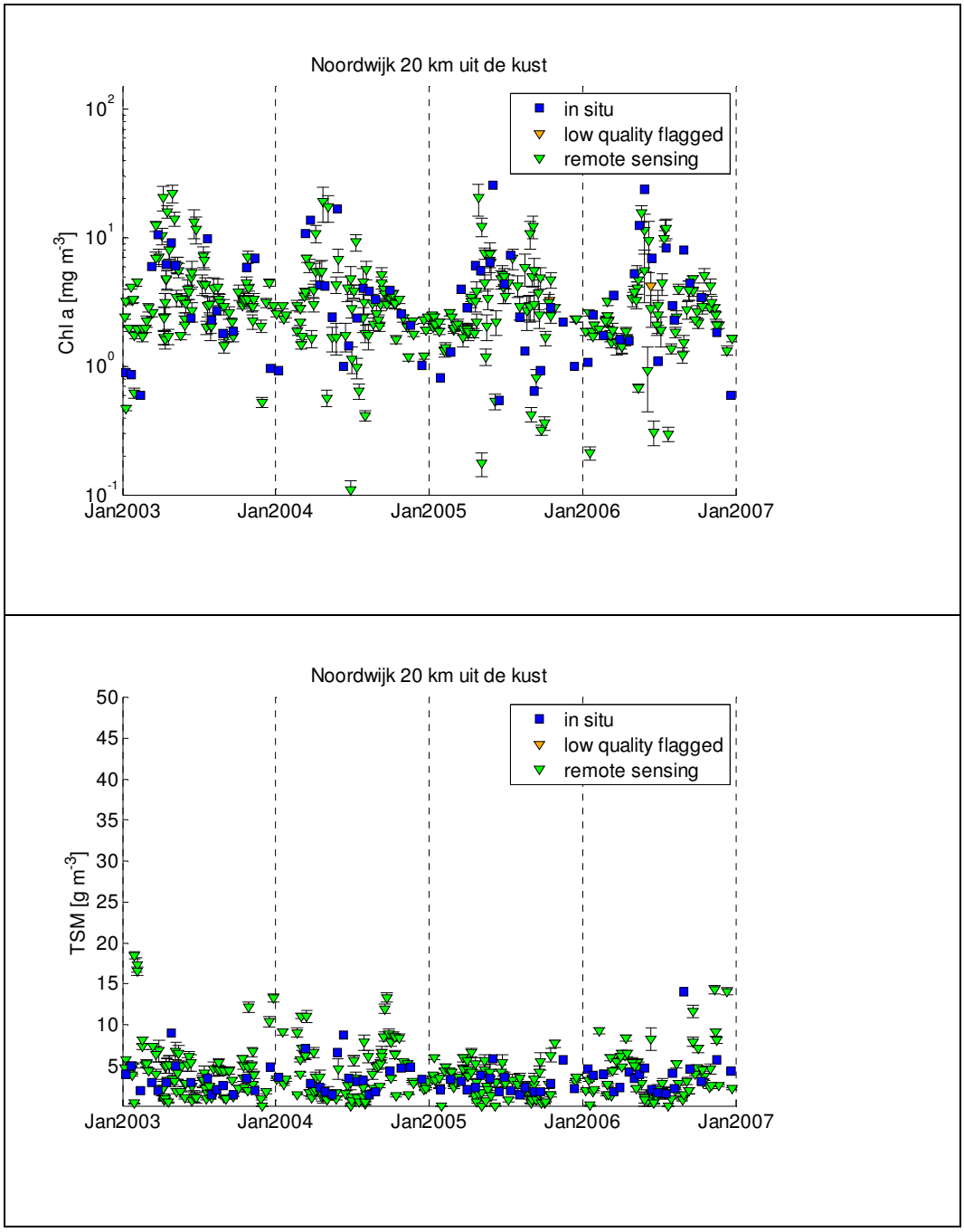


*Figure I.8 Station "Noordwijk 20 km uit de kust": Time series of Chl-a and TSM (blue squares = MWTL and green triangles = MERIS-best-2006-0011). Shown are the results for "high yield" data screening.*

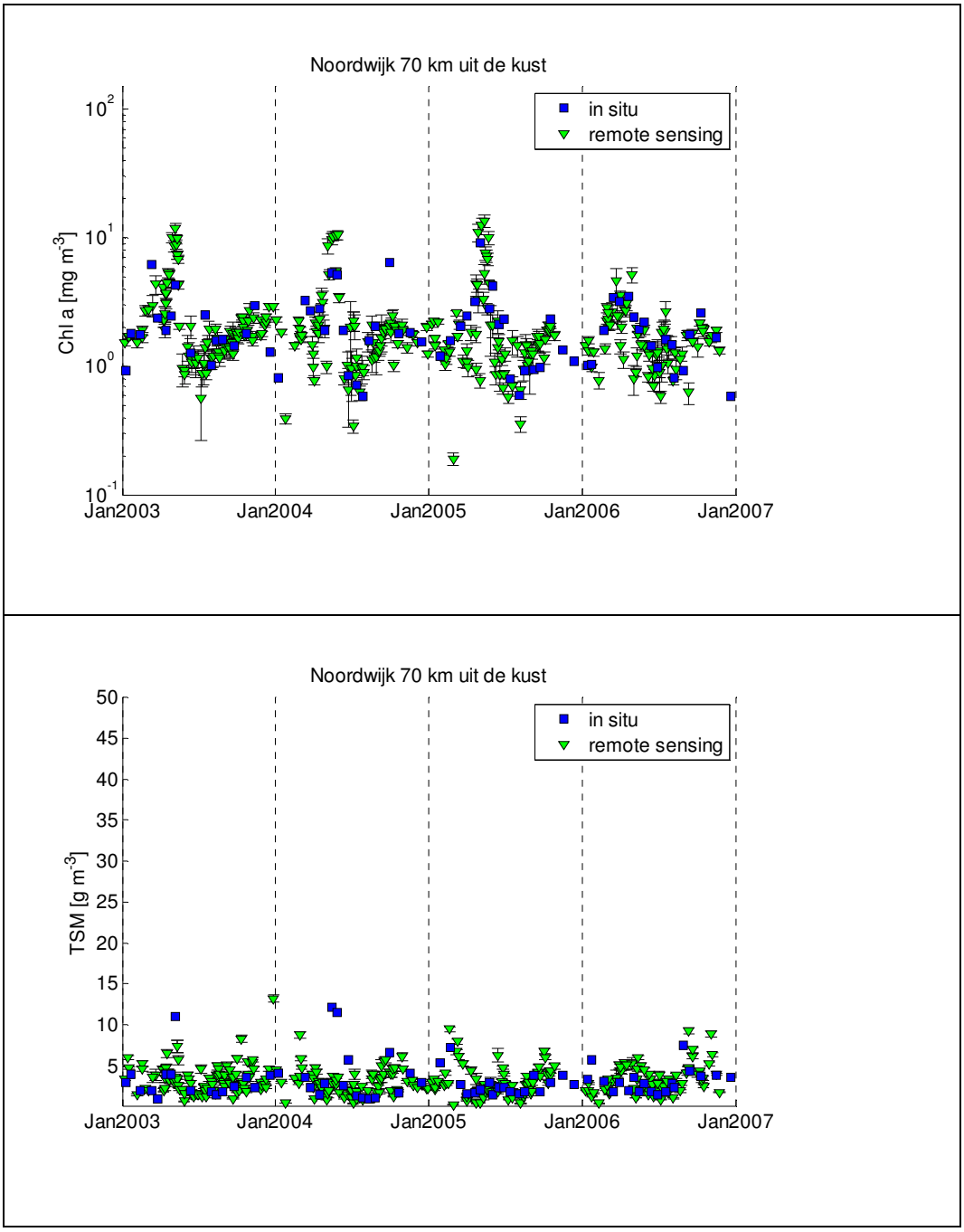


*Figure I.9 Station "Noordwijk 70 km uit de kust": Time series of Chl-a and TSM (blue squares = MWTL and green triangles = MERIS-best-2006-0011). Shown are the results for "high yield" data screening.*

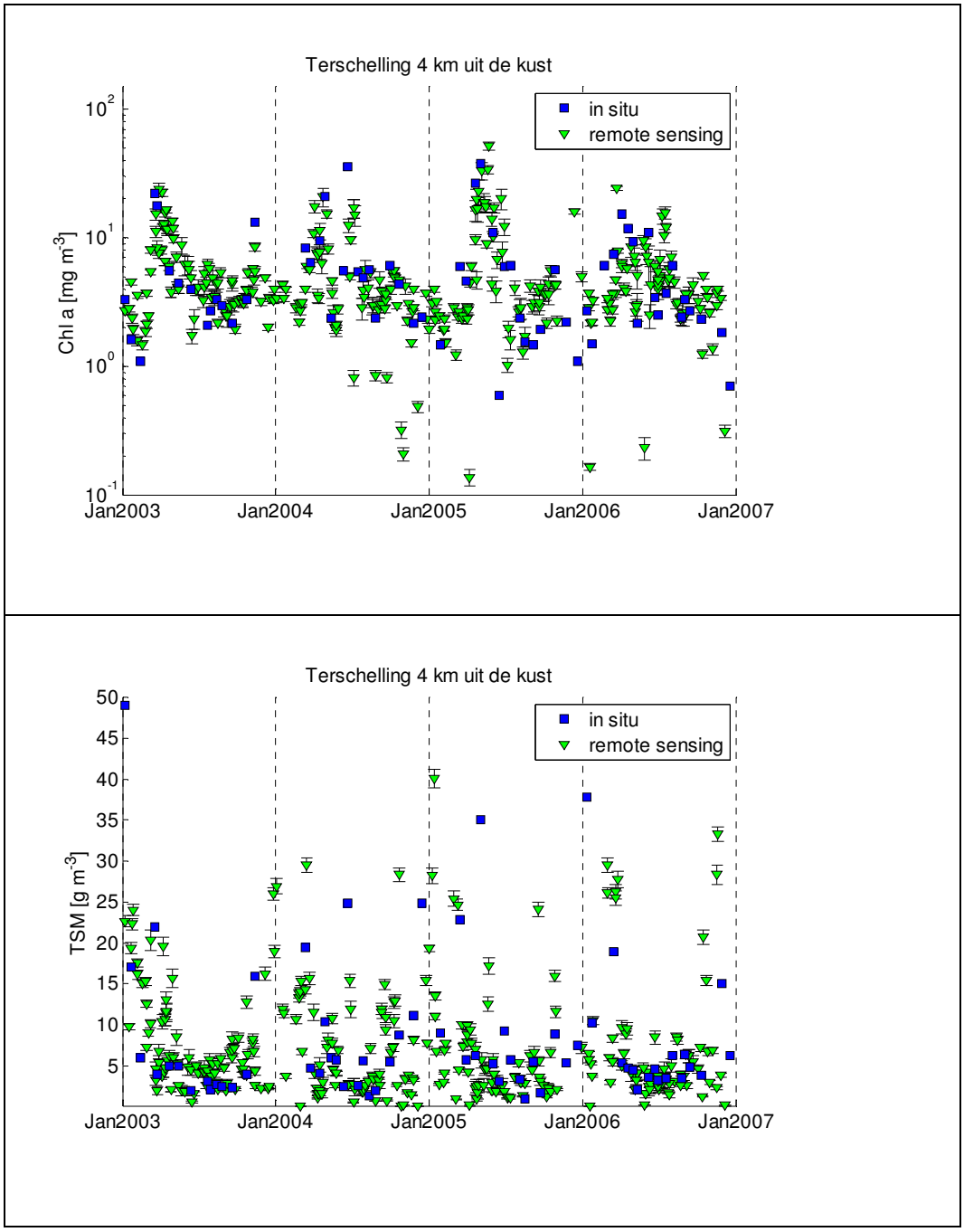


*Figure I.10: Station "Terschelling 4 km uit de kust": Time series of Chl-a and TSM (blue squares = MWTL and green triangles = MERIS-best-2006-0011). Shown are the results for "high yield" data screening.*

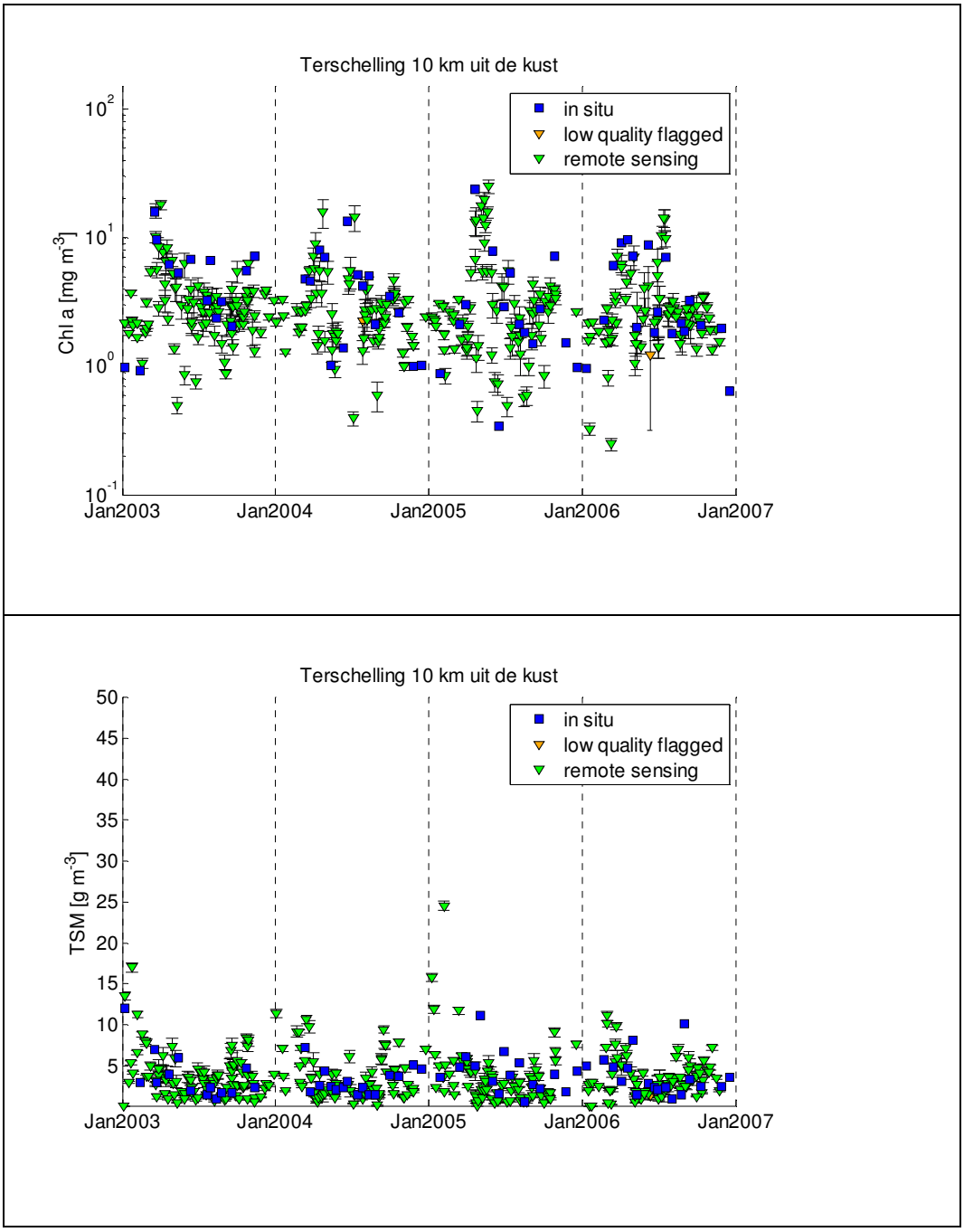


*Figure I.11: Station "Terschelling 10 km uit de kust": Time series of Chl-a and TSM (blue squares = MWTL and green triangles = MERIS-best-2006-0011). Shown are the results for "high yield" data screening.*

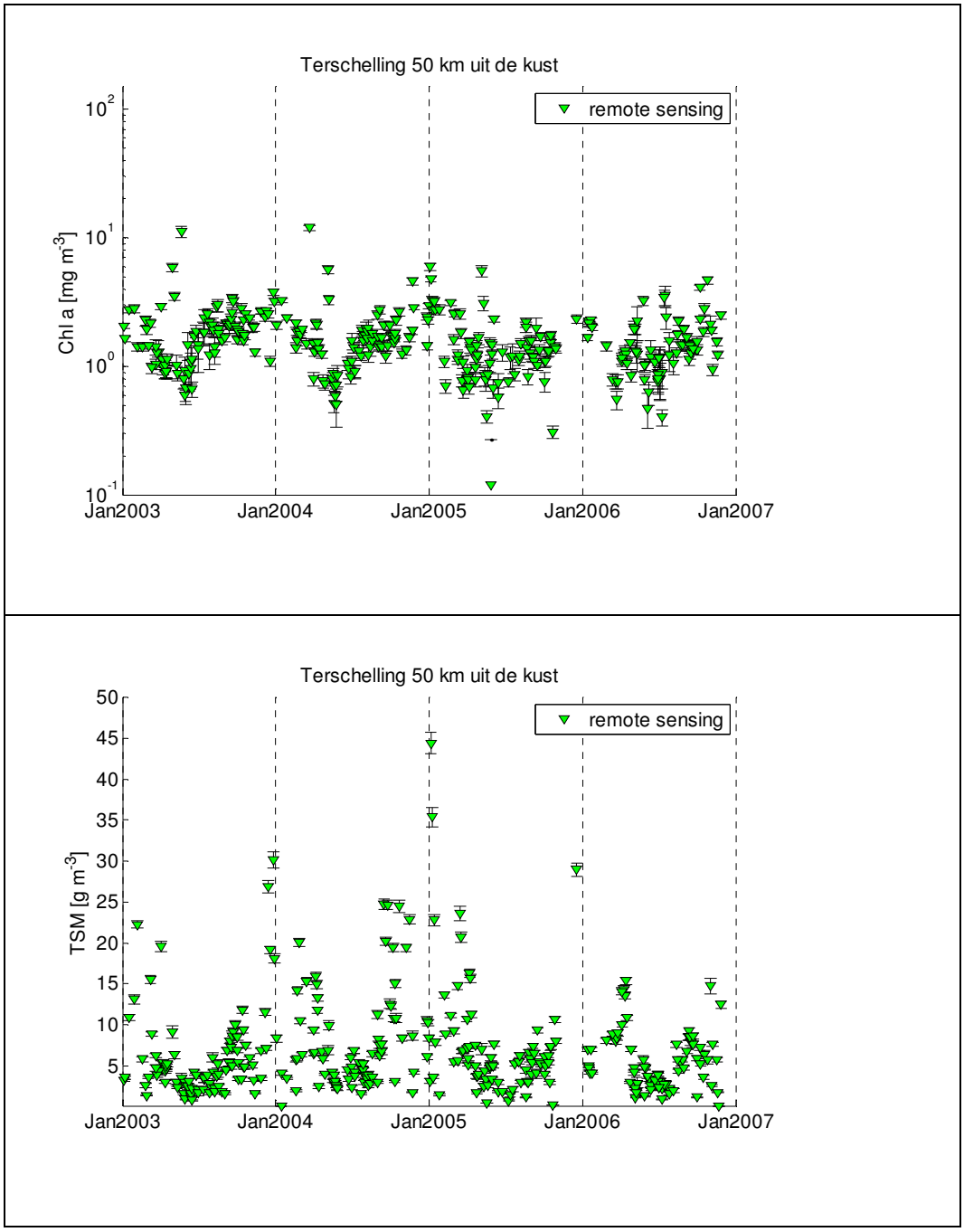


*Figure I.12: Station "Terschelling 50 km uit de kust": Time series of Chl-a and TSM (blue squares = MWTL and green triangles = MERIS-best-2006-0011). Shown are the results for "high yield" data screening.*

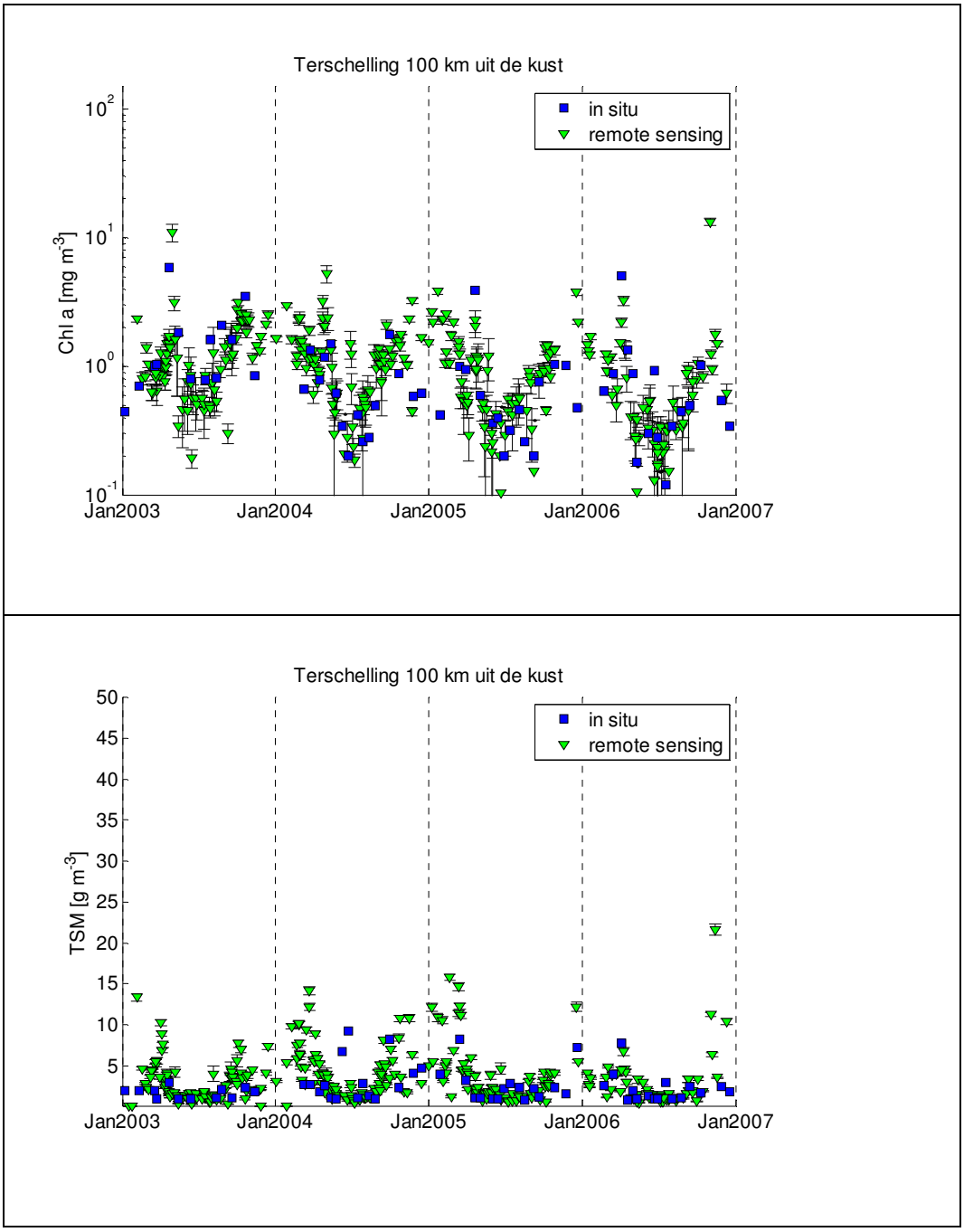


*Figure I.13: Station "Terschelling 100 km uit de kust": Time series of Chl-a and TSM (blue squares = MWTL and green triangles = MERIS-best-2006-0011). Shown are the results for "high yield" data screening.*

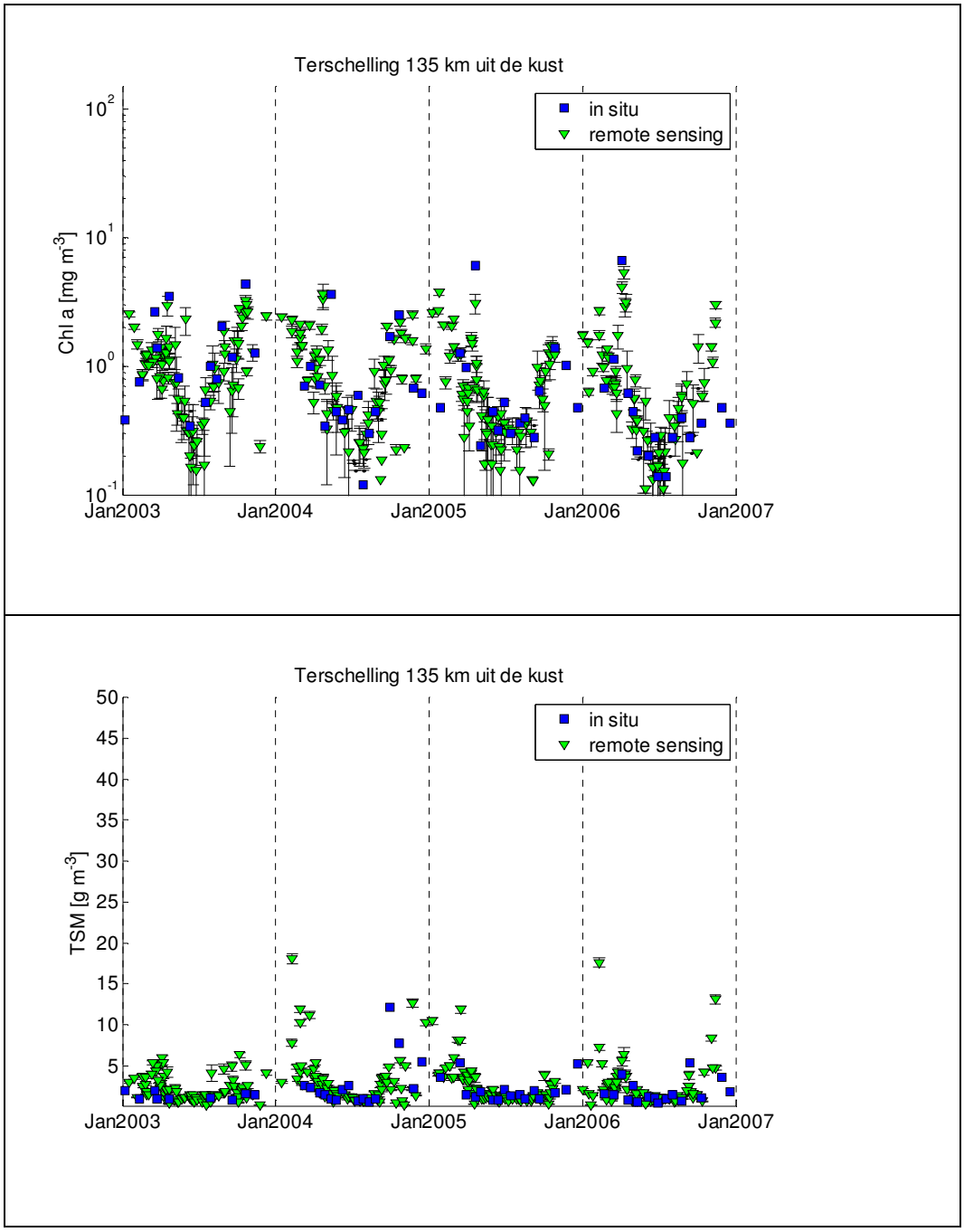


*Figure I.14: Station "Terschelling 135 km uit de kust": Time series of Chl-a and TSM (blue squares = MWTL and green triangles = MERIS-best-2006-0011). Shown are the results for "high yield" data screening.*

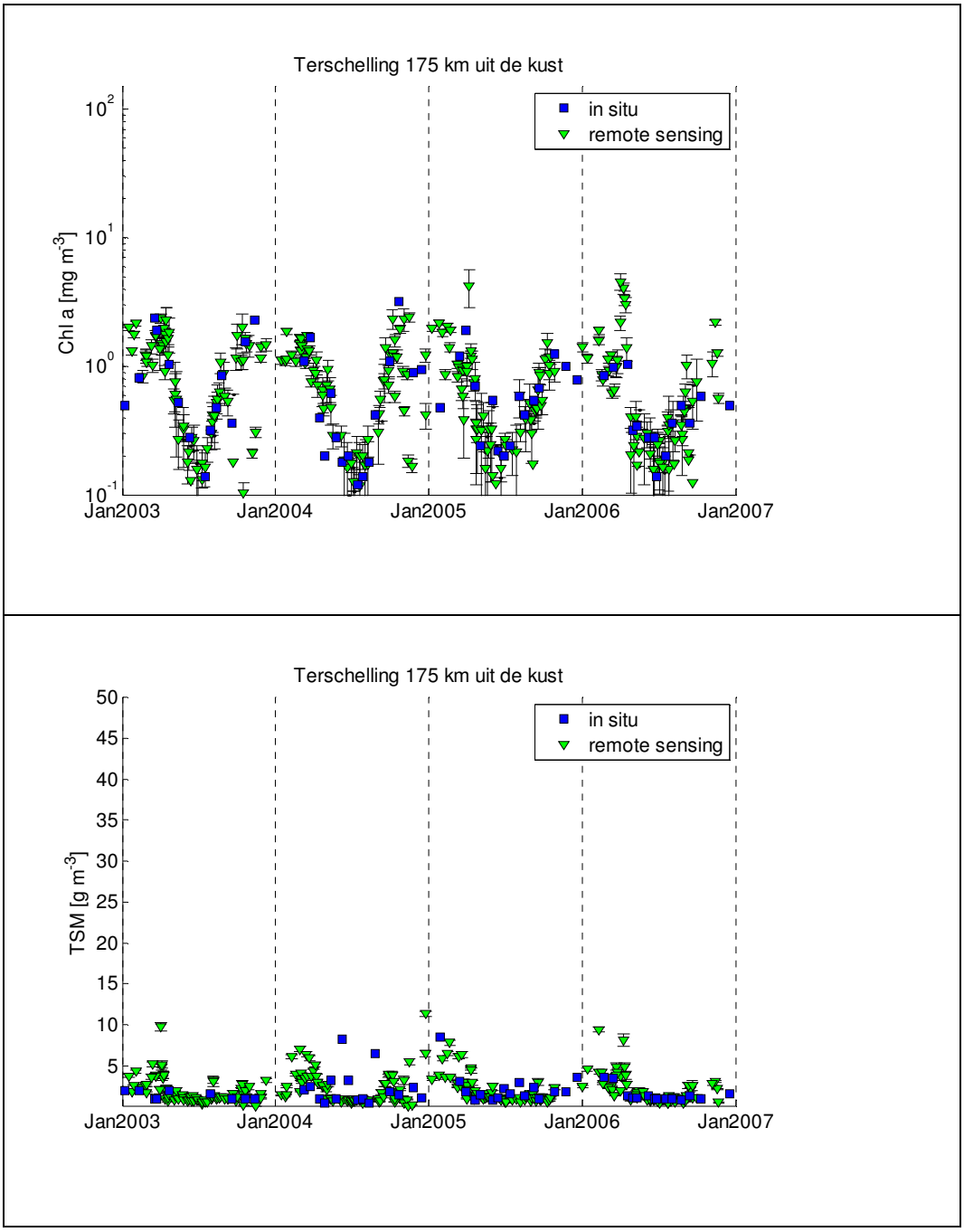


*Figure I.15: Station "Terschelling 175 km uit de kust": Time series of Chl-a and TSM (blue squares = MWTL and green triangles = MERIS-best-2006-0011). Shown are the results for "high yield" data screening.*

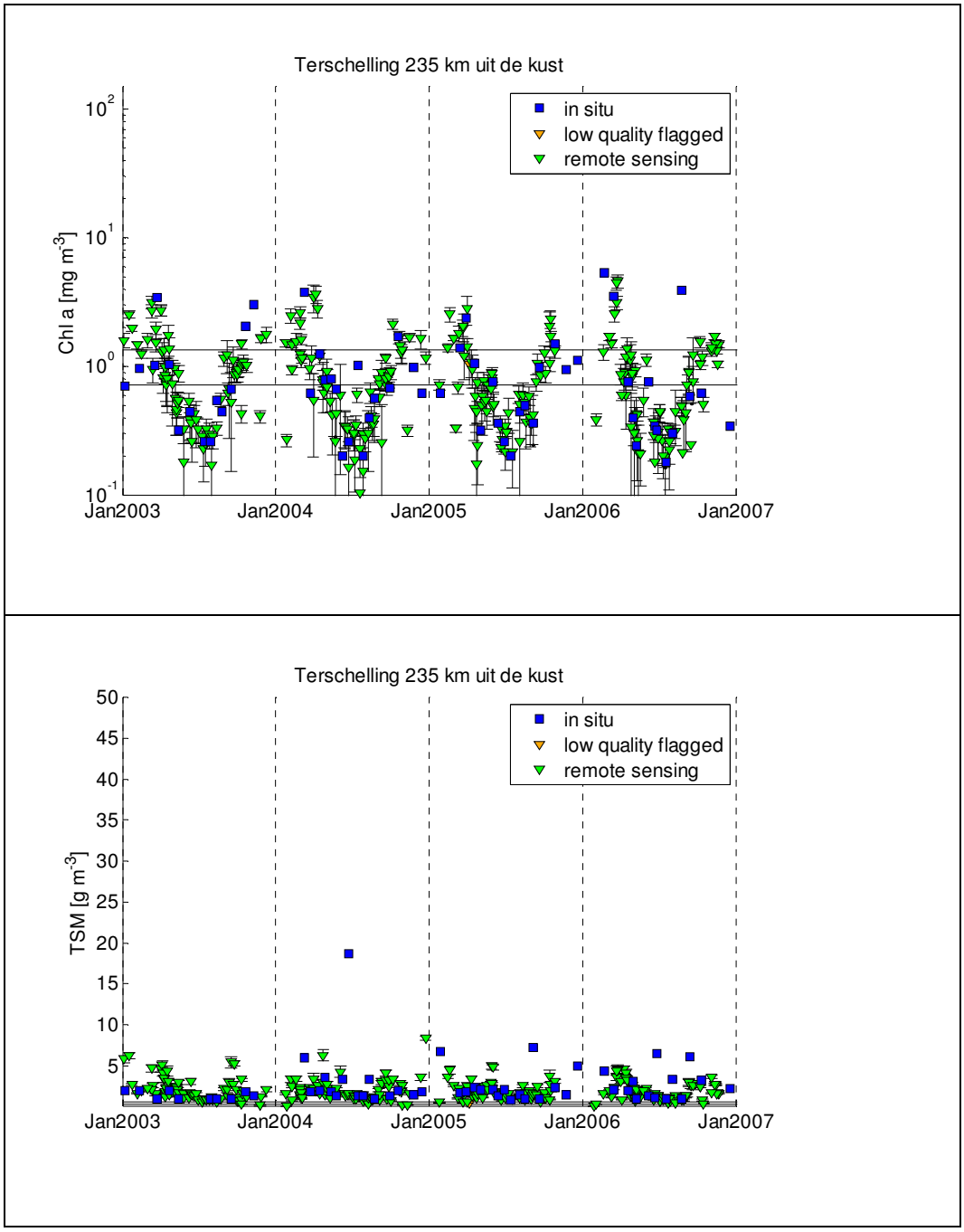


*Figure I.16: Station "Terschelling 235 km uit de kust": Time series of Chl-a and TSM (blue squares = MWTL and green triangles = MERIS-best-2006-0011). Shown are the results for "high yield" data screening.*

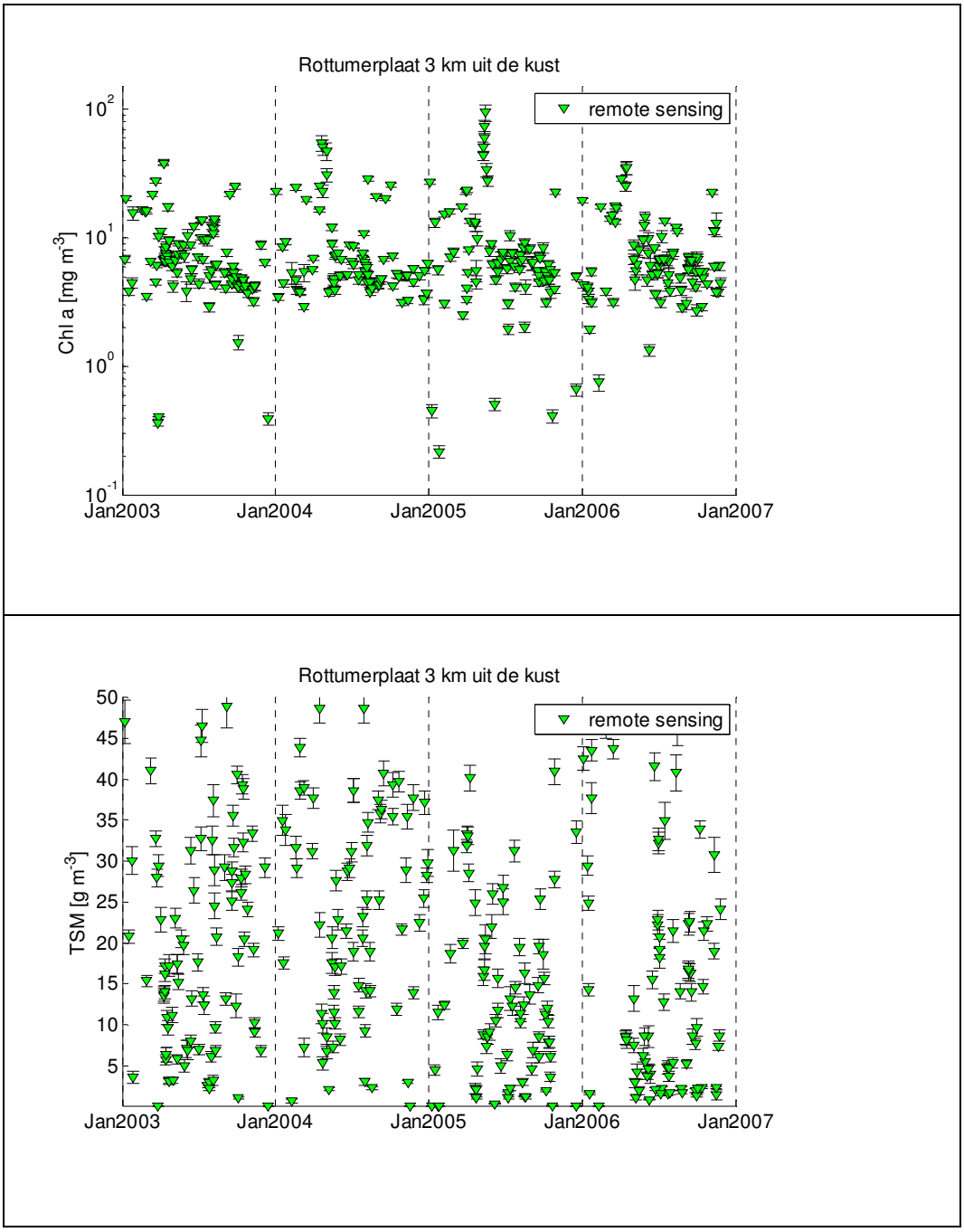


*Figure I.17: Station "Rottumerplaat 3 km uit de kust": Time series of Chl-a and TSM (blue squares = MWTL and green triangles = MERIS-best-2006-0011). Shown are the results for "high yield" data screening.*

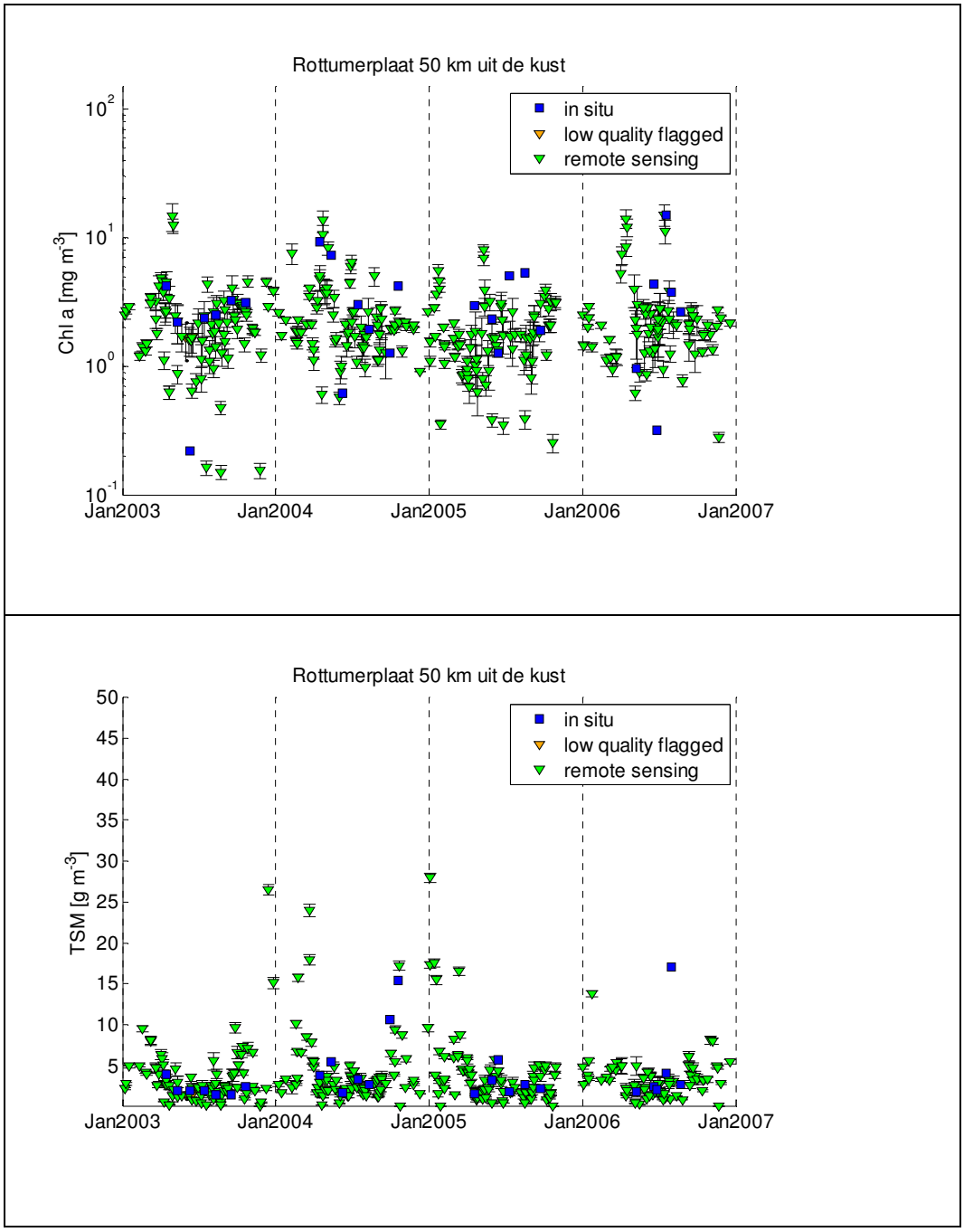


*Figure I.18: Station "Rottumerplaat 50 km uit de kust": Time series of Chl-a and TSM (blue squares = MWTL and green triangles = MERIS-best-2006-0011). Shown are the results for "high yield" data screening.*

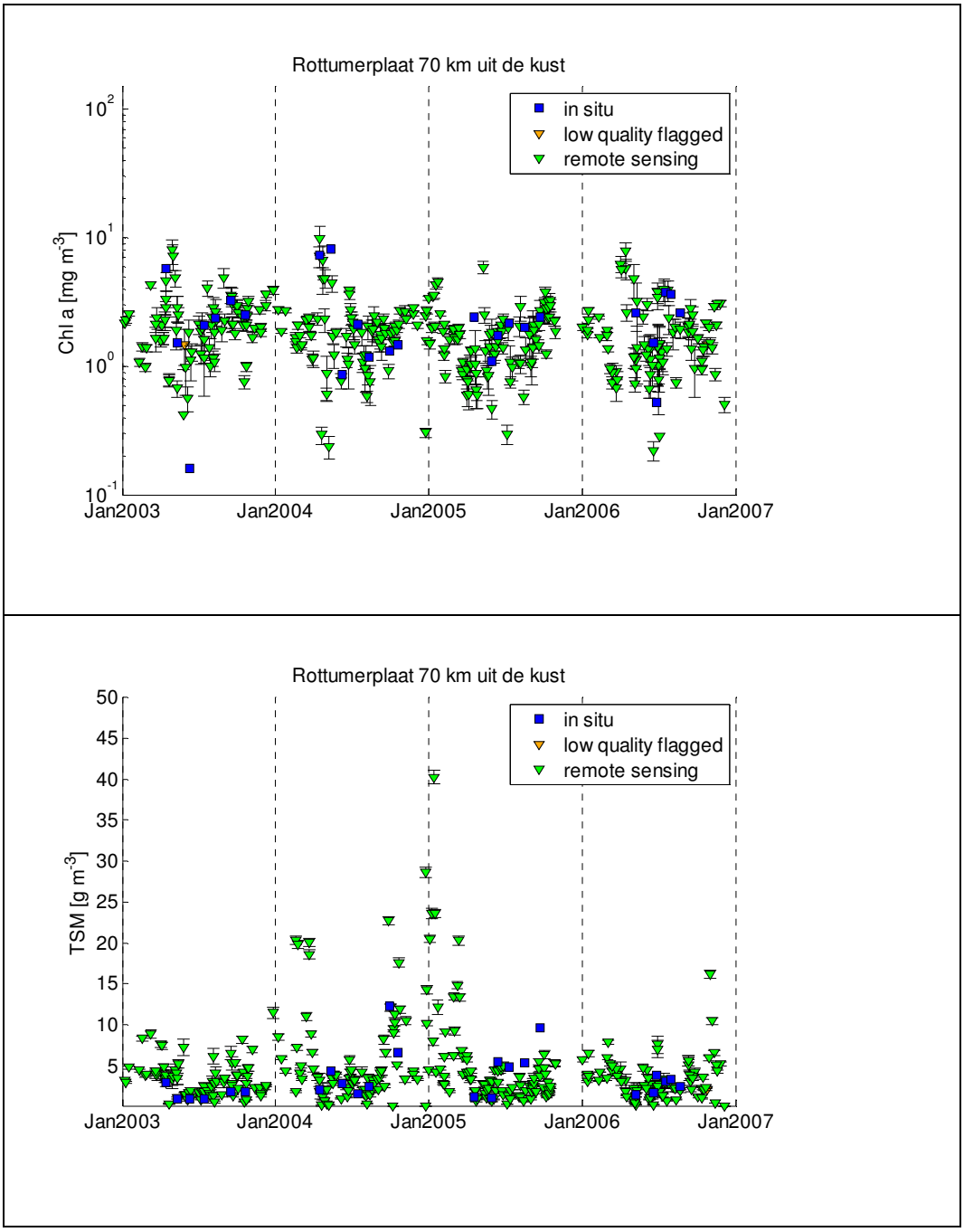


*Figure I.19: Station "Rottumerplaat 70 km uit de kust": Time series of Chl-a and TSM (blue squares = MWTL and green triangles = MERIS-best-2006-0011). Shown are the results for "high yield" data screening.*

# Appendix II. Format of MERIS and MODIS results on MWTL locations as submitted to RWS for validation

The file: testRWSout2.csv is a comma separated values file containing all relevant data for statistical analysis:

The columns are:

1. Year
2. Month
3. Day
4. Station name
5. Station latitude
6. Station longitude
7. CHL [mg m-3]
8. TSM [g m-3]
9. –log(P) [-]
10. dCHL [mg m-3]
11. dTSM [g m-3]

# Appendix III. Description of the dataset of delivered processing results (MERIS 2003 – 2006 and MODIS 2003 and 2004)

The dataset of processed images is organized per year and per day

Per year there is one subdirectory

2003

2004

2005

2006

In the 'year' directory each image has a subdirectory characterized by a code for date and time (yyyymmdd_hhmmss)

2003\20030101_102653

In each image directory the results can be found of the HYDROPT MERIS or MODIS processing. The files are always the same

Here an example is given of the filenames and as general description is provided of the contents

*MER_RR__2CQACR20030101_102653_000026172012_00323_04385_0000_hydropt74.mat*

The hydropt74.mat files contain the most important results of the processing, namely

1. C = concentrations (1=water, 2=chl, 3=tsm and 4 =cdom).
2. Dc = standard errors in the concentrations of (1=water, 2=chl, 3=tsm and 4 =cdom).
3. Kd = Kd in 8 meris bands
4. Msk = mask of all suitable MERIS pixels
5. Chisq = Chi2 : measure of the fit of the simulated HYDROPT on the measured MERIS/MODIS spectrum.
6. P : cumulative probability of Chi2
7. Metadata : information on HYDROPT settings. version and image data

*MER_RR__2CQACR20030101_102653_000026172012_00323_04385_0000_long_results.csv*

The long-results.csv files are Excel compatible comma separated text files containing all results of the processing (concentrations, errors, flags etc.) at the MWTL locations, also the results are given for averages in 3x3 pixel windows centred at the MWTL station locations.

*MER_RR__2CQACR20030101_102653_000026172012_00323_04385_0000_short_results.csv*

The short_results.csv files contain only the concentration values at the MWTL stations

*MER_RR__2CQACR20030101_102653_000026172012_00323_04385_0000_l2flags.mat*

This file contains the flag codings as delivered by ESA

*MER_RR__2CQACR20030101_102653_000026172012_00323_04385_0000_latlon.mat*

The latlon file contains a.o.. the variables biglat and biglon that contain the location per pixel.

*20030101_102653_metadata.mat*

The metadata.mat file contains the name and the date/time information of the image.

*2003\20030101_102653\higres*

Within each image directory there is a subdirectory higres containing jpeg images of all results for area 2 (North Sea) and area 3 (Voordelta). The images show the ESA flags (Medium glint, High glint and PCD-1-13), the concentrations (Chl-a, TSM and CDOM0; the standard errors in the concentrations (dChl-a, dTSM and dCDOM); the Kd at 550 nm and the –log(P($\chi$2)) flag ('P').

From the reflectances the true colour image is produced as jpeg. From the Chl-a images a threshold image is produced showing Chl-a exceeding the threshold of 10 mg/m-3.

*IVM_MER_RR__2CNACR_20030101T102653_prod_Wind velocity_area_3_300.jpg*

*IVM_MER_RR__2CNACR_20030101T102653_prod_Wind velocity_area_2_300.jpg*

*IVM_MER_RR__2CNACR_20030101T102653_prod_P_area_3_300.jpg*

*IVM_MER_RR__2CNACR_20030101T102653_prod_P_area_2_300.jpg*

*IVM_MER_RR__2CNACR_20030101T102653_prod_Medium Glint_area_3_300.jpg*

*IVM_MER_RR__2CNACR_20030101T102653_prod_Medium Glint_area_2_300.jpg*

*IVM_MER_RR__2CNACR_20030101T102653_prod_High Glint_area_3_300.jpg*

*IVM_MER_RR__2CNACR_20030101T102653_prod_High Glint_area_2_300.jpg*

*IVM_MER_RR__2CNACR_20030101T102653_prod_PCD113_area_3_300.jpg*

*IVM_MER_RR__2CNACR_20030101T102653_prod_PCD113_area_2_300.jpg*

*IVM_MER_RR__2CNACR_20030101T102653_prod_Highchl_area_3_300.jpg*

*IVM_MER_RR__2CNACR_20030101T102653_prod_Highchl_area_2_300.jpg*

*IVM_MER_RR__2CNACR_20030101T102653_prod_True_Color_Image_area_3_300.jpg*

*IVM_MER_RR__2CNACR_20030101T102653_prod_True_Color_Image_area_2_300.jpg*

*IVM_MER_RR__2CNACR_20030101T102653_prod_Kd550_area_3_300.jpg*

*IVM_MER_RR__2CNACR_20030101T102653_prod_Kd550_area_2_300.jpg*

*IVM_MER_RR__2CNACR_20030101T102653_prod_dg440_area_3_300.jpg*

*IVM_MER_RR__2CNACR_20030101T102653_prod_dg440_area_2_300.jpg*

*IVM_MER_RR__2CNACR_20030101T102653_prod_g440_area_3_300.jpg*

*IVM_MER_RR__2CNACR_20030101T102653_prod_g440_area_2_300.jpg*

*IVM_MER_RR__2CNACR_20030101T102653_prod_dtsm_area_3_300.jpg*

*IVM_MER_RR__2CNACR_20030101T102653_prod_dtsm_area_2_300.jpg*

*IVM_MER_RR__2CNACR_20030101T102653_prod_tsm_area_3_300.jpg*

*IVM_MER_RR__2CNACR_20030101T102653_prod_tsm_area_2_300.jpg*

*IVM_MER_RR__2CNACR_20030101T102653_prod_dchl_area_3_300.jpg*

*IVM_MER_RR__2CNACR_20030101T102653_prod_dchl_area_2_300.jpg*

*IVM_MER_RR__2CNACR_20030101T102653_prod_chl_area_3_300.jpg*